ELUCIDATING THE ROLE OF PEPTIDYLARGININE DEIMINASE 2 (PADI2) IN MAMMARY TUMOR PROGRESSION

A Dissertation

Presented to the Faculty of the Graduate School

of Cornell University

In Partial Fulfillment of the Requirements for the Degree of

Doctor of Philosophy

by

Sachi Horibata

May 2016

ROLE OF PEPTIDYLARGININE DEIMINASE ENZYME 2 IN MAMMARY TUMOR PROGRESSION

Sachi Horibata, Ph. D.

Cornell University 2016

Peptidylarginine deiminase 2 (PADI2) post-translationally converts positively charged protein arginine residues to neutrally charged citrulline, a process known as citrullination or deimination. We first demonstrated that PADI2 is expressed in mammary gland and its expression is regulated by estrogen. We and others have also found that PADI2 is often overexpressed in breast cancer. To test the ability of PADI2 to alter the tumorigenic properties of breast cancer cells, we either depleted PADI2 from breast cancer cells or suppressed PADI2 activity using PADI inhibitors. We found that PADI2 depletion or inhibition suppresses cell migration and alters the morphology of breast cancer cells. *In vivo*, we found that PADI2 overexpression results in mammary gland hyperbranching, a phenotype often observed during carcinogenesis. In addition, we found that inhibition of PADI2 activity with the PADI inhibitor, BB-Cl-Amidine, suppresses EGF-induced ductal invasion in our mammary gland organoid study. Together, our work suggests that PADI2 plays a critical role in breast cancer cell migration and invasion.

Our previous transcriptomics studies revealed that PADI2 expression is highly correlated with the expression of the oncogene, HER2, across more than 50 breast cancer cell lines. Thus, we investigated the relationship between PADI2 and HER2. Results show that PADI2 appears to be involved in HER2 signaling, both up and downstream of HER2. We have also demonstrated

that PADI2 functions as an estrogen receptor (ER) cofactor by citrullinating histone arginine residues at ER binding sites, thereby promoting stable ER binding and target gene expression. The observation that PADI2 appears to play key roles in both ER and HER2 signaling in breast cancer cells suggests that PADI2 likely plays a critical role in breast cancer progression. The goal of my thesis work was to further investigate the mechanisms by which PADI2 regulates these signal transduction pathways in breast cancer.

BIOGRAPHICAL SKETCH

Sachi Horibata was born on January 1, 1988, in Naga, Philippines. She grew up in Manila, Philippines and Hyogo, Japan. She was the eldest of three siblings. She attended the International School Manila where she met her biology teacher, Mr. Joseph Conte, who encouraged her to pursue her studies in the biological sciences. Upon graduation from high school in 2006, Sachi attended the University of Wisconsin – Madison in Madison, WI, where she majored in Biochemistry. This is when her grandmother was diagnosed and later passed away from ovarian cancer. This motivated her to join the laboratory of Dr. Manish Patankar during her sophomore year, to study the role of MUC16 in epithelial ovarian cancer. She closely worked with Dr. Jennifer Gubbels. Having great role models, she was inspired to become a researcher. Sachi developed a cell-based assay that measure cell-cell interaction that led to the discoveries of multiple roles of MUC16 in ovarian cancer. While working in the Patankar Lab, during her junior year, she also did research in the lab of Dr. Yoshihiro Kawaoka, where she investigated the entry of Ebola virus into host cells. During her last year at UW-Madison, Sachi completed an Honors Thesis on immune cell-ovarian tumor cell adhesion through MUC16 and immunocytokines. With encouragement from her mentors, Sachi applied to graduate school and was accepted at Cornell University. Sachi graduated from UW-Madison with honors and a B.S. in Natural Sciences with a concentration in Biochemistry.

After coming to Cornell University in 2010, Sachi joined the laboratory of Dr. Scott Coonrod. She worked on molecular cell biology and epigenetics, studying a novel histone modifier known as peptidylarginine deiminase 2 (PADI2). Her studies focused on understanding the role of PADI2 in breast cancer progression and potential therapeutic target. During her

graduate studies, she volunteered at the Cancer Resource Center where she received inspiration to pursue a career in cancer biology. Together, this furthered her desire to continue in the field of cancer biology with a strong goal to find better cancer therapies. It was also during her graduate study where she met her husband, Tommy Vo. He is the most motivated graduate student anyone can ever find and he further inspired her to excel in research.

After completing her Ph.D., Sachi plans to begin her postdoctoral work in the laboratory of Dr. Michael Gottesman at the National Cancer Institute in Bethesda, Maryland. The research focus of the laboratory is to understand the mechanisms that reduce accumulation of cytotoxic drugs in cancer cells by ABC transporters. Sachi will be working on investigating the mechanism of cisplatin resistance. She hopes to continue to pursue a career in cancer biology.

In memory of my grandmother, Meriam A. Glinoga –

For giving me strength and courage to pursue cancer research.

ACKNOWLEDGMENTS

I would like to thank my family for their unconditional love and support. They are always supportive of my decisions and encouraged me to pursue my dream. When I fail, they are always there to help me get back up. To my father, even though there is 12 hours of time difference between the United States and the Philippines, thank you for always picking up my phone calls (often around 3 to 6 am) whenever I have something exciting or troubling to share. To my mother, thank you for always cheering me up and teaching me how to enjoy life to the fullest. She is the happiest person I know and she can turn anything into something positive. To my two amazing brothers, thank you for always entertaining me, going on trips with me to clear my mind, sending me boxes of food, or visiting me just to cook for me. To my in-laws and brother-in-laws, thank you for welcoming me into your family and being so supportive of all my decisions.

I am grateful to Dr. Scott Coonrod for his guidance over the years and letting me be part of his lab. He has taught me how to think, speak, and write like a scientist. But more importantly, he gave me the freedom to explore my ideas, try new techniques, write grants, and attend workshops that greatly enhanced my skills that allowed me to get my dream job. He has been so patient with me and I would not ask for any better mentor. I would also like to thank my thesis committee members, Dr. Richard Cerione, Dr. Mark Roberson, and Dr. Robert Weiss for their counsel, suggestions, and their support throughout my graduate career. I cannot thank them enough for all the time they invested to make sure that I am on the right track.

I would like to thank the members in my lab, Dr. John McElwee for teaching me multiple experimental skills and being a great friend, Lynne Anguish for helping me with my orders and histology slides but more importantly, she was there for me like a mother, Kelly Sams for bringing smiles to the lab, Dr. Sunish Mohanan for being a wonderful colleague, Dr. Brian Cherrington for being my mentor who taught me all the necessary techniques run in the lab, Dr.

Xuesen Zhang for teaching me how to run ChIP, Dr. Rui Kan for being a wonderful office mate and Dr. Boram Kim for being a fun lab mate and a good friend. I especially want to thank my students, David Sadegh, Katherine Rogers (Rin), Iva Cvitas, Dalton McLean, and Hamza Oglat. They truly helped me, especially David and Rin, throughout my PhD career. I was very fortunate to have students who are passionate to learn. I would also like to thank my next door lab neighbor, Dr. Chinatsu Mukai and Dr. Roy Cohen for giving me life advice throughout my PhD career. I became very close to Chinatsu and she is like a sister that I can go to.

I also would like to thank Dr. Weiss for introducing me to the Cancer Resource Center (CRC). CRC is now a family to me and they give me reasons to why I am doing what I am doing. I would especially like to thank Bob Riter and the members of the Young Adults Group for welcoming me and giving me courage throughout my graduate career.

I would like to thank Dr. Maurine Linder for her support throughout my graduate career. She always came to my talks or seminars and gave me advice and suggestions. She believed in my ability and I always wanted to work hard to prove that she is right.

I would also like to thank Dr. Dave Lin for making the BBS program the program that it is today. He dedicated his time to make sure all the students would get the education that we need to be a successful graduate student.

I had a pleasure of working with Dr. Charles Danko and his lab members in the later part of my graduate career. Especially, I would like to thank Ed Rice for helping me with my PRO-seq experiments for a whole year. I had a wonderful time collaborating with their lab.

I would like to thank Dr. Marc Antonyak for giving me advice and inspiration during my graduate career. I have never met anyone who can turn any ideas into something brilliant.

I would like to thank Dr. Jim Casey and Fina for treating me like their daughter. They make wonderful Filipino food for me whenever I miss home.

I cannot survive my graduate career without the help of Janna Lamey, Arla Hourigan, Carina Ayar, Cindy Grey, Debbie Crane, Merry Buckley, Shelagh Johnston, and Sue Williams. They truly helped me with every single paper work that I had to file.

Throughout my graduate career, I have made wonderful friends. Without them, I really do now know how I would have been. I would like to thank all my classmates and colleagues in the BBS program for giving me such an amazing graduate life. I also would like to thank the students from the BMCB program in my year for welcoming me to their group and for inviting me to their events and gatherings even though I am not part of their program. I also would like to thank the Filipino community for welcoming me and taking good care of me like a family. I cannot thank them all enough for letting me have such a spectacular graduate life.

Last, but not the least, I would like to thank my loving and supportive husband, Tommy Vo. There have been many ups and downs throughout my graduate career and he was there right next to me. When I have accomplishments, he is so happy, in fact, happier than me. When I have my downs, he will not hold my hand to lift me up, but he will be right next to me, to make sure that I can stand up on my own. He truly helped me become who I am and to not be afraid of failures. He is truly my other half and I am so thankful to have him throughout my graduate career.

TABLE OF CONTENTS

LIST OF FIGURES

CHAPTER ONE

CHAPTER TWO

CHAPTER THREE

CHAPTER FOUR

CHAPTER FIVE

CHAPTER SIX

LIST OF TABLES

CHAPTER ONE

LIST OF ABBREVIATIONS

AD – Alzheimer's disease

AFA – Antifilaggrin autoantibody

AKA – Anti-keratin antibodies

APF – Antiperinuclear factor

Biotin-NTP – Biotin-labeled ribonucleotide triphosphate analogs

CBP – CREB binding protein

ChIP – Chromatin immunoprecipitation

CNS – Central nervous system

DCIS – Ductal carcinoma *in situ*

dREG – Discriminative regulatory element detection from GRO-seq/PRO-seq

E2 – Estrogen or 17β-*estradiol*

ECM – Extracellular matrix

EGF – Epidermal growth factor

EGFR – Epidermal growth factor receptor

EMT – Epithelial-to-mesenchymal transition

ER – Estrogen receptor

ERE – Estrogen response element

eRNA – Enhancer RNA

GDNF – Glial cell line-derived neurotrophic factor

GFAP – Glial fibrillary acidic protein

H3R26 – Histone H3 arginine residue 26

HDAC3 – Histone deacetylase 3

HER2 – Human epidermal growth factor receptor 2

KI/KO – ER binding mutant

KM – Kaplan-Meier

MBP – Myelin basic protein

MNase – Micrococcal nuclease

MS – Multiple sclerosis

NCoR – Nuclear receptor co-repressor

NET – Neutrophil extracellular trap

NK – Natural killer

NLS – Nuclear localization signal

PADI – Peptidylarginine deiminase

PI3K – Phosphatidyl-inositol 3-kinase

PR – Progesterone receptor

PRO-seq – Precision global Run-On and Sequencing assay

RA – Rheumatoid arthritis

RE – Regulatory elements

RTK – Receptor tyrosine kinase

SERM – Selective estrogen-receptor modulator

αERKO – ER α knockout mice

CHAPTER ONE

INTRODUCTION

Portions of this chapter (Figure 1.2 and 1.4) were published in Horibata, S., Coonrod, S.A., and Cherrington, B.D. (2012). Role for peptidylarginine deiminase enzymes in disease and female reproduction. J Reprod Dev *58*, 274-282 (1) and in Mohanan, S., Cherrington, B.D., Horibata, S., McElwee, J.L., Thompson, P.R., and Coonrod, S.A. (2012). Potential role of peptidylarginine deiminase enzymes and protein citrullination in cancer pathogenesis. Biochem Res Int *2012*, 895343 (2).

My thesis is organized according to the work-flow diagram shown in **Figure 1.1**.

Figure 1.1: Work-flow diagram of dissertation.

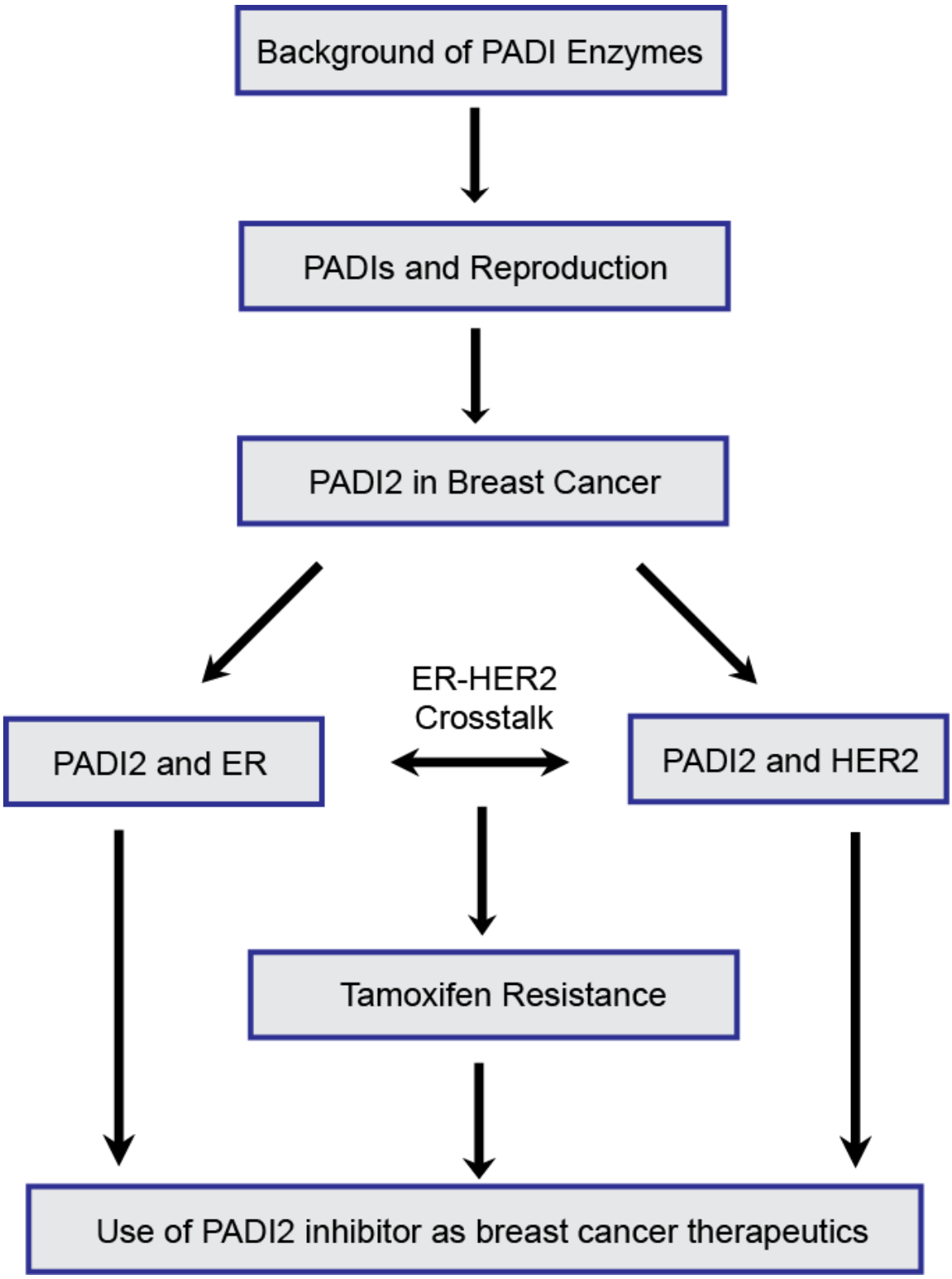
Background of PADI Enzymes
PADIs and Reproduction
PADI2 in Breast Cancer
ER-HER2
Crosstalk
PADI2 and ER
PADI2 and HER2
Tamoxifen Resistance
Use of PADI2 inhibitor as breast cancer therapeutics

Background of PADI Enzymes

Peptidylarginine deiminase enzymes (PADIs) are calcium-dependent enzymes that post-translationally convert positively charged arginine residues to neutrally charged citrulline (1,3,4). This process is known as citrullination or deimination. The loss of charge can result in protein unfolding, proteolytic degradation, or potential loss of intramolecular interactions **(Figure 1.2)** (1,3,5-9). There are 5 PADI family members, PADI1, PADI2, PADI3, PADI4, and PADI6 and they are clustered together on human chromosome 1p36.13 (3). PADI2 is thought to be the ancestral homologue of the PADIs, with the remaining PADs being derived from PADI2 by gene duplication (3). The PADIs have very different tissue distribution and cellular localization patterns **(Table 1.1 and Discussed in Chapter 2)**. PADI1 is localized in epidermis (10-14) whereas PADI2 is the most widely expressed among the PADI family and is localized in brain, skeletal muscle, epidermis, and many other tissues (3,4,12,14-20). On the other hand, PADI3 is predominantly expressed in hair follicles and epidermis (12,21,22) and PADI4 is found in cells of hematopoietic lineages such as eosinophils, neutrophils, granulocytes and monocytes (23-26). Lastly, PADI6 is expressed primarily in oocytes (27,28).

PADIs and Female Reproduction

The earliest PADI literature documented PADI expression in the mouse and rat uterus (14). Aside from our findings on the role of PADI6 in female fertility (29-31) and the role of PADIs in gene regulation in mammary epithelial cells (32), the link between PADIs and reproduction has not been extensively explored. To examine the importance of PADIs in female reproduction, in **Chapter 2**, we first examined the distribution patterns of PADIs in female reproductive tissues. We found that both PADI2 and PADI4 are expressed in the mouse uterine

Figure 1.2: The enzymatic activity of peptidylarginine deiminase (PADI) enzymes. (A) PADI enzymes post-translationally catalyze the conversion of positively charged arginine residues on protein into a neutrally charged citrulline. This process is termed citrullination or deimination. **(B)** The conversion of charge can lead to protein unfolding, proteolytic degradation, or loss of intramolecular interactions (Figure obtained from Horibata, S., *et al.* (2012) *J Reprod Dev* **58**, 274-282) (1).

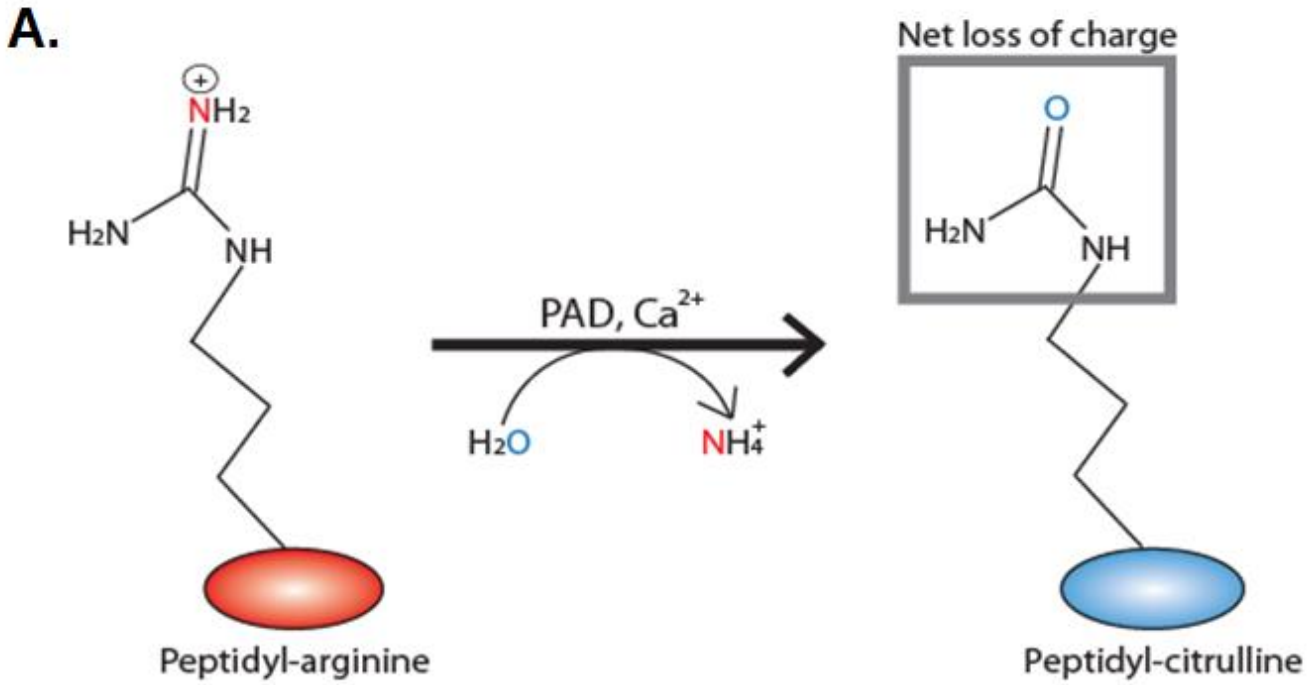
A.
Net loss of charge
PAD, Ca2+
Peptidyl-arginine
Peptidyl-citrulline

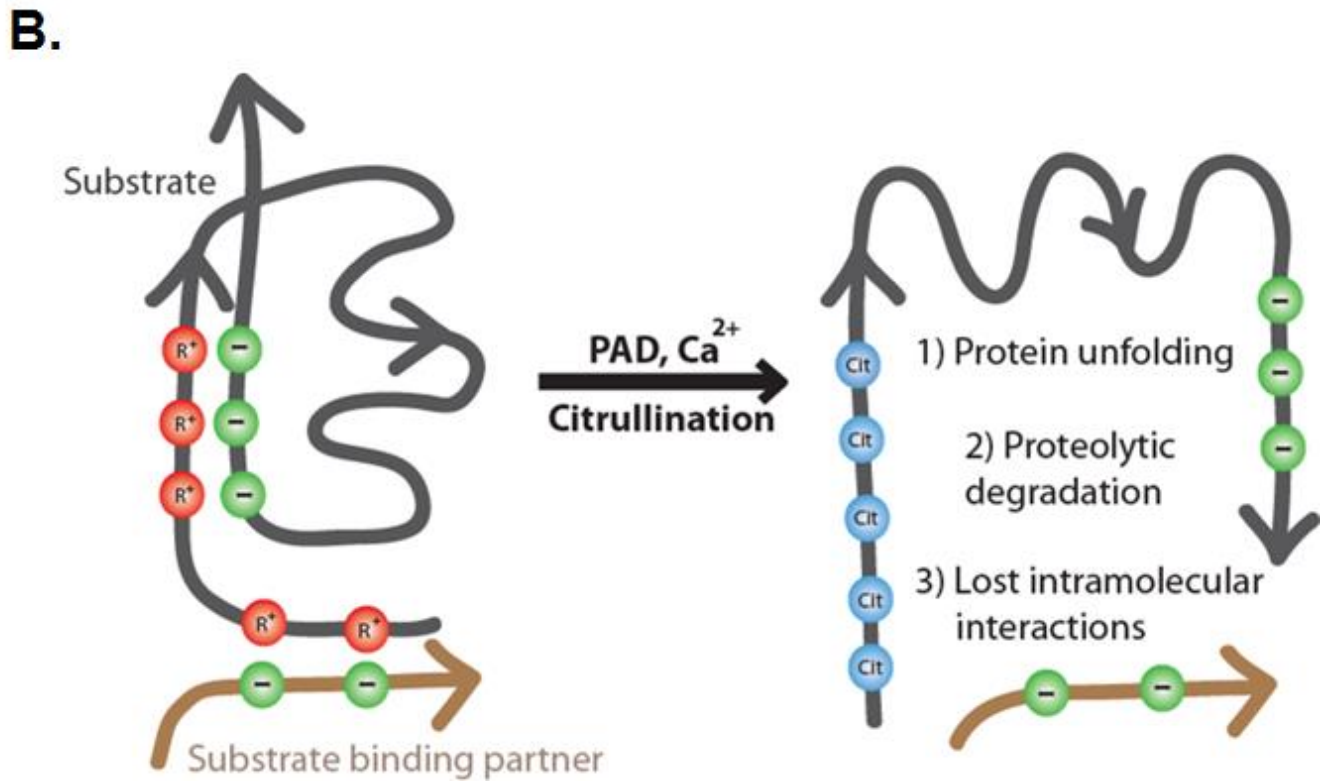
B.
Substrate
PAD, Ca2+
Citrullination
1) Protein unfolding
2) Proteolytic degradation
3) Lost intramolecular interactions
Substrate binding partner

Table 1.1: Subcellular localizations and tissue distributions of PADI enzymes. (Adapted and edited from Vossenaar, E.R., *et al.* (2003) *Bioessays* **25**, 1106-1118) (3).

PADI enzymes	Subcellular Localizations	Tissue Distributions
PADI1	Cytoplasm	epidermis
PADI2	Cytoplasm and Nucleus	brain, skeletal muscle, epidermis, uterus, pituitary gland, mammary gland and many other tissues
PADI3	Cytoplasm	hair follicles and epidermis
PADI4	Cytoplasm and Nucleus	Eosinophils, neutrophils, granulocytes, monocytes, uterus, mammary gland
PADI6	Cytoplasm	Oocytes

and mammary epithelial cells (1). Interestingly, we also found that the expression patterns of PADI2 and PADI4 in uteri and mammary glands are regulated by estrogen (1).

Subcellular localization of PADI enzymes

Previous studies suggested that PADIs 1,2,3, and 6 localize to the cytoplasm while PADI4 localizes to the nucleus via a nuclear localization signal (NLS) composed of 3 lysine residues followed by one proline residue (K-K-K-P) as sequence residues 45-74 (25). In the nucleus, PADI4 can target the N-terminal histone tails for citrullination. Specifically, PADI4 can citrullinate histone H2A arginine residue 3, histone H3 arginine residues 2, 8, 17 and 26, and histone H4 arginine residue 3 to promote chromatin decondensation (33,34).

Recently, we found that PADI2 also localizes to the nucleus in human mammary epithelial cells and binds to chromatin (32). In addition, we also found that the expression of PADI2 correlates with histone citrullination level in canine mammary tissues (35). These findings suggest that PADI2 is likely able to promote histone citrullination similar to PADI4. In fact, we found that PADI2 can target histone H3 arginine residue 26 (H3R26) for citrullination and regulate estrogen receptor (ER) target gene activity (36). Thus, we now know that both PADI2 and PADI4 target histones for citrullination and causing histone modification and chromatin decondensation **(Figure 1.3)** (2).

PADIs and Diseases

PADI4 is the most highly studied PADI family member because of its association with rheumatoid arthritis (RA) (37,38). Patients with RA have high levels of citrullinated proteins in their sera, and anti-citrullinated protein antibodies are used as a diagnostic marker for RA

Figure 1.3: Citrullination of histone tails by PADI enzyme leads to chromatin decondensation. Histone tails have positively charged arginine residues that are interacting with the negatively charged DNA, keeping a condensed chromatin structure. In the presence of PADI enzymes, PADI-mediated citrullination of histone tails results in loss of positively charged arginine residue. The disruption of the interaction between the positively charged arginine residue with DNA results in chromatin decondensation. This transcriptionally poised structure will now expose sites where DNA binding proteins such as transcription factors to bind and to promote transcription of a target gene. (Figure drawn by Sachi Horibata from Mohanan, S., *et al.* (2012) *Biochem Res Int* **2012**, 895343) (2).

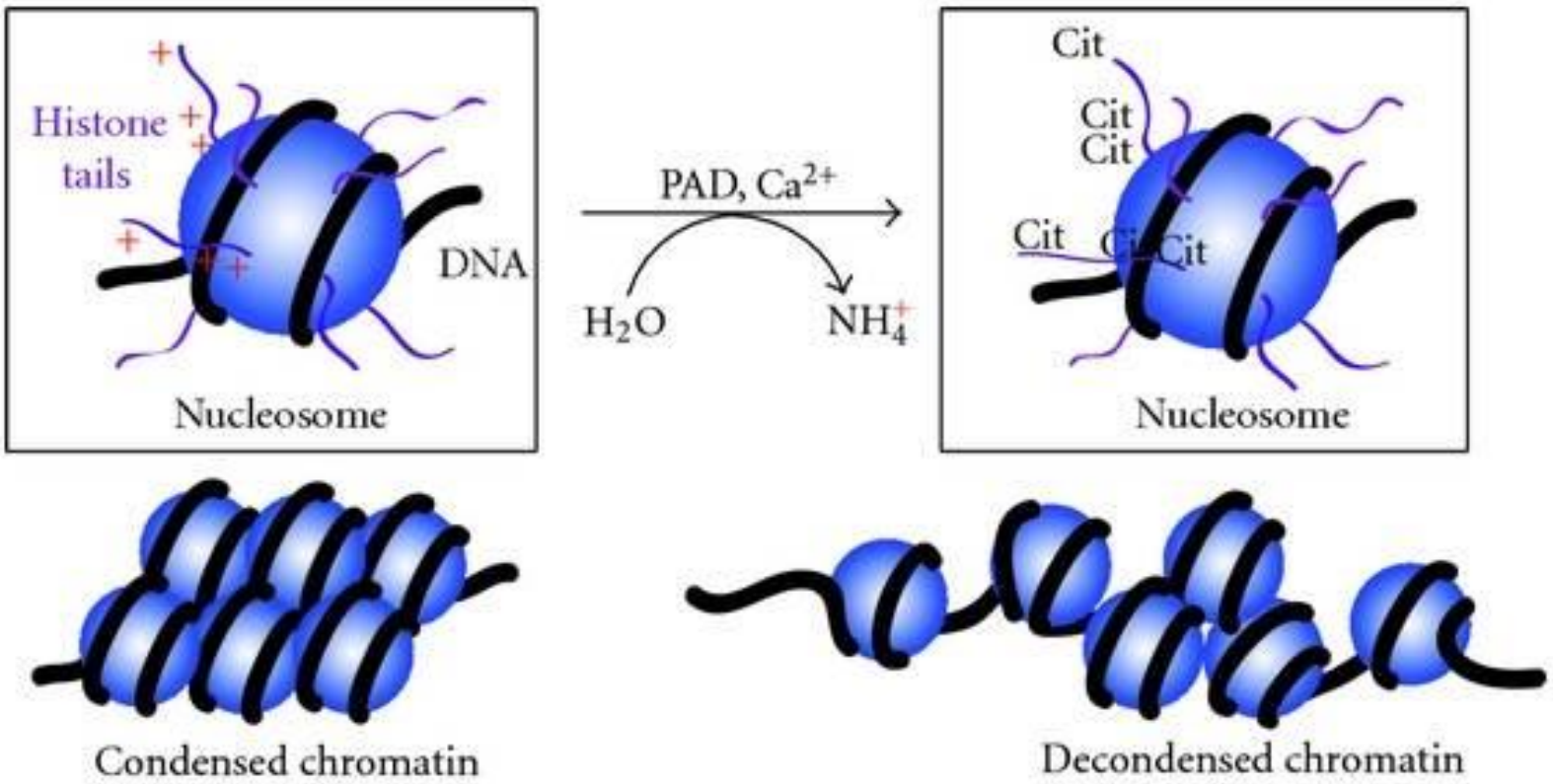
Histone tails
DNA
Nucleosome
PAD, Ca2+
H2O
NH4+
Cit
Cit
Cit
Cit
Cit
Cit
Nucleosome
Condensed chromatin
Decondensed chromatin

(39,40). RA is 3 times more prevalent in women compared to men, suggesting the potential role of sex hormones (41). In addition to RA, PADI4 has also been implicated in Alzheimer's disease where accumulation of PADI4-mediated citrullinated proteins was found in hippocampus of patients (7).

Furthermore, PADI4 is also suggested to be involved in cancer. Chang et al. immunostained a tissue array containing 47 tumors and found increased PADI4 expression in "adenocarcinoma samples from the colon, duodenum, esophagus, fallopian tube, gall bladder, lung, ovary, parotid, pancreas, prostate, rectum, small intestine, stomach, thyroid, and uterus" (6). In a subsequent study, they performed immunohistochemistry staining of patients' tumor samples from China, and found PADI4 expression in "breast carcinoma, lung adenocarcinomas, hepatocellular carcinomas, esophageal squamous cancer cells, colorectal adenocarcinomas, renal cancer cells, ovarian adenocarcinomas, endometrial carcinomas, uterine adenocarcinomas, bladder carcinomas, chondromas" and in other cancers (42).

PADI2 and Breast Cancer

Given the link between PADI4 and cancer, we asked if PADI2 might similarly be involved in cancer progression. PADI2 was of particular interest because large-scale screenings have suggested a potential link between PADI2 and cancer. Bertucci et al. investigated the gene expression profiles of 213 breast tumors and 16 breast cancer cell lines by performing microarray studies and found PADI2 to be one of the 29 genes overexpressed in *ERBB2*-positive breast cancer (43). Mackay et al. characterized 24 breast cancer cell lines and found 753 genes where their expression correlated with their copy number. Of the target hits, PADI2 was one of the genes to have highly significant expression in luminal breast cancer compared to the basal breast

cancer (44). These studies have found PADI2 as one of the top hit genes correlated with breast cancer; however, no study has investigated the role of PADI2 in breast cancer progression. Thus, we investigated the potential role of PADI2 in breast cancer progression.

As a model system, we used the MCF10AT breast cancer cell lines that mimic the 1) normal, 2) transformed, 3) ductal carcinoma *in* situ (DCIS), and 4) invasive DCIS stages **(Figure 1.4)**. These cell lines were generated by Dr. Fred Miller (45-48). He took the normal MCF10A cells (49) and transformed with an oncogene *H-Ras* (MCF10AT cells) (45). After 2067 days of MCF10AT culture, he injected the cells into immunodeficient nude mice. The nude mice developed small DCIS *comedo* lesions (MCF10DCIS.com cells). Lastly, he cultured the cells that progressed to carcinoma and invaded out from the DCIS (MCF10CA1 cells) (45,50). We have previously found PADI2 to be highly expressed in the three transformed lines, MCF10AT, MCF10DCIS.com, and MCF10CA1 cells, with the highest PADI2 expression in MCF10DCIS.com cells (51). Using the MCF10DCIS.com cells, in **Chapter 3**, I investigated the role of PADI2 in breast cancer progression. Specifically, I found that depletion of PADI2 altered cell morphology of the MCF10DCIS.com breast cancer cells, from elongated cell structure to more epithelial-like structure. This led me to investigate the role of PADI2 in tumor cell migration and invasion.

PADI inhibitors

Due to the importance of PADI enzymes in multiple diseases, particularly in RA, PADI inhibitors were generated by our close collaborator, Dr. Paul Thompson. There are currently several PADI inhibitors with, Cl-Amidine (first-generation) and BB-Cl-Amidine (second-generation) showing the most promise in specifically blocking PADI activity (52-54). Cl-

Figure 1.4: MCF10AT breast cancer progression cell lines model. Normal immortalized mammary cells, MCF10A, were transformed with an oncogene *H-Ras*. These transformed mammary cells, MCF10AT, were injected into a nude mouse. The mouse formed ductal carcinoma *in situ* lesions that include *comedo*-ductal carcinoma *in situ* (MCF10DCIS.com cells) and invasive ductal carcinoma (MCF10CA1 cells) (45,46,48).

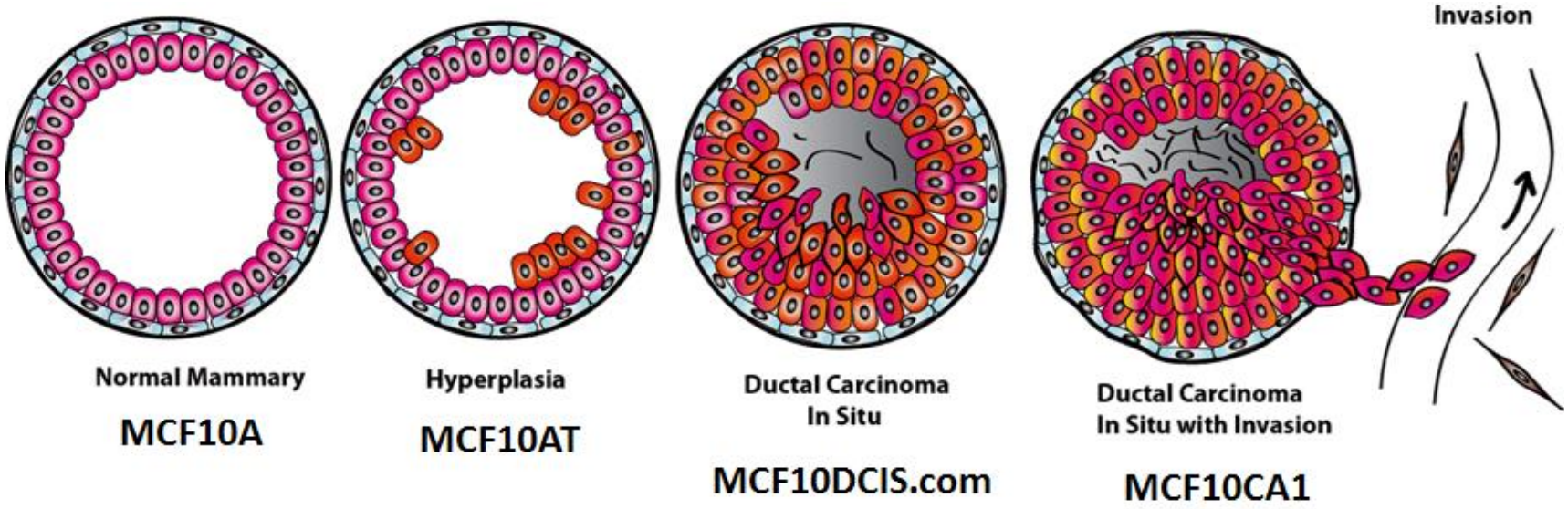
Invasion
Normal Mammary
MCF10A
Hyperplasia
MCF10AT
Ductal Carcinoma
In Situ
MCF10DCIS.com
Ductal Carcinoma
In Situ with Invasion
MCF10CA1

Amidine was generated based on a PADI substrate, benzoyl arginine amide (53). BB-Cl-Amidine was synthesized from Cl-Amidine but with modifications to the C-terminus and N-terminus. The C-terminus is replaced with benzimidazole and N-terminus is replaced by biphenyl moiety (54). This results in better cellular uptake and potency **(Figure 1.5)**. To test the effect of this new PADI inhibitor, in **Chapter 4**, I investigated the effect of BB-Cl-Amidine in MCF10DCIS.com cells.

Breast Cancer Subtypes

Breast tumors are heterogeneous in their nature with diverse responses to treatments. With major advances in genomics-based technologies, we are more able to accurately identify breast cancer subtypes. Perou et al. performed cDNA microarrays and hierarchical clustering on human breast tumors and found 496 genes, that differed between tumors (55). Furthermore, in their subsequent study, they defined to four subtypes, Luminal A, Luminal B, ERBB-positive (HER2+), and basal-like (56).

Breast cancer subtypes are defined by the estrogen receptor (ER), progesterone receptor (PR), and human epidermal growth factor receptor 2 (HER2). Luminal A subtype is ER+ (and/or PR+) and HER2-; Luminal B subtype is ER+ (and/or PR+) and HER2-; basal like subtype, also called triple negative, is ER- (and PR-) and HER2-; and ERBB-positive subtype is ER- (and PR-) and HER2+ **(Table 1.2)** (57-59).

We recently reported that PADI2 expression is correlated with HER2 expression and is involved in *in vitro* and *in vivo* proliferation of mammary tumors (51). However, the functional relationship of PADI2 and HER2 is unknown. Thus, in **Chapter 5**, we investigated the role of PADI2 in HER2-positive breast cancer.

Figure 1.5: Chemical structure of first generation (Cl-Amidine) and second generation (BB-Cl-Amidine) PADI inhibitors. Cl-amidine was generated based on the structure of a small molecule PADI substrate (benzoyl arginine amide). BB-Cl-amidine was synthesized basing on Cl-amidine as a structural backbone where the C-terminus is relaced with benzimidazole and N-terminus is replaced by biphenyl moiety for better cellular uptake and potency. (Figure adapted from Knight, J.S., *et al.* (2015) *Ann Rheum Dis* **74**, 2199-2206) (54).

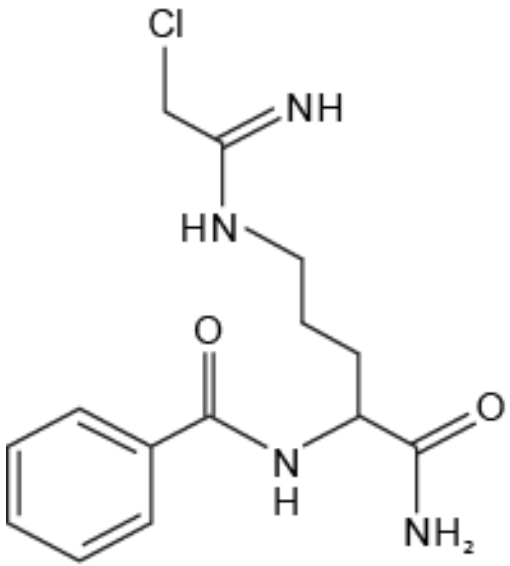

Cl-Amidine
(1st Generation)

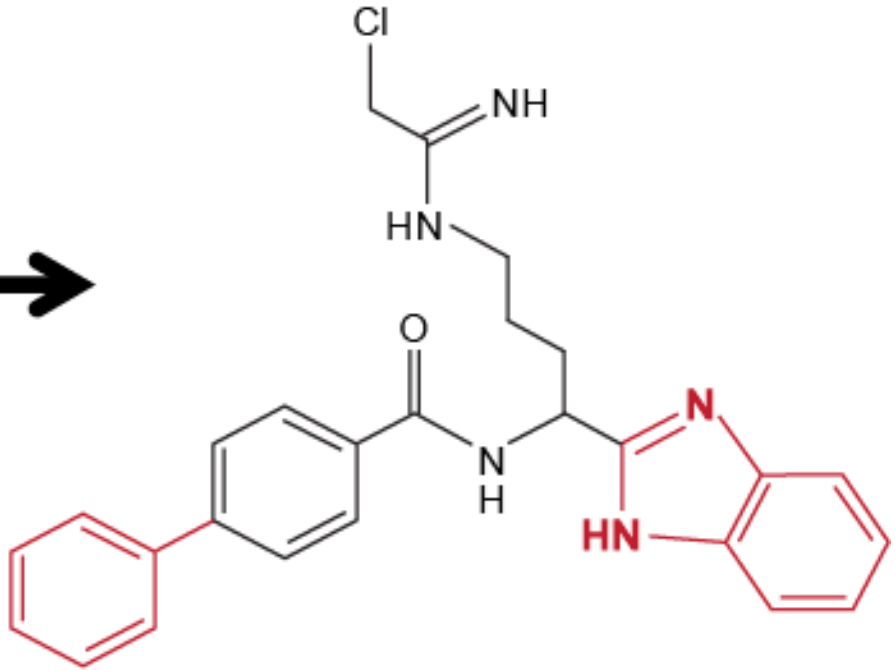

BB-Cl-Amidine
(2nd Generation)

Table 1.2: Prevalence of breast cancer subtypes. (Adapted from Susan G. Komen and (57-59)).

Subtypes	ER/PR/HER2 status	Prevalence
Luminal A	ER+ (and/or PR+) and HER2-	30-70%
Luminal B	ER+ (and/or PR+) and HER2+	10-20%
Basal-like (Triple Negative)	ER- (and PR-) and HER2-	15-20%
HER2-positive	ER- (and PR-) and HER2+	5-15%

PADI2 and ER

As mentioned earlier, we found that PADI2 can target histone H3R26 for citrullination and promote ER target gene activity (36). Specifically, Zhang et al. found that after estrogen stimulation, PADI2-mediated citrullination of H3R26 results in an open chromatin state at the estrogen response element (ERE) of target gene promoters (36). Furthermore, Zhang et al. found that both depletion of PADI2 via shRNA or inhibition of PADI2 activity by Cl-Amidine treatment suppresses transcriptional activity of canonical ER target genes (36). These results suggest that PADI2 mediated histone citrullination at H3R26 is critical for estrogen mediated ER target gene activation.

Guertin et al. investigated estrogen induced histone citrullination at high spatial and temporal resolution (60). They found that ER binding and histone H3R26 citrullination are highly correlated after estrogen treatment (60). To test the effect of PADI2-mediated citrullination in ER binding, they performed chromatin immunoprecipitation (ChIP) – qPCR on PADI2 depleted MCF-7 breast cancer cells and found that PADI2 depletion inhibits citrullination of H3R26 and ER binding (60). Furthermore, their MNase ChIP-seq experiment showed that citrullination of histone H3 arginine residue 26 changes nucleosome structure to a structurally poised state for efficient ER binding (60). Together, these data show that PADI2 acts as a co-factor and is required for efficient ER target gene activation.

Endocrine Therapy

Approximately, 70% of breast cancer patients have ER+ tumors. Thus, selective estrogen-receptor modulators (SERMs), particularly tamoxifen (ER antagonist), are widely used as a treatment (61). Tamoxifen therapy works by preventing the activity of ER by blocking

estrogen-mediated target gene activation. For example, in the absence of tamoxifen, estrogen binds to ER and that complex binds to estrogen response DNA elements (ERE), causing transcriptional activation or repression of target genes. However, in the presence of tamoxifen, tamoxifen outcompetes estrogen for ER binding, preventing transcriptional activity of ER (62,63) **(Figure 1.6)**. Despite promising initial responses to tamoxifen therapy, it is suggested that 40 to 50% of patients undergoing tamoxifen therapy will eventually develop tamoxifen-resistant breast cancer (64,65). Thus, there is a need to elucidate the mechanism of tamoxifen resistance for better treatment outcomes.

Tamoxifen Resistance via ER-HER2 Crosstalk

Recent studies suggest that cross-phosphorylation and activation of epidermal growth factor receptor (EGFR/HER2) pathway as a mechanism of tamoxifen resistance. The studies lead by the laboratory of Dr. Schiff found that ER+ MCF-7 breast cancer cells, when overexpressed with HER2, promote tamoxifen-stimulated tumor growth (66). They found that in the absence of HER2, tamoxifen treatment results in recruitment of co-repressors such as nuclear receptor co-repressor (NCoR) and histone deacetylase 3 (HDAC3) to suppress ER target gene activation. However, in the presence of HER2, tamoxifen treatment results in recruitment of co-activators such as ER, nuclear receptor co-activator (NCoA or AIB1), CREB binding protein (CBP), and p300, and promotes ER target gene activation (67). These suggest a potential escape pathway developed by cancer cells against endocrine therapy.

As mentioned earlier, our laboratory identified PADI2 as an ER co-factor. In addition, as discussed in **Chapter 5**, we found that PADI2 regulates HER2 expression via binding to the

Figure 1.6: Schematic diagram of the effect of estrogen and tamoxifen on ER target gene transcription. (A) Estrogen activates ER and recruits co-activator complex and binds to the ERE. This results in transcriptional activation of ER target genes. **(B)** However, in the presence of tamoxifen, tamoxifen binds to ER competitively with estrogen. This results in recruitment of co-repressors and promotes suppression of ER target genes.

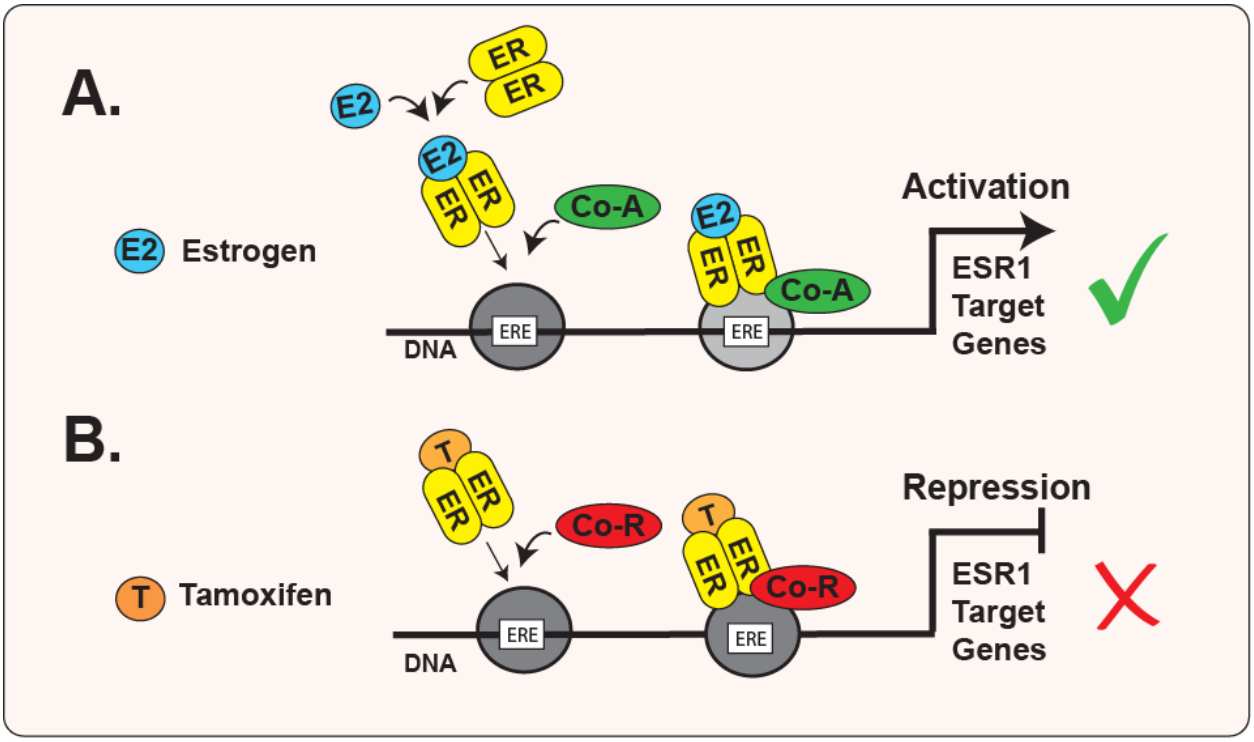
A.
E2
ER
ER
E2
ER
ER
Co-A
E2
ER
ER
Co-A
Activation
E2 Estrogen
ESR1
Target
Genes
DNA
ERE
ERE
B.
T
ER
ER
Co-R
T
ER
ER
Co-R
Repression
T Tamoxifen
ESR1
Target
Genes
DNA
ERE
ERE
E2 Estrogen
Co-A
Co-Activator
Complex
ER
ER
Estrogen
Receptor
T Tamoxifen
Co-R
Co-Repressor
Complex
ERE
Estrogen
Response
Element

promoter of HER2 and potentially promoting target gene transcription. Since PADI2 is involved in both ER and HER2 signaling pathways, I explored the role of PADI2 in tamoxifen resistance.

A Genome-Wide Approach to Study Tamoxifen Resistance

Although many advances have been made in understanding endocrine resistance, it is still one of the major dilemmas in the field. The most widely used breast cancer cell line to study ER+ tumors is MCF-7 cells. Recently, it has been shown that the MCF-7 cell line contains pools of subclones that are either tamoxifen sensitive or resistant de novo (68). Gonzalez-Malerva et al. took advantage of this clonal variation and isolated tamoxifen sensitive ($B7^{TamS}$ and $C11^{TamS}$) and resistant ($H9^{TamR}$ and $G11^{TamR}$) MCF-7 subclones (68). We obtained these cell lines to test whether PADI2 may also play a role in tamoxifen resistance.

In **Chapter 6**, I conducted Precision global Run-On and Sequencing (PRO-seq) assay on TamS and TamR cells to comprehensively and precisely map genomic regions with RNA polymerase II (Pol II) transcriptional activity **(Figure 1.7)** (69). This enabled me to map the location and activities of all genes. I particularly paid close attention to the area in the genome with divergent transcription, a phenomenon when there are transcription initiations in opposing directions on positive (+) and negative (-) DNA strands because these are the regions where I can find active promoters and enhancers (70,71). We used the discriminative regulatory element detection from GRO-seq/PRO-seq (dREG) program to identify the regulatory elements, (RE) such as promoters and enhancers, to understand the molecular differences between the two TamS and TamR lines (72). From this assay, I further investigated where PADI2 fits within the mechanism of tamoxifen resistance.

Figure 1.7: Schematic diagram of PRO-seq experiment. First, 5 x 10^6 tamoxifen sensitive ($B7^{TamS}$ or $C11^{TamS}$) or resistant ($H9^{TamR}$ and $G11^{TamR}$) cells are cultured. Next, nuclear isolation is performed on these cells. Once the nuclei are isolated, the following experimental steps are performed: (1) removal of impediments using Sarkosyl, (2) nuclear Run-On reactions using biotin-labeled ribonucleotide triphosphate analogs (biotin-NTP), (3) base hydrolysis, (4) bead binding and enrichment, (5) 3' adaptor ligation, (6) 2^{nd} bead binding and enrichment, (7) 5' de-capping with the use of RppH probe, (8) 5' adaptor ligation, (9) 3^{rd} bead binding and enrichment, (10) reverse transcription, (11) amplification using an index or barcode sequence, (12) purification using SDS-PAGE, and lastly, (13) next-generation sequencing on an Illumina NextSeq 500 platform (Figure adapted from manuscript in preparation from Chapter 6 and (69)).

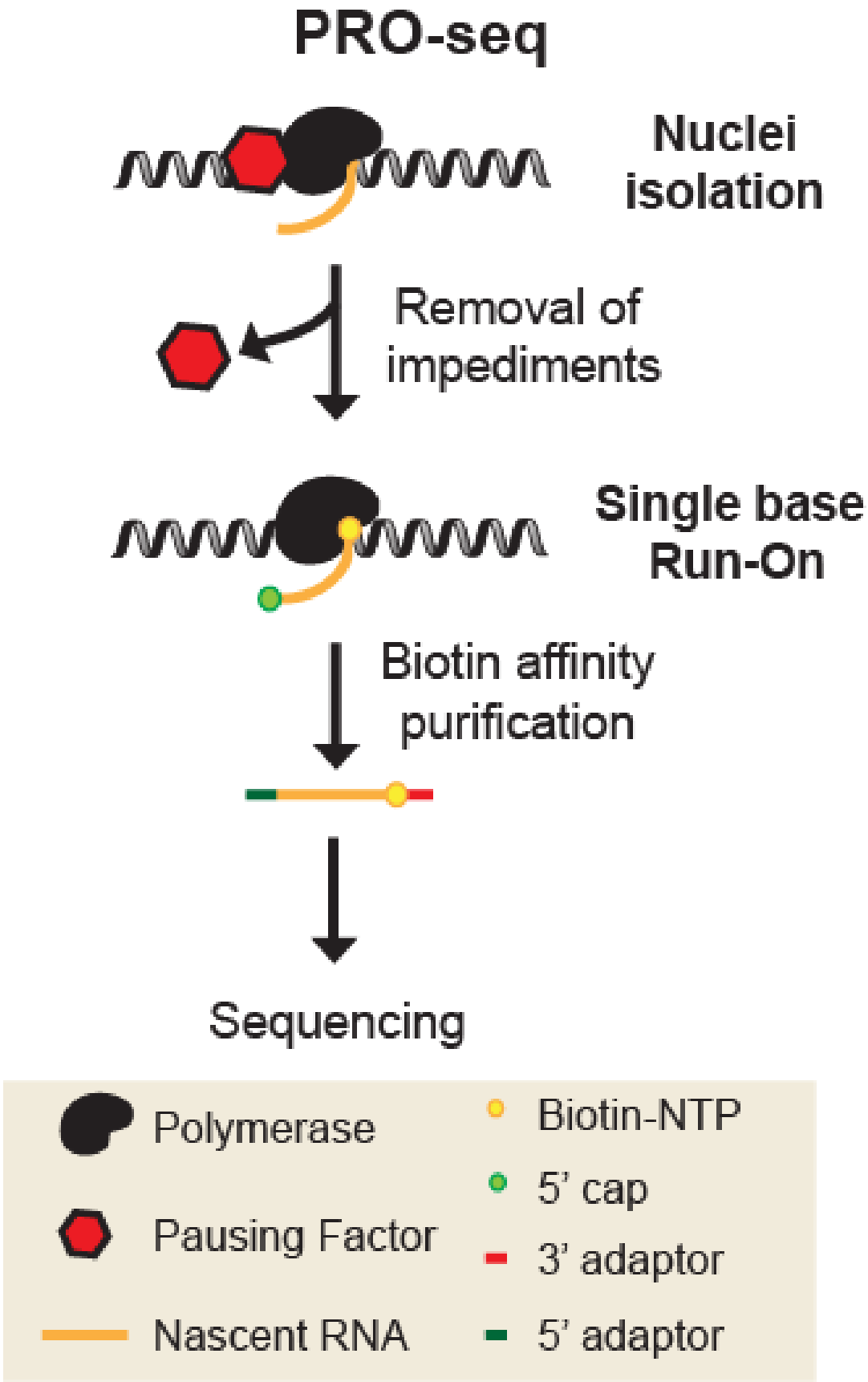
PRO-seq
Nuclei isolation
Removal of impediments
Single base Run-On
Biotin affinity purification
Sequencing
Polymerase
Pausing Factor
Nascent RNA
Biotin-NTP
5' cap
3' adaptor
5' adaptor

In my concluding chapter, **Chapter 6**, I provided summaries of my main findings in each chapter and provided future directions for PADI2 studies. In addition, I provided data on my ongoing genome-wide study investigating the role of PADI2 in development of tamoxifen resistance.

Overview:

Although PADI2 is often an upregulated gene in breast cancers, no previous study to our knowledge, has investigated in detail the mechanistic role of PADI2 in breast cancer progression. In my thesis, I discuss my discoveries on the role of PADI2 in breast cancer progression.

REFERENCES

1. Horibata, S., Coonrod, S. A., and Cherrington, B. D. (2012) Role for peptidylarginine deiminase enzymes in disease and female reproduction. *J Reprod Dev* **58**, 274-282

2. Mohanan, S., Cherrington, B. D., Horibata, S., McElwee, J. L., Thompson, P. R., and Coonrod, S. A. (2012) Potential role of peptidylarginine deiminase enzymes and protein citrullination in cancer pathogenesis. *Biochem Res Int* **2012**, 895343

3. Vossenaar, E. R., Zendman, A. J., van Venrooij, W. J., and Pruijn, G. J. (2003) PAD, a growing family of citrullinating enzymes: genes, features and involvement in disease. *Bioessays* **25**, 1106-1118

4. Watanabe, K., and Senshu, T. (1989) Isolation and characterization of cDNA clones encoding rat skeletal muscle peptidylarginine deiminase. *J Biol Chem* **264**, 15255-15260

5. Tarcsa, E., Marekov, L. N., Mei, G., Melino, G., Lee, S. C., and Steinert, P. M. (1996) Protein unfolding by peptidylarginine deiminase. Substrate specificity and structural relationships of the natural substrates trichohyalin and filaggrin. *J Biol Chem* **271**, 30709-30716

6. Chang, X., and Han, J. (2006) Expression of peptidylarginine deiminase type 4 (PAD4) in various tumors. *Mol Carcinog* **45**, 183-196

7. Ishigami, A., Ohsawa, T., Hiratsuka, M., Taguchi, H., Kobayashi, S., Saito, Y., Murayama, S., Asaga, H., Toda, T., Kimura, N., and Maruyama, N. (2005) Abnormal accumulation of citrullinated proteins catalyzed by peptidylarginine deiminase in hippocampal extracts from patients with Alzheimer's disease. *J Neurosci Res* **80**, 120-128

8. Mastronardi, F. G., Mak, B., Ackerley, C. A., Roots, B. I., and Moscarello, M. A. (1996) Modifications of myelin basic protein in DM20 transgenic mice are similar to those in myelin basic protein from multiple sclerosis. *J Clin Invest* **97**, 349-358

9. Suzuki, A., Yamada, R., Chang, X., Tokuhiro, S., Sawada, T., Suzuki, M., Nagasaki, M., Nakayama-Hamada, M., Kawaida, R., Ono, M., Ohtsuki, M., Furukawa, H., Yoshino, S., Yukioka, M., Tohma, S., Matsubara, T., Wakitani, S., Teshima, R., Nishioka, Y., Sekine, A., Iida, A., Takahashi, A., Tsunoda, T., Nakamura, Y., and Yamamoto, K. (2003) Functional haplotypes of PADI4, encoding citrullinating enzyme peptidylarginine deiminase 4, are associated with rheumatoid arthritis. *Nat Genet* **34**, 395-402

10. Guerrin, M., Ishigami, A., Mechin, M. C., Nachat, R., Valmary, S., Sebbag, M., Simon, M., Senshu, T., and Serre, G. (2003) cDNA cloning, gene organization and expression analysis of human peptidylarginine deiminase type I. *Biochem J* **370**, 167-174

11. Senshu, T., Kan, S., Ogawa, H., Manabe, M., and Asaga, H. (1996) Preferential deimination of keratin K1 and filaggrin during the terminal differentiation of human epidermis. *Biochem Biophys Res Commun* **225**, 712-719

12. Terakawa, H., Takahara, H., and Sugawara, K. (1991) Three types of mouse peptidylarginine deiminase: characterization and tissue distribution. *J Biochem* **110**, 661-666

13. Kubilus, J., Waitkus, R. F., and Baden, H. P. (1980) Partial purification and specificity of an arginine-converting enzyme from bovine epidermis. *Biochim Biophys Acta* **615**, 246-251

14. Tsuchida, M., Takahara, H., Minami, N., Arai, T., Kobayashi, Y., Tsujimoto, H., Fukazawa, C., and Sugawara, K. (1993) cDNA nucleotide sequence and primary structure of mouse uterine peptidylarginine deiminase. Detection of a 3'-untranslated nucleotide sequence common to the mRNA of transiently expressed genes and rapid turnover of this enzyme's mRNA in the estrous cycle. *Eur J Biochem* **215**, 677-685

15. Ishigami, A., Ohsawa, T., Asaga, H., Akiyama, K., Kuramoto, M., and Maruyama, N. (2002) Human peptidylarginine deiminase type II: molecular cloning, gene organization, and expression in human skin. *Arch Biochem Biophys* **407**, 25-31

16. Watanabe, K., Akiyama, K., Hikichi, K., Ohtsuka, R., Okuyama, A., and Senshu, T. (1988) Combined biochemical and immunochemical comparison of peptidylarginine deiminases present in various tissues. *Biochim Biophys Acta* **966**, 375-383

17. Nagata, S., Yamagiwa, M., Inoue, K., and Senshu, T. (1990) Estrogen regulates peptidylarginine deiminase levels in a rat pituitary cell line in culture. *J Cell Physiol* **145**, 333-339

18. Senshu, T., Akiyama, K., Nagata, S., Watanabe, K., and Hikichi, K. (1989) Peptidylarginine deiminase in rat pituitary: sex difference, estrous cycle-related changes, and estrogen dependence. *Endocrinology* **124**, 2666-2670

19. Urano, Y., Watanabe, K., Sakaki, A., Arase, S., Watanabe, Y., Shigemi, F., Takeda, K., Akiyama, K., and Senshu, T. (1990) Immunohistochemical demonstration of peptidylarginine deiminase in human sweat glands. *Am J Dermatopathol* **12**, 249-255

20. Akiyama, K., Inoue, K., and Senshu, T. (1989) Immunocytochemical study of peptidylarginine deiminase: localization of its immunoreactivity in prolactin cells of female rat pituitaries. *Endocrinology* **125**, 1121-1127

21. Kanno, T., Kawada, A., Yamanouchi, J., Yosida-Noro, C., Yoshiki, A., Shiraiwa, M., Kusakabe, M., Manabe, M., Tezuka, T., and Takahara, H. (2000) Human peptidylarginine deiminase type III: molecular cloning and nucleotide sequence of the

cDNA, properties of the recombinant enzyme, and immunohistochemical localization in human skin. *J Invest Dermatol* **115**, 813-823

22. Nishijyo, T., Kawada, A., Kanno, T., Shiraiwa, M., and Takahara, H. (1997) Isolation and molecular cloning of epidermal- and hair follicle-specific peptidylarginine deiminase (type III) from rat. *J Biochem* **121**, 868-875

23. Asaga, H., Nakashima, K., Senshu, T., Ishigami, A., and Yamada, M. (2001) Immunocytochemical localization of peptidylarginine deiminase in human eosinophils and neutrophils. *J Leukoc Biol* **70**, 46-51

24. Nakashima, K., Hagiwara, T., Ishigami, A., Nagata, S., Asaga, H., Kuramoto, M., Senshu, T., and Yamada, M. (1999) Molecular characterization of peptidylarginine deiminase in HL-60 cells induced by retinoic acid and 1alpha,25-dihydroxyvitamin D(3). *J Biol Chem* **274**, 27786-27792

25. Nakashima, K., Hagiwara, T., and Yamada, M. (2002) Nuclear localization of peptidylarginine deiminase V and histone deimination in granulocytes. *J Biol Chem* **277**, 49562-49568

26. Vossenaar, E. R., Nijenhuis, S., Helsen, M. M., van der Heijden, A., Senshu, T., van den Berg, W. B., van Venrooij, W. J., and Joosten, L. A. (2003) Citrullination of synovial proteins in murine models of rheumatoid arthritis. *Arthritis Rheum* **48**, 2489-2500

27. Chavanas, S., Mechin, M. C., Takahara, H., Kawada, A., Nachat, R., Serre, G., and Simon, M. (2004) Comparative analysis of the mouse and human peptidylarginine deiminase gene clusters reveals highly conserved non-coding segments and a new human gene, PADI6. *Gene* **330**, 19-27

28. Zhang, J., Dai, J., Zhao, E., Lin, Y., Zeng, L., Chen, J., Zheng, H., Wang, Y., Li, X., Ying, K., Xie, Y., and Mao, Y. (2004) cDNA cloning, gene organization and expression analysis of human peptidylarginine deiminase type VI. *Acta Biochim Pol* **51**, 1051-1058

29. Esposito, G., Vitale, A. M., Leijten, F. P., Strik, A. M., Koonen-Reemst, A. M., Yurttas, P., Robben, T. J., Coonrod, S., and Gossen, J. A. (2007) Peptidylarginine deiminase (PAD) 6 is essential for oocyte cytoskeletal sheet formation and female fertility. *Mol Cell Endocrinol* **273**, 25-31

30. Yurttas, P., Vitale, A. M., Fitzhenry, R. J., Cohen-Gould, L., Wu, W., Gossen, J. A., and Coonrod, S. A. (2008) Role for PADI6 and the cytoplasmic lattices in ribosomal storage in oocytes and translational control in the early mouse embryo. *Development* **135**, 2627-2636

31. Kan, R., Yurttas, P., Kim, B., Jin, M., Wo, L., Lee, B., Gosden, R., and Coonrod, S. A. (2011) Regulation of mouse oocyte microtubule and organelle dynamics by PADI6 and the cytoplasmic lattices. *Dev Biol* **350**, 311-322

32. Cherrington, B. D., Zhang, X., McElwee, J. L., Morency, E., Anguish, L. J., and Coonrod, S. A. (2012) Potential role for PAD2 in gene regulation in breast cancer cells. *PLoS One* **7**, e41242

33. Wang, Y., Li, M., Stadler, S., Correll, S., Li, P., Wang, D., Hayama, R., Leonelli, L., Han, H., Grigoryev, S. A., Allis, C. D., and Coonrod, S. A. (2009) Histone hypercitrullination mediates chromatin decondensation and neutrophil extracellular trap formation. *J Cell Biol* **184**, 205-213

34. Tanikawa, C., Espinosa, M., Suzuki, A., Masuda, K., Yamamoto, K., Tsuchiya, E., Ueda, K., Daigo, Y., Nakamura, Y., and Matsuda, K. (2012) Regulation of histone modification and chromatin structure by the p53-PADI4 pathway. *Nat Commun* **3**, 676

35. Cherrington, B. D., Morency, E., Struble, A. M., Coonrod, S. A., and Wakshlag, J. J. (2010) Potential role for peptidylarginine deiminase 2 (PAD2) in citrullination of canine mammary epithelial cell histones. *PLoS One* **5**, e11768

36. Zhang, X., Bolt, M., Guertin, M. J., Chen, W., Zhang, S., Cherrington, B. D., Slade, D. J., Dreyton, C. J., Subramanian, V., Bicker, K. L., Thompson, P. R., Mancini, M. A., Lis, J. T., and Coonrod, S. A. (2012) Peptidylarginine deiminase 2-catalyzed histone H3 arginine 26 citrullination facilitates estrogen receptor alpha target gene activation. *Proc Natl Acad Sci U S A* **109**, 13331-13336

37. Chang, X., Yamada, R., Suzuki, A., Sawada, T., Yoshino, S., Tokuhiro, S., and Yamamoto, K. (2005) Localization of peptidylarginine deiminase 4 (PADI4) and citrullinated protein in synovial tissue of rheumatoid arthritis. *Rheumatology (Oxford)* **44**, 40-50

38. Chang, X., Zhao, Y., Sun, S., Zhang, Y., and Zhu, Y. (2009) The expression of PADI4 in synovium of rheumatoid arthritis. *Rheumatol Int* **29**, 1411-1416

39. van Boekel, M. A., Vossenaar, E. R., van den Hoogen, F. H., and van Venrooij, W. J. (2002) Autoantibody systems in rheumatoid arthritis: specificity, sensitivity and diagnostic value. *Arthritis Res* **4**, 87-93

40. Reparon-Schuijt, C. C., van Esch, W. J., van Kooten, C., Schellekens, G. A., de Jong, B. A., van Venrooij, W. J., Breedveld, F. C., and Verweij, C. L. (2001) Secretion of anti-citrulline-containing peptide antibody by B lymphocytes in rheumatoid arthritis. *Arthritis Rheum* **44**, 41-47

41. Feldmann, M., Brennan, F. M., and Maini, R. N. (1996) Rheumatoid arthritis. *Cell* **85**, 307-310

42. Chang, X., Han, J., Pang, L., Zhao, Y., Yang, Y., and Shen, Z. (2009) Increased PADI4 expression in blood and tissues of patients with malignant tumors. *BMC Cancer* **9**, 40

43. Bertucci, F., Borie, N., Ginestier, C., Groulet, A., Charafe-Jauffret, E., Adelaide, J., Geneix, J., Bachelart, L., Finetti, P., Koki, A., Hermitte, F., Hassoun, J., Debono, S., Viens, P., Fert, V., Jacquemier, J., and Birnbaum, D. (2004) Identification and validation of an ERBB2 gene expression signature in breast cancers. *Oncogene* **23**, 2564-2575

44. Mackay, A., Tamber, N., Fenwick, K., Iravani, M., Grigoriadis, A., Dexter, T., Lord, C. J., Reis-Filho, J. S., and Ashworth, A. (2009) A high-resolution integrated analysis of genetic and expression profiles of breast cancer cell lines. *Breast Cancer Res Treat* **118**, 481-498

45. Miller, F. R., Soule, H. D., Tait, L., Pauley, R. J., Wolman, S. R., Dawson, P. J., and Heppner, G. H. (1993) Xenograft model of progressive human proliferative breast disease. *J Natl Cancer Inst* **85**, 1725-1732

46. Miller, F. R. (1996) Models of progression spanning preneoplasia and metastasis: the human MCF10AneoT.TGn series and a panel of mouse mammary tumor subpopulations. *Cancer Treat Res* **83**, 243-263

47. Santner, S. J., Dawson, P. J., Tait, L., Soule, H. D., Eliason, J., Mohamed, A. N., Wolman, S. R., Heppner, G. H., and Miller, F. R. (2001) Malignant MCF10CA1 cell lines derived from premalignant human breast epithelial MCF10AT cells. *Breast Cancer Res Treat* **65**, 101-110

48. Miller, F. R., Santner, S. J., Tait, L., and Dawson, P. J. (2000) MCF10DCIS.com xenograft model of human comedo ductal carcinoma in situ. *J Natl Cancer Inst* **92**, 1185-1186

49. Soule, H. D., Maloney, T. M., Wolman, S. R., Peterson, W. D., Jr., Brenz, R., McGrath, C. M., Russo, J., Pauley, R. J., Jones, R. F., and Brooks, S. C. (1990) Isolation and characterization of a spontaneously immortalized human breast epithelial cell line, MCF-10. *Cancer Res* **50**, 6075-6086

50. Dawson, P. J., Wolman, S. R., Tait, L., Heppner, G. H., and Miller, F. R. (1996) MCF10AT: a model for the evolution of cancer from proliferative breast disease. *Am J Pathol* **148**, 313-319

51. McElwee, J. L., Mohanan, S., Griffith, O. L., Breuer, H. C., Anguish, L. J., Cherrington, B. D., Palmer, A. M., Howe, L. R., Subramanian, V., Causey, C. P., Thompson, P. R., Gray, J. W., and Coonrod, S. A. (2012) Identification of PADI2 as a potential breast cancer biomarker and therapeutic target. *BMC Cancer* **12**, 500

52. Knuckley, B., Causey, C. P., Pellechia, P. J., Cook, P. F., and Thompson, P. R. (2010) Haloacetamidine-based inactivators of protein arginine deiminase 4 (PAD4): evidence that general acid catalysis promotes efficient inactivation. *Chembiochem* **11**, 161-165

53. Luo, Y., Arita, K., Bhatia, M., Knuckley, B., Lee, Y. H., Stallcup, M. R., Sato, M., and Thompson, P. R. (2006) Inhibitors and inactivators of protein arginine deiminase 4: functional and structural characterization. *Biochemistry* **45**, 11727-11736

54. Knight, J. S., Subramanian, V., O'Dell, A. A., Yalavarthi, S., Zhao, W., Smith, C. K., Hodgin, J. B., Thompson, P. R., and Kaplan, M. J. (2015) Peptidylarginine deiminase inhibition disrupts NET formation and protects against kidney, skin and vascular disease in lupus-prone MRL/lpr mice. *Ann Rheum Dis* **74**, 2199-2206

55. Perou, C. M., Sorlie, T., Eisen, M. B., van de Rijn, M., Jeffrey, S. S., Rees, C. A., Pollack, J. R., Ross, D. T., Johnsen, H., Akslen, L. A., Fluge, O., Pergamenschikov, A., Williams, C., Zhu, S. X., Lonning, P. E., Borresen-Dale, A. L., Brown, P. O., and Botstein, D. (2000) Molecular portraits of human breast tumours. *Nature* **406**, 747-752

56. Sorlie, T., Perou, C. M., Tibshirani, R., Aas, T., Geisler, S., Johnsen, H., Hastie, T., Eisen, M. B., van de Rijn, M., Jeffrey, S. S., Thorsen, T., Quist, H., Matese, J. C., Brown, P. O., Botstein, D., Lonning, P. E., and Borresen-Dale, A. L. (2001) Gene expression patterns of breast carcinomas distinguish tumor subclasses with clinical implications. *Proc Natl Acad Sci U S A* **98**, 10869-10874

57. Fan, C., Oh, D. S., Wessels, L., Weigelt, B., Nuyten, D. S., Nobel, A. B., van't Veer, L. J., and Perou, C. M. (2006) Concordance among gene-expression-based predictors for breast cancer. *N Engl J Med* **355**, 560-569

58. Voduc, K. D., Cheang, M. C., Tyldesley, S., Gelmon, K., Nielsen, T. O., and Kennecke, H. (2010) Breast cancer subtypes and the risk of local and regional relapse. *J Clin Oncol* **28**, 1684-1691

59. Howlader, N., Altekruse, S. F., Li, C. I., Chen, V. W., Clarke, C. A., Ries, L. A., and Cronin, K. A. (2014) US incidence of breast cancer subtypes defined by joint hormone receptor and HER2 status. *J Natl Cancer Inst* **106**

60. Guertin, M. J., Zhang, X., Anguish, L., Kim, S., Varticovski, L., Lis, J. T., Hager, G. L., and Coonrod, S. A. (2014) Targeted H3R26 deimination specifically facilitates estrogen receptor binding by modifying nucleosome structure. *PLoS Genet* **10**, e1004613

61. Robertson, J. F. (1996) Oestrogen receptor: a stable phenotype in breast cancer. *Br J Cancer* **73**, 5-12

62. Carroll, J. S., Meyer, C. A., Song, J., Li, W., Geistlinger, T. R., Eeckhoute, J., Brodsky, A. S., Keeton, E. K., Fertuck, K. C., Hall, G. F., Wang, Q., Bekiranov, S., Sementchenko, V., Fox, E. A., Silver, P. A., Gingeras, T. R., Liu, X. S., and Brown, M. (2006) Genome-wide analysis of estrogen receptor binding sites. *Nat Genet* **38**, 1289-1297

63. Hah, N., Danko, C. G., Core, L., Waterfall, J. J., Siepel, A., Lis, J. T., and Kraus, W. L. (2011) A rapid, extensive, and transient transcriptional response to estrogen signaling in breast cancer cells. *Cell* **145**, 622-634

64. Ma, C. X., Sanchez, C. G., and Ellis, M. J. (2009) Predicting endocrine therapy responsiveness in breast cancer. *Oncology (Williston Park)* **23**, 133-142

65. Ali, S., and Coombes, R. C. (2002) Endocrine-responsive breast cancer and strategies for combating resistance. *Nat Rev Cancer* **2**, 101-112

66. Massarweh, S., Osborne, C. K., Creighton, C. J., Qin, L., Tsimelzon, A., Huang, S., Weiss, H., Rimawi, M., and Schiff, R. (2008) Tamoxifen resistance in breast tumors is driven by growth factor receptor signaling with repression of classic estrogen receptor genomic function. *Cancer Res* **68**, 826-833

67. Shou, J., Massarweh, S., Osborne, C. K., Wakeling, A. E., Ali, S., Weiss, H., and Schiff, R. (2004) Mechanisms of tamoxifen resistance: increased estrogen receptor-HER2/neu cross-talk in ER/HER2-positive breast cancer. *J Natl Cancer Inst* **96**, 926-935

68. Gonzalez-Malerva, L., Park, J., Zou, L., Hu, Y., Moradpour, Z., Pearlberg, J., Sawyer, J., Stevens, H., Harlow, E., and LaBaer, J. (2011) High-throughput ectopic expression screen for tamoxifen resistance identifies an atypical kinase that blocks autophagy. *Proc Natl Acad Sci U S A* **108**, 2058-2063

69. Kwak, H., Fuda, N. J., Core, L. J., and Lis, J. T. (2013) Precise maps of RNA polymerase reveal how promoters direct initiation and pausing. *Science* **339**, 950-953

70. Kapranov, P., Willingham, A. T., and Gingeras, T. R. (2007) Genome-wide transcription and the implications for genomic organization. *Nat Rev Genet* **8**, 413-423

71. Core, L. J., Waterfall, J. J., and Lis, J. T. (2008) Nascent RNA sequencing reveals widespread pausing and divergent initiation at human promoters. *Science* **322**, 1845-1848

72. Danko, C. G., Hyland, S. L., Core, L. J., Martins, A. L., Waters, C. T., Lee, H. W., Cheung, V. G., Kraus, W. L., Lis, J. T., and Siepel, A. (2015) Identification of active transcriptional regulatory elements from GRO-seq data. *Nat Methods* **12**, 433-438

CHAPTER TWO

ROLE FOR PEPTIDYLARGININE DEIMINASE ENZYMES IN DISEASE AND FEMALE REPRODUCTION

* Published previously as Horibata, S., Coonrod, S. A., and Cherrington, B. D. (2012) Role for peptidylarginine deiminase enzymes in disease and female reproduction. *J Reprod Dev* **58**, 274-282

Contributions:

Manuscript preparation: Horibata, S.

Edits: Horibata, S., Coonrod, S.A., and Cherrington, B.D.

Revisions: Horibata, S.

Conception and Design: Horibata, S., Coonrod, S.A., and Cherrington, B.D.

Experiments: Cherrington, B.D.

Figures 2.1 to 2.3: Horibata, S.

Figures 2.4 to 2.7: Cherrington, B.D.

ABSTRACT

The peptidylarginine deiminases (PADs) are a family of calcium-dependent enzymes that post-translationally convert positively charged arginine residues to neutrally charged citrulline in a process called citrullination. There are five PAD family members (PAD1-4 and 6), each with unique tissue distribution patterns and functional roles including: cellular differentiation, nerve growth, apoptosis, inflammation, gene regulation, and early embryonic development. Previous review articles have focused on the expression and function of PADs and on their catalytic activity, citrullination, while other, more recent reviews have addressed the role of these enzymes in disease (1-3). What has not been previously reviewed in any level of detail is the role that PAD proteins play in female reproduction. Given that: (1) PAD family members are highly represented in female reproductive tissues, (2) that some of the earlier PAD literature suggests that PADs play a critical role in female reproduction, and (3) that our studies have demonstrated that oocyte and early embryo restricted PAD6 is essential for female reproduction, we felt that a more comprehensive review of this topic was warranted.

INTRODUCTION

The peptidylarginine deiminases (PADs, PADIs or protein-L-arginine iminohydrolase [EC 3.5.3.15]) are a family of calcium-dependent enzymes that post-translationally convert positively charged arginine residues on target proteins to neutrally charged citrulline (3). This activity is termed citrullination or deimination (Fig. 1) and the modification results in the disruption of ionic and hydrogen bonds within the substrate proteins causing wide-ranging effects on target protein structure, function, and protein-protein interactions (1,4) (Fig. 2). The PAD gene family consists of five members (PAD1-4 and PAD6) located within a highly organized gene cluster on human chromosome 1p36.13 and on the orthologous region of mouse chromosome 4 (3,5). PAD2 is believed to be the ancestral homologue, while the other PADs appear to have been derived from PAD2 via a series of gene duplications (3). Each PAD enzyme has a unique tissue distribution pattern and substrate preferences which likely confers biological specificity.

Expression and function of PAD family members in non-reproductive tissues

PAD1 is expressed from the basal to granular layer of the epidermis and a major function of this PAD in keratinocytes is to promote differentiation by citrullinating the intermediate filaments, keratin (including K1 and K10) and filaggrin (3,6). The loss of charge following citrullination is believed to lead to disassembly of the cytokeratin-filaggrin complex and proteolytic degradation, thereby generating an amino acid pool that is required for maintenance of stratum corneum's barrier function (7-9). Additionally, citrullination also reduces the flexibility of the keratin cytoskeleton due, in part, to cross-linking of keratin and filaggrin filaments, thus forming a rigid matrix that facilitates epidermal cornification (10-12).

Figure 2.1: Peptidylarginine deiminase (PAD) enzymes convert protein arginine residues to citrulline in a process called citrullination.

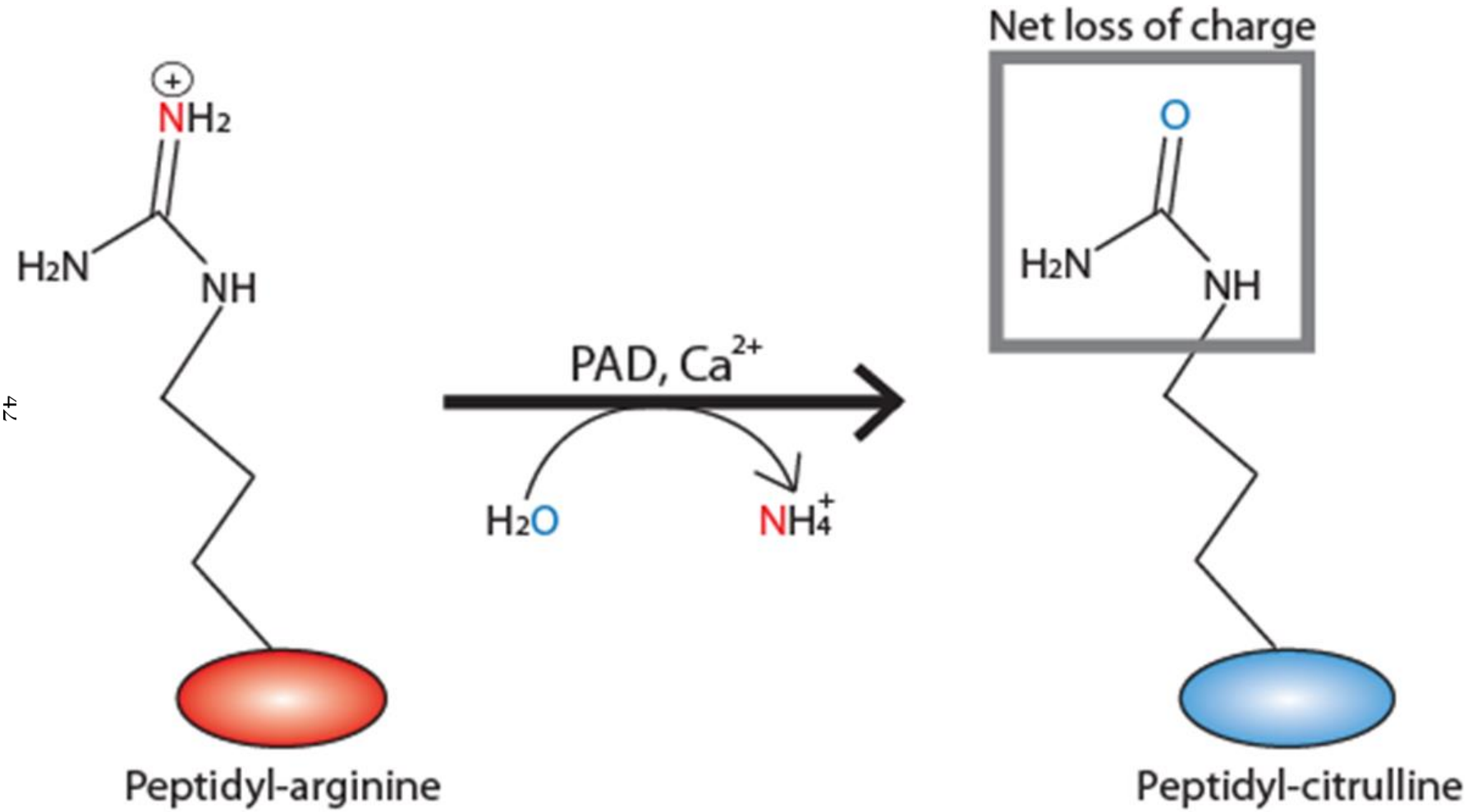
Net loss of charge
NH2
H2N
NH
O
PAD, Ca2+
H2O
NH4+
Peptidyl-arginine
Peptidyl-citrulline

Figure 2.2: The effects of PAD-catalyzed citrullination

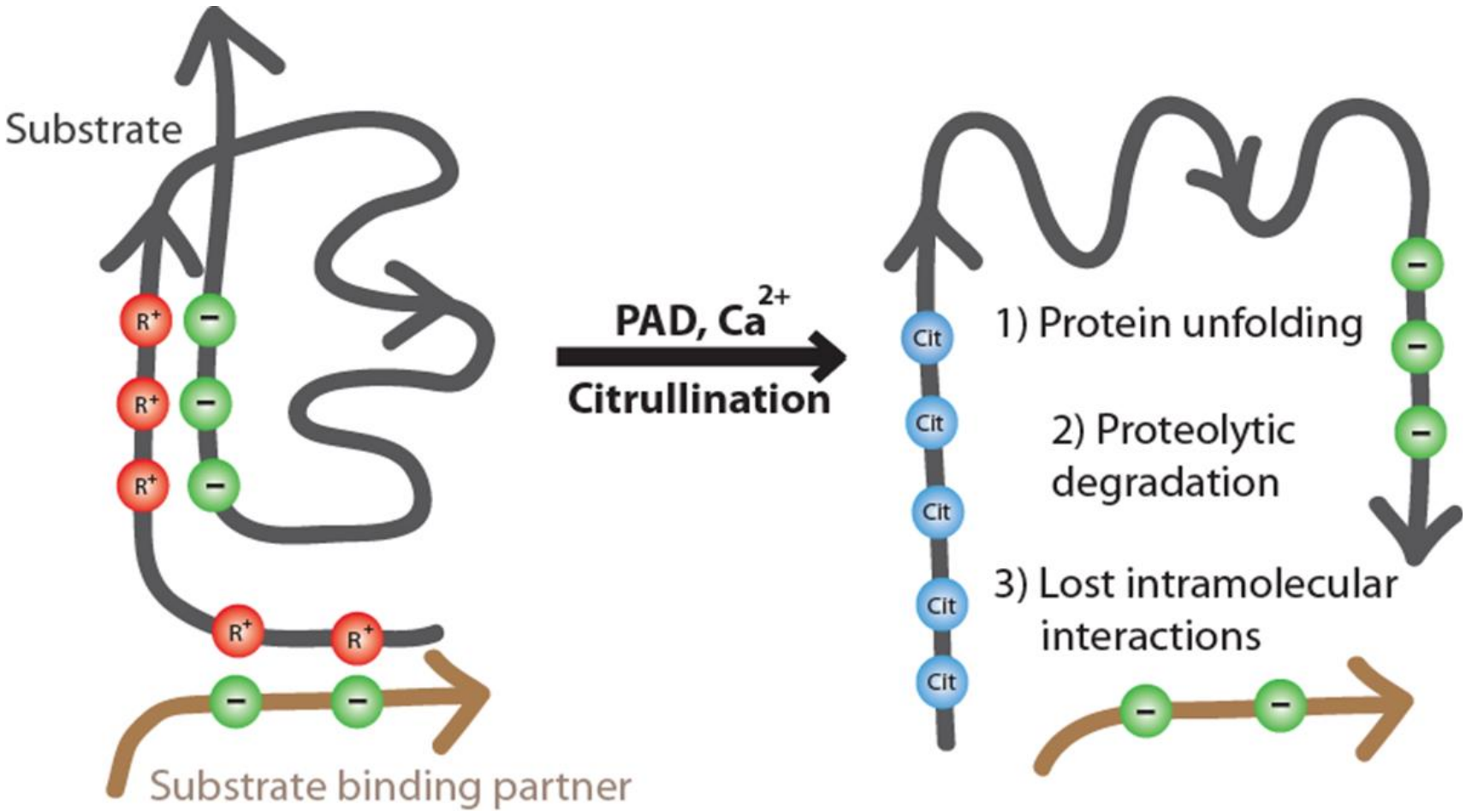
Substrate
R+
R+
R+
R+
R+
PAD, Ca2+
Citrullination
Cit
Cit
Cit
Cit
Cit
1) Protein unfolding
2) Proteolytic degradation
3) Lost intramolecular interactions
Substrate binding partner

PAD2 is the most widely expressed isoform and is present in a range of tissues including the brain, spinal cord, oligodendrocytes, skeletal muscle, pancreas, salivary gland, sweat gland, spleen, macrophage, bone marrow, and yolk sac (3,13,14). While citrullination appears to be sparse in normal nervous tissue, a major substrate for PAD2 during the onset of neurodegenerative disease is myelin basic protein (MBP), a constituent of the myelin sheath. PAD2 is highly expressed in skeletal muscle, yet a role for this PAD in muscle function has not been described and levels of citrullinated proteins in skeletal muscle tissue actually appear to be very low (15). In macrophages, PAD2 can citrullinate vimentin, a type 3 intermediate filament, resulting in filament network breakdown (16) and, eventually, apoptosis. Recently, PAD2 was linked to cytokine signaling during the immune response where it citrullinates IKKγ in macrophages, causing suppression of NF-kB activity (17). Additionally, PAD2 mediated citrullination of CXCL8 was also associated with suppression of the inflammatory response (18). Regarding PAD2's subcellular localization, PAD2 has been previously characterized as localizing to the cytoplasm. However, newer evidence suggests that, in mammary epithelium and neural tissue at least, PAD2 is also found in the nucleus (19,20). Our finding that PAD2 appears to target histones for citrullination suggests that, similar to PAD4, PAD2 may also play a role in gene regulation.

PAD3 expression seems to be limited to hair follicles and the epidermis (21). In follicles, PAD3 has been found to citrullinate the structural protein, trichohyalin, in the inner root sheath cells causing conformational changes during hair growth (22). It is believed that this activity results in a more soluble form of trichohyalin, thus facilitating trichohyalin's association with cytokeratins and cross-linking by transglutaminase to allow for directional hair growth (4,23,24). Along with filaggrin, PAD3 is also expressed in keratinocytes of the highly differentiated

epidermal granular layer where citrullination of filaggrin enhances its association with keratin to form a fibrous matrix that is required for cornification. Dysregulated citrullination of filaggrin by PAD3 in the epidermis is implicated with impaired epidermal homeostasis and loss of barrier function (25).

PAD4 is best characterized in cells of the hematopoietic lineage including monocytes, T cells, B cells, neutrophils, eosinophils, natural killer (NK) cells, and granulocytes (26,27). Newer reports, however, indicate that PAD4 is also expressed in mammary epithelial cells (28,29). PAD4 is the only family member which possesses a canonical nuclear localization signal, and, in the nucleus, PAD4 has been found to citrullinate a range of factors involved in transcriptional regulation including; histone proteins, transcription factors, and transcription co-factors (28-31). PAD4 was also recently found to regulate apoptosis and the cell cycle by regulating the expression of the p53 target genes p21, OKL38, CIP1 and WAF1; thus linking PAD4 activity with cancer (32,33). Additionally, PAD4 has also been found to mediate chromatin decondensation in HL-60 granulocytes and neutrophils via histone hypercitrullination (34).

PAD6 expression is limited to oocytes and early embryos and will be discussed in the Reproduction section below.

PADs and disease

Recently, dysregulation of PADs has been associated with multiple disease states including rheumatoid arthritis, multiple sclerosis, Alzheimer's disease, and, increasingly, cancer. A discussion of the links between PADs and disease follows.

Rheumatoid Arthritis (RA)

Among the PAD family members, PAD4 is perhaps the best characterized due to its close association with rheumatoid arthritis (RA). PAD4-mediated citrullination of fibrin and fibrinogen is frequently elevated in the synovial tissues of patients with RA (35,36) and autoantibodies generated against citrullinated proteins are present in sera from patients with RA (37). Additionally, antifilaggrin autoantibody (AFA) titer is closely correlated with RA severity and is, therefore, frequently used as serological markers to detect RA (38,39). Aside from AFAs, other known autoantibodies against citrullinated proteins include antiperinuclear factor (APF) and anti-keratin antibodies (AKA). Due to the strong correlation between PAD-mediated citrullination of synovial proteins and RA, understanding the causes and mechanisms of PAD catalyzed citrullination will likely provide insights into RA pathogenesis and also better define this clear target for therapeutic intervention.

Multiple Sclerosis (MS)

PAD2-catalyzed citrullination of myelin basic protein (MBP) is thought to play an important role in demyelination of central nervous system (CNS) neurons in MS patients (40). Under physiological conditions, MBP interacts with negatively charged phospholipids to stabilize the multilayered myelin. However, deregulation of PAD2 activity in the brain leads to increased MBP citrullination and the resulting loss of positive charge disrupts MBP-phospholipid interactions and increases myelin sheath instability (41-43). MBP hypercitrullination also induces a more open MBP configuration, leading to cathepsin D-mediated enzymatic degradation and increased T-cell sensitivity (44,45). Interestingly, other substrates may also be targeted for citrullination in MS. For example, TNF-α has been found to

promote nuclear translocation of PAD4 in brain tissue followed by PAD4-mediated histone H3 citrullination. This observation suggests that dysregulation of PAD4-mediated gene regulation may also play a role in the progression of MS (46).

Alzheimer's disease (AD)

Abnormal accumulation of citrullinated proteins such as vimentin and GFAP (glial fibrillary acidic protein) are found in the hippocampus of AD brains and these modified proteins show increased immunoreactivity compared to proteins from normal brain. Studies have also shown that citrullination of cerebral proteins by PAD2 occurs in regions undergoing neurodegeneration, suggesting that citrullination may promote the progression of neurodegenerative disease (47,48).

PADs and Inflammation

Given the strong associations with RA, MS, and Alzheimer's disease, PADs have previously been primarily linked to inflammatory autoimmune diseases. However, PAD-mediated citrullination is also elevated in a range of inflammatory states which lack a strong autoimmune component including myositis, tobacco induced pulmonary disease, and tonsillitis (15). Additionally, a very recent study found that PAD expression and activity were elevated in a mouse biopsy wound healing assay that models physiological inflammatory conditions (49). Lastly, we have found that PAD4-mediated histone hypercitrullination plays a critical role in chromatin release during neutrophil extracellular trap (NET) formation in granulocytes (34). NET formation occurs in response to inflammatory mediators and does not necessarily involve an autoimmune component. These observations suggest that PAD-mediated citrullination may

play a fundamental role in the inflammatory process and, thus, is likely to be involved in a wider range of physiological and pathological processes than previously envisioned. While the link between PADs and inflammation has recently developed in non-reproductive tissues, such an association has yet to be investigated in reproductive tissues.

RESULTS

A Role for PADs in Female Reproduction

As discussed below, some of the earliest PAD literature documented PAD expression and activity in female reproductive tissues. However, in more recent years, other than our work documenting the role of PAD6 in female fertility and on the role of PADs in gene regulation in mammary epithelial cells, the link between PADs and reproduction has not been further developed. To highlight the potential importance of PADs in female reproductive tissue, we examined PAD tissue distribution patterns in datasets utilizing modern transcriptomic techniques. For example, Massively Parallel Signature Sequencing (which can determine absolute gene expression profiles) was utilized to evaluate mRNA expression patterns across a broad range of mouse tissues (50). Analysis of this dataset found that expression levels of PADs 1, 2, 4, and 6 across more than 50 tissues was highest in female reproductive tissues such as the uterus, cervix, and vagina. Analysis of data from cDNA microarrays by Hewitt *et al*. further strengthens the association of PADs with reproduction by showing that estrogen induces the expression of PAD1, 2, and 4 in uterine tissue (51). In this study, ovariectomized mice were treated with estrogen and uterine samples harvested at 0.5, 2, 6, 12, and 24 hours post treatment. The microarray data shows that estrogen treatment increases uterine PAD1 and PAD2 expression by > 3 fold within 2 hours of treatment and this level of increase is achieved for PAD4 after 12

hours. Expression of PAD mRNA levels was also compared in the uteri of ovariectomized wild type, αERKO (ER α knockout mice), and KI/KO (ER binding mutant) mice after estrogen treatment (52). Both αERKO and KI/KO mice uteri show decreased levels of PAD1, 2 and 4 expression compared to wild type uteri at 2 and 24 hours indicating that ERα appears to be involved in the expression of these PAD family members. Strengthening the link between ER and PAD expression, PAD1 appears to contain 2 EREs (Estrogen Response Element) while PAD4 appears to have one canonical ERE (53). PAD3, which also appears to contain a canonical ERE, is not expressed in uterine tissue while PAD2, which does not appear to contain an ERE, is expressed in the uterus. PAD2's estrogen responsiveness, however, may potentially be explained by ERα interactions with the transcription factor Sp1, which binds the PAD2 promoter at multiple sites (54).

This newer transcriptome data supports a strong association between PADs and female reproduction and reinforces the existing literature characterizing the localization and distribution of the PAD gene family in female reproductive organs. A summary of PAD expression in the reproductive tract is shown in Figure 3. Before discussing the older literature, it is important to first note here that the initial studies on PAD biology focused on a single enzyme termed "peptidylarginine deiminase" or alternatively called "skeletal muscle peptidylarginine deiminase" before the discovery of the different isoforms of the family. With availability of full genome sequences, it is now clear that the first cDNA clones isolated from rat skeletal muscle and mouse uterus are in fact PAD2 (55,56). However, the use of enzymatic activity assays on whole tissue extracts and potentially cross-reactive antibodies makes it difficult to pinpoint exactly which isoform is being discussed in some of these early studies.

Figure 2.3: PAD localization in the reproductive tissues: pituitary gland, mammary gland, ovary, and uterus.

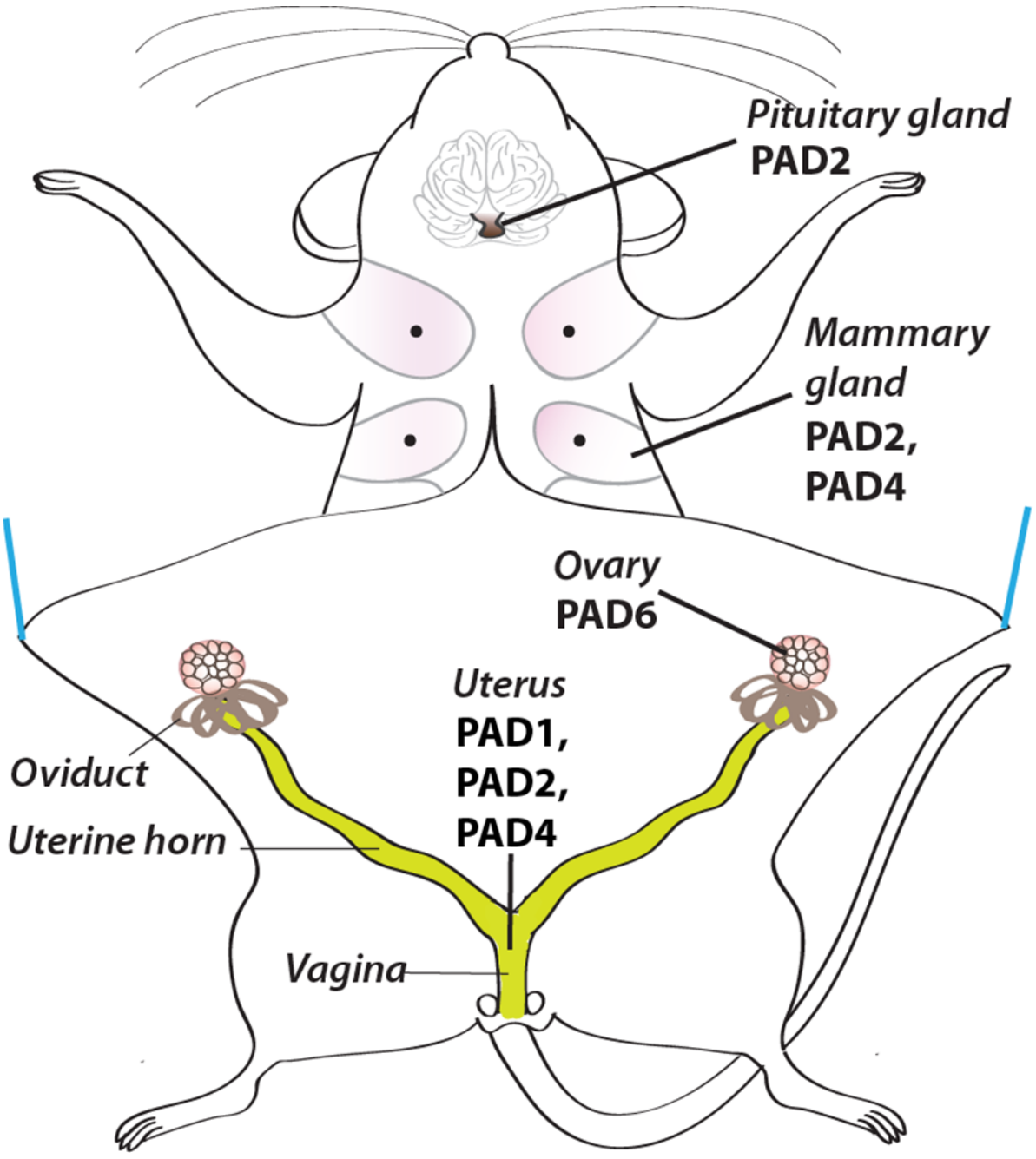
Pituitary gland
PAD2
Mammary gland
PAD2, PAD4
Ovary
PAD6
Uterus
PAD1, PAD2, PAD4
Oviduct
Uterine horn
Vagina

Pituitary

One of the first tissues studied in PAD biology was the pituitary gland. Based on the cDNA sequence, tissue isolation, and antibodies, the isoform detected in the pituitary appears likely to be PAD2 (56,57). Using pituitary lysates, investigators noticed a strong sexual dimorphism with a high level of PAD activity in the female rat pituitary, while little enzymatic activity was seen in the pituitary gland from males. Negligible PAD enzymatic activity was detected in 3-week old female pituitary, but by about 4 months of age, activity increased substantially, suggesting that sexual maturation contributes to PAD expression (58). In rats, serum estrogen (17β-estradiol) concentration varies during the estrous cycle, gradually increasing during metestrus, peaking at proestrus, followed by a sharp decrease during estrus (59). Estrous cycle-staged rats showed a two-fold higher PAD activity level in pituitary lysates during proestrus and estrus than during metestrus and diestrus stages. Thus, the rise in 17β-estradiol serum levels just prior to increased PAD activity levels suggests that the fluctuations of the hormone during the estrous cycle plays an important role in PAD expression in the pituitary (58).

Further studies strengthened the role of estrogen in PAD expression. First, Senshu *et al.* showed that ovariectomy of rats causes a severe drop in pituitary PAD activity; however, this activity could be restored by repeated injections of 17β-estradiol (58,60). Interestingly, they also found that, in the pituitary, PAD mRNA levels did not directly correlate with enzymatic activity, leading the authors to speculate that PAD mRNA might be regulated at the translational and stability levels (60). Second, investigators found that 17β-estradiol causes a dose-dependent increase in PAD biosynthesis and activity, reaching levels four- to fivefold higher than that of controls in the somato-lactotroph rat pituitary-derived MtT/S cells line (61). At the same time,

the authors found that other steroid hormones such as testosterone, progesterone, and corticosterone did not affect PAD activity in MtT/S cells.

Interestingly, insulin also increases PAD biosynthesis and activity in MtT/S cells in a dose-dependent manner (62). The increase in insulin-induced PAD levels was found to occur prior to prolactin biosynthesis suggesting that elevated PAD levels may be important for regulating prolactin expression in lactotrophs; one of the five hormone-secreting cell types in the anterior pituitary gland. Immunohistochemical and immunofluoresecent studies were carried out in the rat anterior pituitary gland and localized PAD expression to prolactin-secreting lactotrophs (63). A substantial and steady rise in PAD activity is seen from day 7 of pregnancy through day 14 in the rat pituitary. Given that an increase in 17β-estradiol levels normally precedes lactotroph proliferation and prolactin biosynthesis and that, in pregnant rats, estrogen levels remain low during early to mid-pregnancy, this observation suggests that other factors may be regulating PAD expression in the pituitary during pregnancy.

Mammary Gland

The role of PAD expression in the mammary gland is a relatively young field of investigation and, to date, it appears that PAD2 and 4 are the main isoforms expressed in this tissue. The majority of the work studying the role of PAD4 in the mammary gland has focused on epigenetic control of gene expression using human breast cancer cell lines. For example, in 2004 a report by Wang *et al.* documented how human PAD4 can convert methyl-arginine residues on histone H3 and 4 tails to the non-standard residue citrulline (28). In the course of this study, the authors used the human mammary adenocarcinoma-derived MCF-7 cell line to show that endogenous PAD4 plays a role in regulating expression of the estrogen-responsive pS2

gene promoter. The PAD4 promoter was also characterized in MCF-7 cells and found to be estrogen-responsive due to ERα binding and ERα mediated increases in AP-1, Sp1, and NF-Y transcription factor levels (64). Further, work by Zhang *et al.* used a genome-wide approach to show that PAD4 is enriched at transcriptional start sites and is primarily associated with actively transcribed genes in MCF-7 cells. Mechanistically, PAD4 was found to activate transcription of *c-fos* via citrullination of the transcription factor, Elk-1, thus potentiating subsequent Elk-1 phosphorylation and histone H4 acetylation at this target (29). Interestingly, several of the DNA elements associated with PAD4 activity correspond to recognition sites for transcription factors with known roles in mammary gland function such as STAT1, 3, and 5.

Most work to date has focused on the molecular role of PAD4 in gene regulation in cancer cells, with little emphasis on normal reproductive function or mammary tissue expression patterns. In an effort to address this issue, in this report we examined PAD4 expression patterns over the course of the estrous cycle in the mouse mammary fat pad and found that PAD4 is expressed at low but detectable levels in epithelial cells during estrus (Fig. 4a). In estrogen supplemented ovariectomized mice, PAD4 expression levels appear to increase in the nuclei of mammary epithelial cells compared to the placebo control, indicating that estrogen appears to regulate PAD4 expression *in vivo* (Fig 4b). The observation that PAD4 is expressed in the mouse mammary epithelium and that its expression is regulated by estrogen is supported by microarray data from the Korach lab (51).

Regarding PAD2, we found that its expression in the canine mammary gland appears to initiate during estrus, with the mRNA and protein levels peaking during diestrus (19). Similar to the dog, here we found that PAD2 is expressed in epithelial cell populations within the mouse mammary fat pad during all stages of the estrus cycle, with the highest PAD2 expression being

Figure 2.4: PAD4 is expressed in epithelial cell populations in the mouse mammary fat pad. **(A)** PAD4 expression is detected during the estrus phase of the mouse estrous cycle. Mice were estrous cycle staged by vaginal cytology and at each stage mammary fat pads were harvested and fixed in formalin. Tissue sections were probed with anti-PAD4 antibody or equal concentration of rabbit IgG as a control and counterstained with hematoxylin (20X). **(B)** PAD4 is expressed in the nuclei of mouse mammary epithelial cells following estrogen treatment. Mice were ovariectomized and implanted with either a slow release estrogen pellet or a placebo pellet as a control. After three weeks, mammary fat pads were collected and examined for PAD4 (green) expression using anti-PAD4 antibody or equal concentration of rabbit IgG as a control. Nuclei are stained with DAPI (blue) (40X).

A.

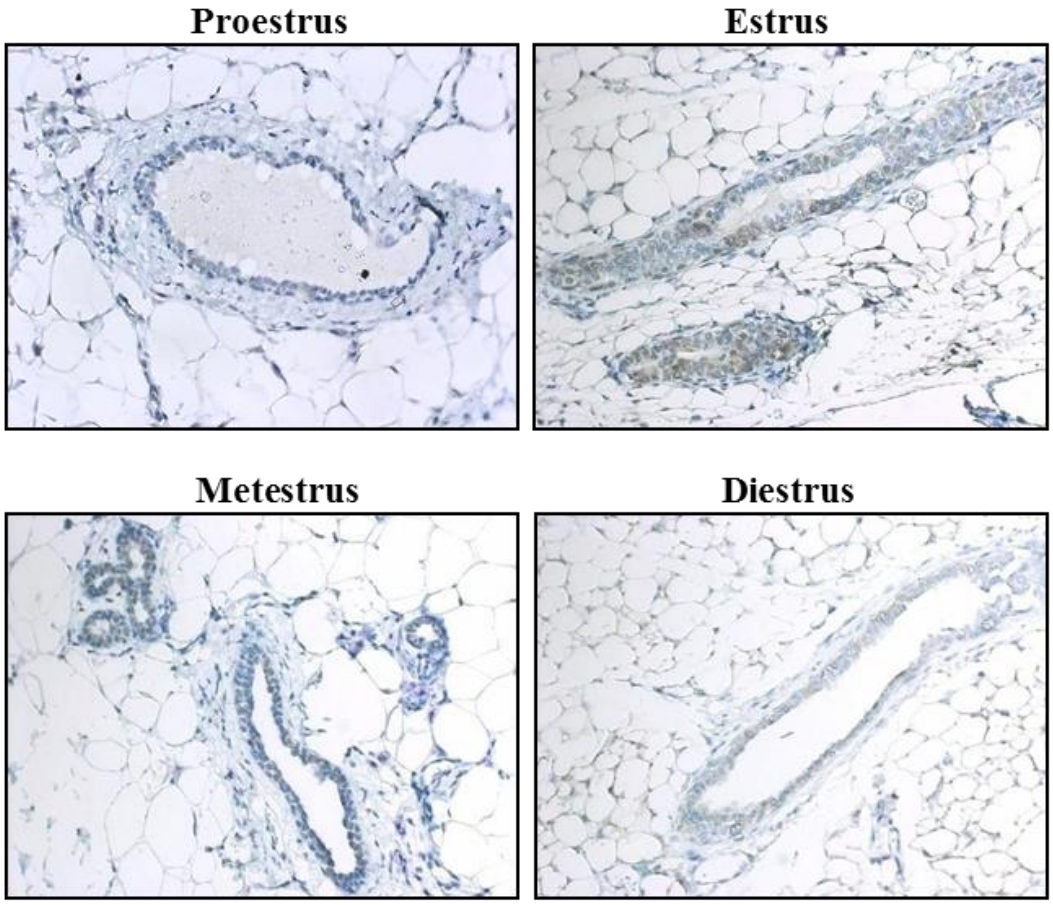
Proestrus
Estrus
Metestrus
Diestrus

B.

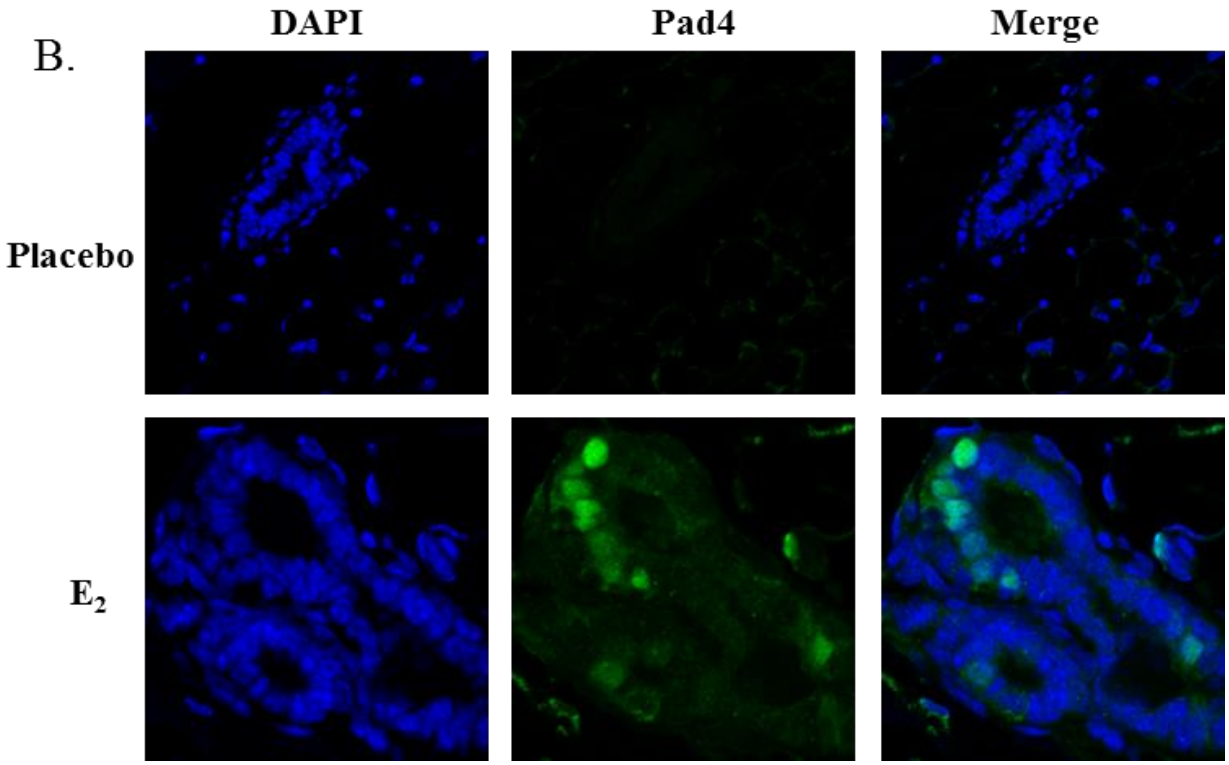
DAPI
Pad4
Merge
Placebo
E2

observed at estrus (Fig. 5a). In estrogen treated ovariectomized mice, PAD2 levels in mammary fat pads increase versus placebo control, clearly indicating a role for estrogen in driving PAD2 expression in mammary epithelial cells (Fig. 5b). Interestingly, PAD2 expression in the canine mammary gland is also estrous cycle dependent but appears to be out of phase with PAD expression patterns in the rodent mammary gland. This difference may be due to unique estrous cycle stage lengths and hormone levels in the two species, especially given that in the canine cycle, the luteal phase can last up to 100 days. Our previous report found that a fraction of PAD2 localizes to the nucleus of luminal epithelial cells in the canine mammary gland and that a major target of PAD2 in these cells appears to be histone H3 (19). These findings, coupled with more recent data from our lab, suggest that future investigations into the roles of PAD2 and PAD4 in gene regulation via histone modification in normal mammary tissue and breast cancer will likely be highly productive.

Uterus

As noted above, recent transcriptomics studies found that, of more than 50 tissues examined, the uterus expresses the highest levels of PADs 1, 2, and 4 in the mouse. Thus, it is somewhat surprising how little is currently known about the role of PADs in uterine biology. In an effort to gain more insight into the localization and regulation of PADs in the uterus, we probed uterine sections from estrous cycle staged mice using an anti-PAD4 antibody. We observed that PAD4 expression varies across the estrous cycle and localizes to luminal and glandular epithelial cells (Fig. 6a). To determine if PAD4 expression in the uterus is estrogen dependent, mice were ovariectomized and given either a placebo or slow release subcutaneous estrogen pellet for 3 weeks prior to immunohistochemical examination. Results showed that

Figure 2.5: PAD2 is expressed in epithelial cell populations in the mouse mammary fat pad. **(A)** PAD2 is detected in all stages of the estrous cycle with highest expression during the estrus phase. Mice were estrous cycle staged by vaginal cytology and at each stage mammary fat pads were harvested and fixed in formalin. Tissue sections were probed with anti-PAD2 antibody or equal concentration of rabbit IgG as a control and counterstained with hematoxylin (100X). **(B)** PAD2 is expressed in mouse mammary epithelial cells following estrogen treatment. Mice were ovariectomized and implanted with either a slow release estrogen pellet or a placebo pellet as a control. After three weeks, mammary fat pads were collected and examined for PAD2 expression using anti-PAD2 antibody or equal concentration of rabbit IgG as a control and counterstained with hematoxylin (40X).

A.

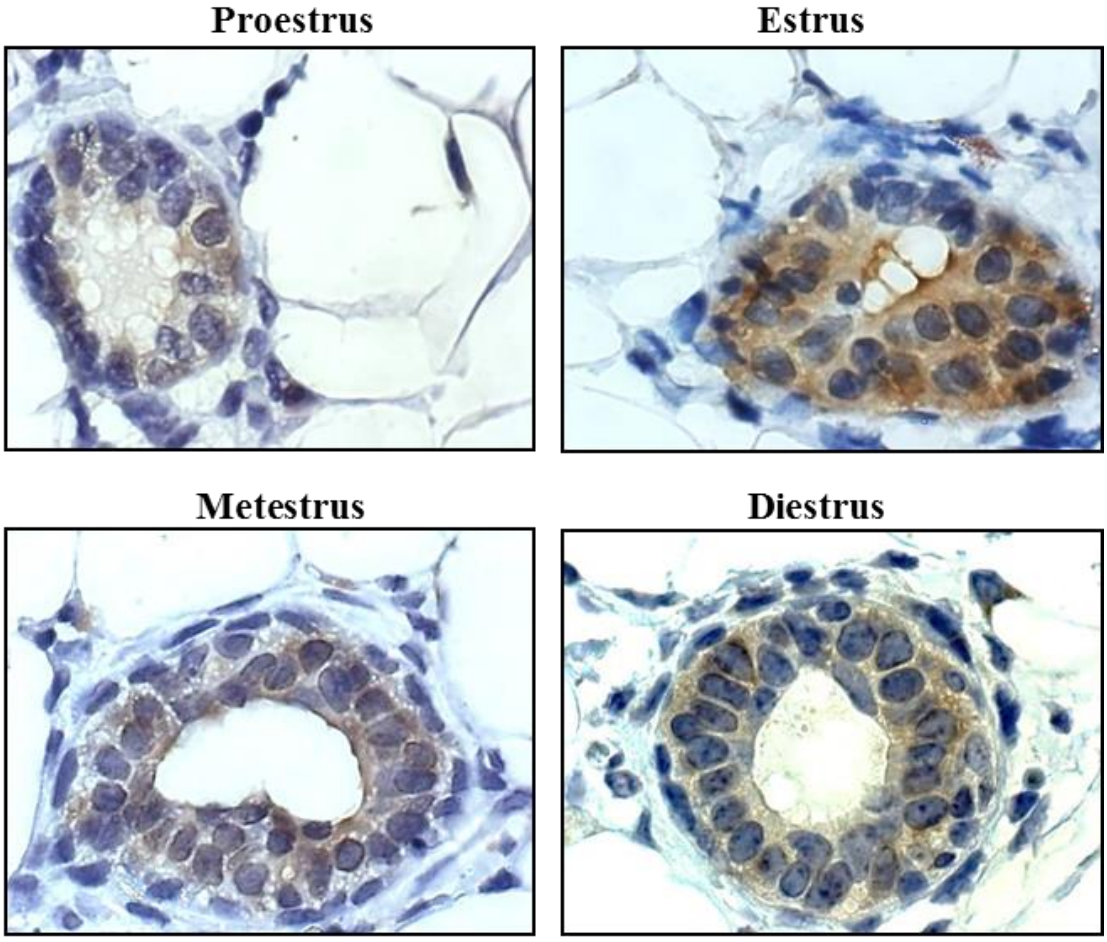

B.

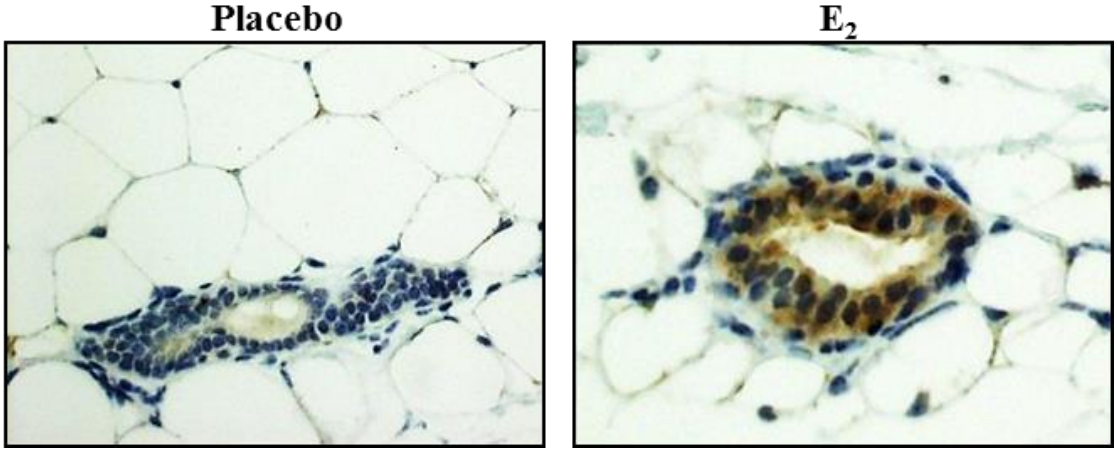

Figure 2.6: PAD4 is expressed in luminal and glandular epithelial cell populations in the mouse uterus. (A) PAD4 expression levels fluctuate across the mouse estrous cycle with highest expression detected during estrus. Mice were estrous cycle staged by vaginal cytology and at each stage uteri were harvested and fixed in formalin. Tissue sections were probed with anti-PAD4 antibody or equal concentration of rabbit IgG as a control and counterstained with hematoxylin (20X). **(B)** PAD4 is expressed in mouse uteri epithelial cells following estrogen treatment. Mice were ovariectomized and implanted with either a slow release estrogen pellet or a placebo pellet as a control. After three weeks, uteri were collected and examined for PAD4 expression using anti-PAD4 antibody or equal concentration of rabbit IgG as a control and counterstained with hematoxylin (20X).

A.

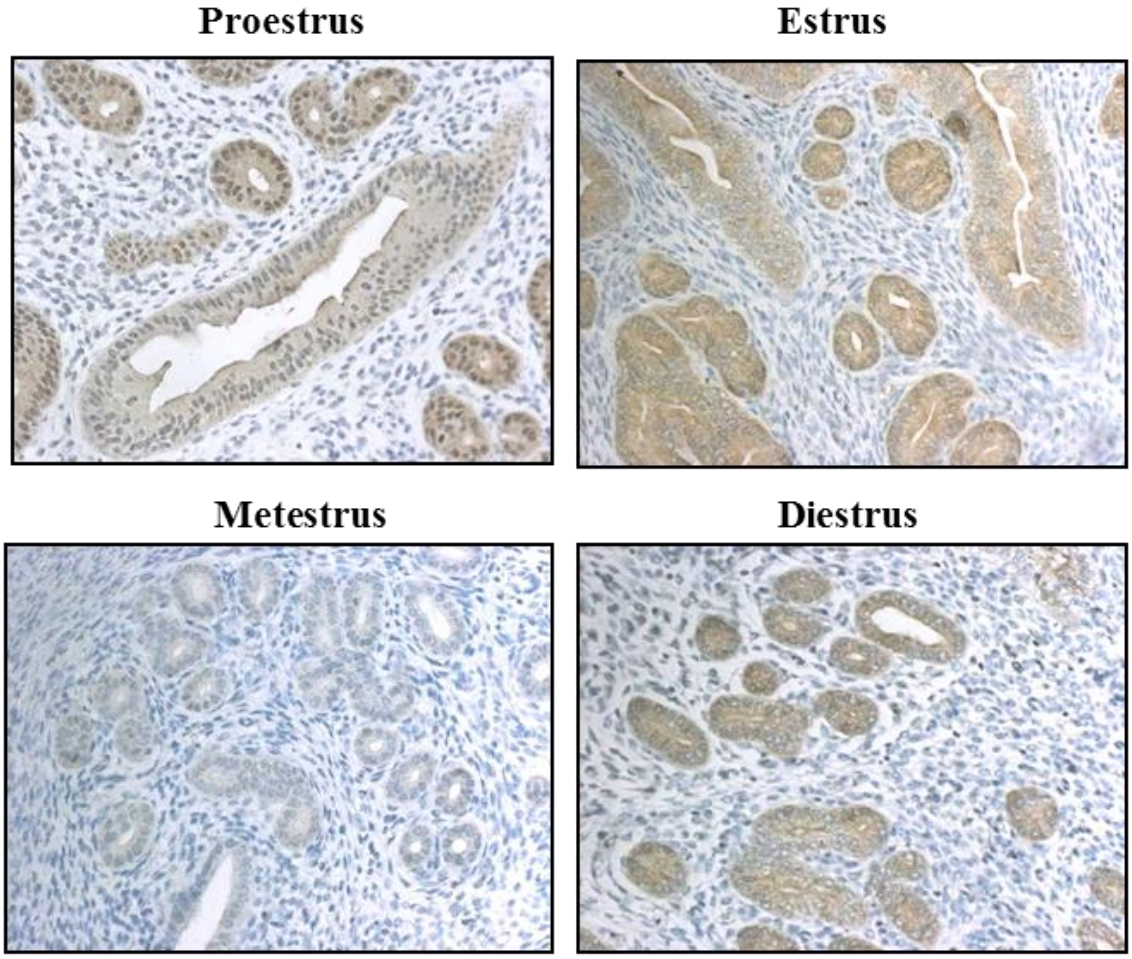

B.

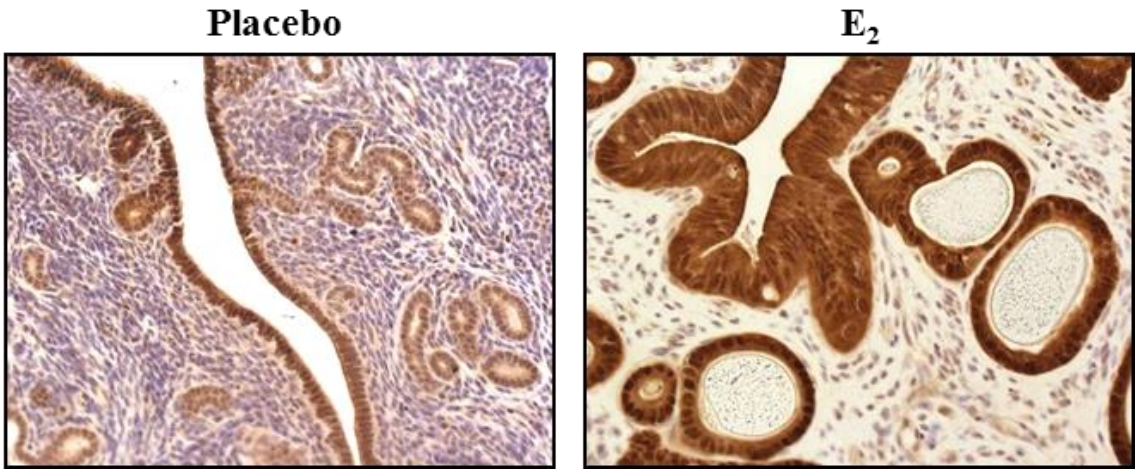

PAD4 expression is detected in the placebo control uterine tissue but that its expression increases following estrogen replacement (Fig 6b).

PAD2 is also expressed in uterine tissue and somewhat more characterized. Takahara *et al.* originally called the enzyme "peptidylarginine deiminase"; however, they subsequently cloned a single isoform from uterine tissue and sequence analysis identified the protein as PAD2 (55,65). In their initial study, they showed that, similar to PADs 1 and 4, PAD2 expression localizes to luminal and glandular epithelia of the uterus and that its expression levels change over the course of the estrous cycle, with a peak in expression being found at proestrus. Similarly, PAD2 levels in the uterus were found to diminish after ovariectomy but were restored following 17β-estradiol injection in a dose dependent manner (66). Herein, we further validated the expression of PAD2 in uterine tissue using a commercially available anti-PAD2 antibody that has previously been determined to be highly specific for PAD2 in that cross-reactivity to other PAD family members was not observed (19). We also found that PAD2 is expressed in luminal and glandular epithelial cell populations within the mouse uterus in an estrous cycle dependent manner but with highest expression being observed during estrus (Fig. 7a). In ovariectomized mice treated with estrogen, PAD2 levels in uteri increase versus placebo control, clearly indicating the role of estrogen in driving PAD2 expression in uterine epithelial cell populations (Fig. 7b).

Regarding PAD1, older reports have found that mouse PAD1 expression in uterine tissue is also estrous cycle dependent with peak expression during proestrus and that PAD1 expression can be rescued after ovariectomy by exogenous estrogen treatment (13,67). Lastly, Takahara *et al.* showed that enzymatic activity in uterine tissue during estrus was 3-4 fold higher than that during diestrus, although this likely represents the combined activity of PADs 1, 2 and 4. Taken

Figure 2.7: PAD2 is expressed in luminal and glandular epithelial cell populations in the mouse uterus. (A) PAD2 expression levels are highest during the estrus phase but present in all stages of the mouse estrous cycle. Mice were estrous cycle staged by vaginal cytology and at each stage uteri were harvested and fixed in formalin. Tissue sections were probed with anti-PAD2 antibody or equal concentration of rabbit IgG as a control and counterstained with hematoxylin (100X). **(B)** PAD2 is expressed in mouse uterine epithelial cells following estrogen treatment. Mice were ovariectomized and implanted with either a slow release estrogen pellet or a placebo pellet as a control. After three weeks, uteri were collected and examined for PAD2 (green) expression using anti-PAD2 antibody, cytokeratin (red) using an anti-cytokeratin antibody or equal concentration of rabbit IgG as a control. All nuclei are stained with DAPI (blue) (40X).

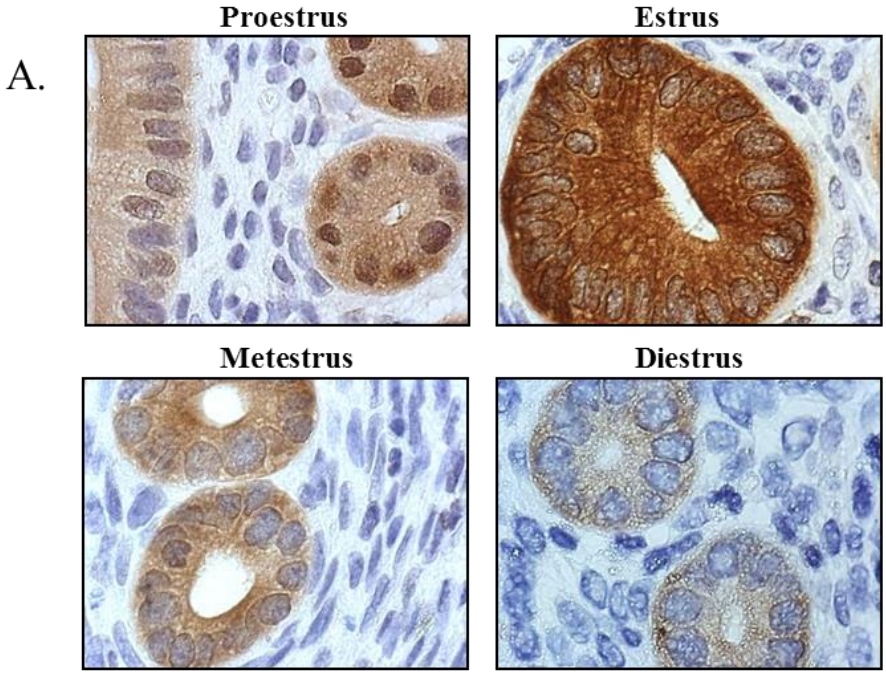
A.
Proestrus
Estrus
Metestrus
Diestrus

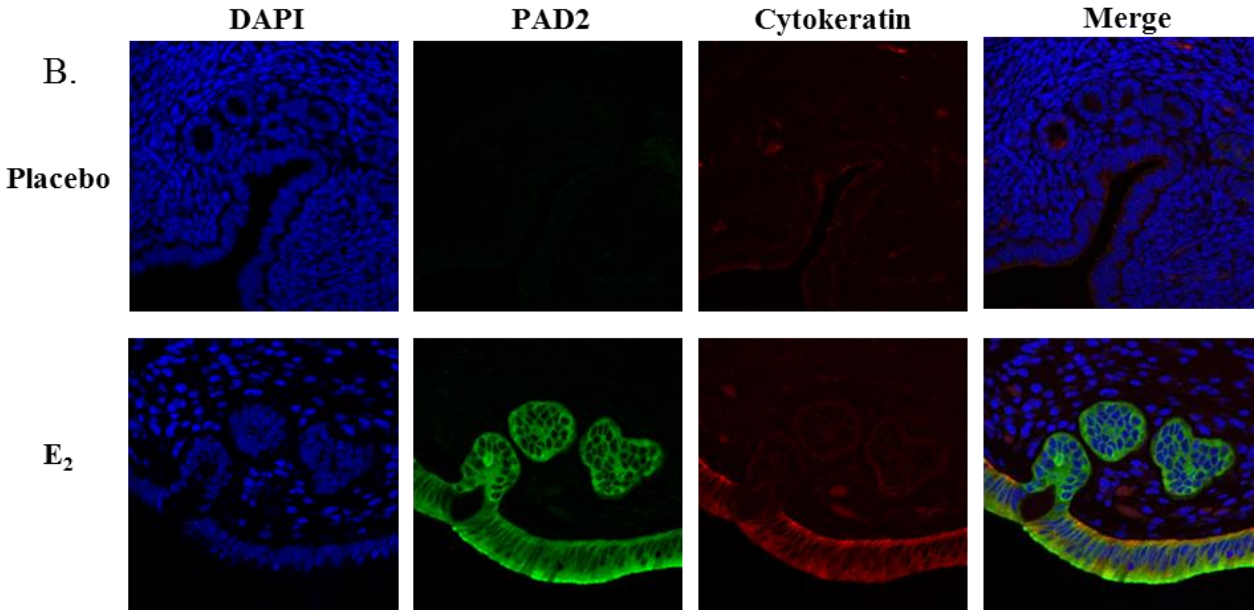
B.
DAPI
PAD2
Cytokeratin
Merge
Placebo
E2

together, these findings support the prediction that multiple PAD family members are expressed in the uterus in an estrogen dependent manner and likely play a functional role in uterine biology.

Ovary

PAD6 appears to represent the major PAD family member in the ovary, with its expression being entirely limited to germ cells within this organ. PAD6 was first identified and cloned based on its absence of expression in somatic tissues and high protein expression levels in oocytes and pre-implantation embryos (14). Through use of mutant mice, we have shown that PAD6 is essential for female fertility with the developmental arrest in PAD6-null mice occurring at the two-cell stage of development (68). Additionally, we found that that PAD6 localizes to a poorly characterized cytoskeletal structure termed lattices located within oocytes and early embryos and that PAD6 is also essential for lattice formation (69). Recently, we found that α-tubulin associates with PAD6 at the lattices, and that PAD6 deletion causes altered microtubule formation and a dramatic suppression of stable microtubules. Further, we found that microtubule mediated organelle repositioning during oocyte maturation was defective in PAD6 null mice, suggesting that PAD6 and the lattices play a critical role regulating microtubule-based activities during oocyte maturation and, potentially, during early development (70). While other PAD isoforms have not been previously described in normal ovaries, recent studies show PAD4 expression appears to be upregulated in ovarian tumors. Specifically, PAD4 is highly expressed in ovarian adenocarcinomas, but minimally expressed in benign ovarian cystadenomas, suggesting a role for PAD4 in the ovarian tumorigenesis (71).

Could PADs play a role in inflammation in the female reproductive tract?

As noted earlier, PADs are increasingly associated with inflammatory processes in non-reproductive tissues. Thus, it is interesting to speculate that PAD-mediated inflammatory activities may also play important roles in the female reproductive tract. For example, reproductive hormone-driven changes in the uterus can be viewed as an inflammatory process, as evidenced by the increased endometrial expression of inflammatory cytokines and chemokines and the accompanying infiltration of natural killer cells and other leucocytes into this tissue (72). During the secretory phase of the estrous cycle, expression of the chemokines CXCL10 and CXCL11 by the human endometrium is high and appears to be regulated by both estradiol and progesterone (73). Interestingly, CXCL10 and CXCL11 have been found to be citrullinated by PAD2, and this modification subsequently alters their chemoattracting and signaling capacity (74). Thus, it is possible that elevated PAD levels in the endometrium during the secretory phase of the estrous cycle may function to citrullinate proteins such as CXCL10 and CXCL11 and thereby modulate the inflammatory response in the uterus. Another clear link to inflammatory pathways in female reproduction is the process of ovulation, which has long been described as an inflammatory reaction (75,76). It is currently unclear if oocyte-derived PAD6 plays any role in the ovulation process, however, our finding that PAD6 appears to play a critical role in oocyte maturation, which precedes ovulation, makes this idea intriguing possibility.

CONCLUSIONS

Given the abundance of PADs 1-4 in female reproductive tissues, it seems possible that, in addition to PAD6, other PADs will likely be found to play important roles in female reproduction. In the coming years, the generation and analysis of mice with mutated versions of

these PADs will likely directly test this hypothesis. Additionally, a range of new isoform-specific PAD inhibitors are also currently in development and the use of these inhibitors in mouse studies will also likely test whether citrullination is required for specific aspects of female reproduction.

REFERENCES

1. Gyorgy, B., Toth, E., Tarcsa, E., Falus, A., and Buzas, E. I. (2006) Citrullination: a posttranslational modification in health and disease. *The international journal of biochemistry & cell biology* **38**, 1662-1677

2. Mechin, M. C., Sebbag, M., Arnaud, J., Nachat, R., Foulquier, C., Adoue, V., Coudane, F., Duplan, H., Schmitt, A. M., Chavanas, S., Guerrin, M., Serre, G., and Simon, M. (2007) Update on peptidylarginine deiminases and deimination in skin physiology and severe human diseases. *International Journal of Cosmetic Science* **29**, 147-168

3. Vossenaar, E. R., Zendman, A. J., van Venrooij, W. J., and Pruijn, G. J. (2003) PAD, a growing family of citrullinating enzymes: genes, features and involvement in disease. *BioEssays : news and reviews in molecular, cellular and developmental biology* **25**, 1106-1118

4. Tarcsa, E., Marekov, L. N., Mei, G., Melino, G., Lee, S. C., and Steinert, P. M. (1996) Protein unfolding by peptidylarginine deiminase. Substrate specificity and structural relationships of the natural substrates trichohyalin and filaggrin. *The Journal of biological chemistry* **271**, 30709-30716

5. Chavanas, S., Mechin, M. C., Takahara, H., Kawada, A., Nachat, R., Serre, G., and Simon, M. (2004) Comparative analysis of the mouse and human peptidylarginine deiminase gene clusters reveals highly conserved non-coding segments and a new human gene, PADI6. *Gene* **330**, 19-27

6. Senshu, T., Kan, S., Ogawa, H., Manabe, M., and Asaga, H. (1996) Preferential deimination of keratin K1 and filaggrin during the terminal differentiation of human epidermis. *Biochemical and biophysical research communications* **225**, 712-719

7. Nachat, R., Mechin, M. C., Takahara, H., Chavanas, S., Charveron, M., Serre, G., and Simon, M. (2005) Peptidylarginine deiminase isoforms 1-3 are expressed in the epidermis and involved in the deimination of K1 and filaggrin. *The Journal of investigative dermatology* **124**, 384-393

8. Rawlings, A. V., and Harding, C. R. (2004) Moisturization and skin barrier function. *Dermatologic therapy* **17 Suppl 1**, 43-48

9. Senshu, T., Akiyama, K., Ishigami, A., and Nomura, K. (1999) Studies on specificity of peptidylarginine deiminase reactions using an immunochemical probe that recognizes an enzymatically deiminated partial sequence of mouse keratin K1. *Journal of dermatological science* **21**, 113-126

10. Gan, S. Q., McBride, O. W., Idler, W. W., Markova, N., and Steinert, P. M. (1991) Organization, structure, and polymorphisms of the human profilaggrin gene. *Biochemistry* **30**, 5814

11. Ishida-Yamamoto, A., Senshu, T., Eady, R. A., Takahashi, H., Shimizu, H., Akiyama, M., and Iizuka, H. (2002) Sequential reorganization of cornified cell keratin filaments involving filaggrin-mediated compaction and keratin 1 deimination. *The Journal of investigative dermatology* **118**, 282-287

12. Simon, M., Haftek, M., Sebbag, M., Montezin, M., Girbal-Neuhauser, E., Schmitt, D., and Serre, G. (1996) Evidence that filaggrin is a component of cornified cell envelopes in human plantar epidermis. *The Biochemical journal* **317 (Pt 1)**, 173-177

13. Terakawa, H., Takahara, H., and Sugawara, K. (1991) Three types of mouse peptidylarginine deiminase: characterization and tissue distribution. *Journal of Biochemistry* **110**, 661-666

14. Wright, P. W., Bolling, L. C., Calvert, M. E., Sarmento, O. F., Berkeley, E. V., Shea, M. C., Hao, Z., Jayes, F. C., Bush, L. A., Shetty, J., Shore, A. N., Reddi, P. P., Tung, K. S., Samy, E., Allietta, M. M., Sherman, N. E., Herr, J. C., and Coonrod, S. A. (2003) ePAD, an oocyte and early embryo-abundant peptidylarginine deiminase-like protein that localizes to egg cytoplasmic sheets. *Developmental biology* **256**, 73-88

15. Makrygiannakis, D., af Klint, E., Lundberg, I. E., Lofberg, R., Ulfgren, A. K., Klareskog, L., and Catrina, A. I. (2006) Citrullination is an inflammation-dependent process. *Annals of the Rheumatic Diseases* **65**, 1219-1222

16. Vossenaar, E. R., Radstake, T. R., van der Heijden, A., van Mansum, M. A., Dieteren, C., de Rooij, D. J., Barrera, P., Zendman, A. J., and van Venrooij, W. J. (2004) Expression and activity of citrullinating peptidylarginine deiminase enzymes in monocytes and macrophages. *Annals of the Rheumatic Diseases* **63**, 373-381

17. Lee, H. J., Joo, M., Abdolrasulnia, R., Young, D. G., Choi, I., Ware, L. B., Blackwell, T. S., and Christman, B. W. (2010) Peptidylarginine deiminase 2 suppresses inhibitory {kappa}B kinase activity in lipopolysaccharide-stimulated RAW 264.7 macrophages. *The Journal of biological chemistry* **285**, 39655-39662

18. Proost, P., Loos, T., Mortier, A., Schutyser, E., Gouwy, M., Noppen, S., Dillen, C., Ronsse, I., Conings, R., Struyf, S., Opdenakker, G., Maudgal, P. C., and Van Damme, J. (2008) Citrullination of CXCL8 by peptidylarginine deiminase alters receptor usage, prevents proteolysis, and dampens tissue inflammation. *The Journal of experimental medicine* **205**, 2085-2097

19. Cherrington, B. D., Morency, E., Struble, A. M., Coonrod, S. A., and Wakshlag, J. J. (2010) Potential role for peptidylarginine deiminase 2 (PAD2) in citrullination of canine mammary epithelial cell histones. *PLoS One* **5**, e11768

20. Jang, B., Shin, H. Y., Choi, J. K., Nguyen du, P. T., Jeong, B. H., Ishigami, A., Maruyama, N., Carp, R. I., Kim, Y. S., and Choi, E. K. (2011) Subcellular localization of peptidylarginine deiminase 2 and citrullinated proteins in brains of scrapie-infected mice: nuclear localization of PAD2 and membrane fraction-enriched citrullinated proteins. *Journal of neuropathology and experimental neurology* **70**, 116-124

21. Kanno, T., Kawada, A., Yamanouchi, J., Yosida-Noro, C., Yoshiki, A., Shiraiwa, M., Kusakabe, M., Manabe, M., Tezuka, T., and Takahara, H. (2000) Human peptidylarginine deiminase type III: molecular cloning and nucleotide sequence of the cDNA, properties of the recombinant enzyme, and immunohistochemical localization in human skin. *The Journal of investigative dermatology* **115**, 813-823

22. Rogers, G., Winter, B., McLaughlan, C., Powell, B., and Nesci, T. (1997) Peptidylarginine deiminase of the hair follicle: characterization, localization, and function in keratinizing tissues. *The Journal of investigative dermatology* **108**, 700-707

23. Guerrin, M., Ishigami, A., Mechin, M. C., Nachat, R., Valmary, S., Sebbag, M., Simon, M., Senshu, T., and Serre, G. (2003) cDNA cloning, gene organization and expression analysis of human peptidylarginine deiminase type I. *The Biochemical journal* **370**, 167-174

24. Tarcsa, E., Marekov, L. N., Andreoli, J., Idler, W. W., Candi, E., Chung, S. I., and Steinert, P. M. (1997) The fate of trichohyalin. Sequential post-translational modifications by peptidyl-arginine deiminase and transglutaminases. *The Journal of biological chemistry* **272**, 27893-27901

25. Chavanas, S., Adoue, V., Mechin, M. C., Ying, S., Dong, S., Duplan, H., Charveron, M., Takahara, H., Serre, G., and Simon, M. (2008) Long-range enhancer associated with chromatin looping allows AP-1 regulation of the peptidylarginine deiminase 3 gene in differentiated keratinocyte. *PLoS One* **3**, e3408

26. Asaga, H., Nakashima, K., Senshu, T., Ishigami, A., and Yamada, M. (2001) Immunocytochemical localization of peptidylarginine deiminase in human eosinophils and neutrophils. *Journal of leukocyte biology* **70**, 46-51

27. Nakashima, K., Hagiwara, T., and Yamada, M. (2002) Nuclear localization of peptidylarginine deiminase V and histone deimination in granulocytes. *The Journal of biological chemistry* **277**, 49562-49568

28. Wang, Y., Wysocka, J., Sayegh, J., Lee, Y. H., Perlin, J. R., Leonelli, L., Sonbuchner, L. S., McDonald, C. H., Cook, R. G., Dou, Y., Roeder, R. G., Clarke, S., Stallcup, M. R., Allis, C. D., and Coonrod, S. A. (2004) Human PAD4 regulates histone arginine methylation levels via demethylimination. *Science (New York, N.Y.)* **306**, 279-283

29. Zhang, X., Gamble, M. J., Stadler, S., Cherrington, B. D., Causey, C. P., Thompson, P. R., Roberson, M. S., Kraus, W. L., and Coonrod, S. A. (2011) Genome-wide analysis reveals PADI4 cooperates with Elk-1 to activate c-Fos expression in breast cancer cells. *PLoS genetics* **7**, e1002112

30. Lee, Y. H., Coonrod, S. A., Kraus, W. L., Jelinek, M. A., and Stallcup, M. R. (2005) Regulation of coactivator complex assembly and function by protein arginine methylation and demethylimination. *Proceedings of the National Academy of Sciences of the United States of America* **102**, 3611-3616

31. Guo, Q., and Fast, W. (2011) Citrullination of inhibitor of growth 4 (ING4) by peptidylarginine deminase 4 (PAD4) disrupts the interaction between ING4 and p53. *J Biol Chem* **286**, 17069-17078

32. Li, P., Yao, H., Zhang, Z., Li, M., Luo, Y., Thompson, P. R., Gilmour, D. S., and Wang, Y. (2008) Regulation of p53 target gene expression by peptidylarginine deiminase 4. *Molecular and cellular biology* **28**, 4745-4758

33. Yao, H., Li, P., Venters, B. J., Zheng, S., Thompson, P. R., Pugh, B. F., and Wang, Y. (2008) Histone Arg modifications and p53 regulate the expression of OKL38, a mediator of apoptosis. *The Journal of biological chemistry* **283**, 20060-20068

34. Wang, Y., Li, M., Stadler, S., Correll, S., Li, P., Wang, D., Hayama, R., Leonelli, L., Han, H., Grigoryev, S. A., Allis, C. D., and Coonrod, S. A. (2009) Histone hypercitrullination mediates chromatin decondensation and neutrophil extracellular trap formation. *The Journal of cell biology* **184**, 205-213

35. Chang, X., Yamada, R., Suzuki, A., Sawada, T., Yoshino, S., Tokuhiro, S., and Yamamoto, K. (2005) Localization of peptidylarginine deiminase 4 (PADI4) and citrullinated protein in synovial tissue of rheumatoid arthritis. *Rheumatology (Oxford, England)* **44**, 40-50

36. van Beers, J. J., Raijmakers, R., Alexander, L. E., Stammen-Vogelzangs, J., Lokate, A. M., Heck, A. J., Schasfoort, R. B., and Pruijn, G. J. (2010) Mapping of citrullinated fibrinogen B-cell epitopes in rheumatoid arthritis by imaging surface plasmon resonance. *Arthritis research & therapy* **12**, R219

37. Schellekens, G. A., de Jong, B. A., van den Hoogen, F. H., van de Putte, L. B., and van Venrooij, W. J. (1998) Citrulline is an essential constituent of antigenic determinants recognized by rheumatoid arthritis-specific autoantibodies. *The Journal of clinical investigation* **101**, 273-281

38. Girbal-Neuhauser, E., Durieux, J. J., Arnaud, M., Dalbon, P., Sebbag, M., Vincent, C., Simon, M., Senshu, T., Masson-Bessiere, C., Jolivet-Reynaud, C., Jolivet, M., and Serre, G. (1999) The epitopes targeted by the rheumatoid arthritis-associated antifilaggrin autoantibodies are posttranslationally generated on various sites of (pro)filaggrin by

deimination of arginine residues. *Journal of immunology (Baltimore, Md.: 1950)* **162**, 585-594

39. Masson-Bessiere, C., Sebbag, M., Girbal-Neuhauser, E., Nogueira, L., Vincent, C., Senshu, T., and Serre, G. (2001) The major synovial targets of the rheumatoid arthritis-specific antifilaggrin autoantibodies are deiminated forms of the alpha- and beta-chains of fibrin. *Journal of immunology (Baltimore, Md.: 1950)* **166**, 4177-4184

40. Lamensa, J. W., and Moscarello, M. A. (1993) Deimination of human myelin basic protein by a peptidylarginine deiminase from bovine brain. *Journal of neurochemistry* **61**, 987-996

41. Moscarello, M. A., Wood, D. D., Ackerley, C., and Boulias, C. (1994) Myelin in multiple sclerosis is developmentally immature. *The Journal of clinical investigation* **94**, 146-154

42. Musse, A. A., Li, Z., Ackerley, C. A., Bienzle, D., Lei, H., Poma, R., Harauz, G., Moscarello, M. A., and Mastronardi, F. G. (2008) Peptidylarginine deiminase 2 (PAD2) overexpression in transgenic mice leads to myelin loss in the central nervous system. *Disease models & mechanisms* **1**, 229-240

43. Wood, D. D., Ackerley, C. A., Brand, B., Zhang, L., Raijmakers, R., Mastronardi, F. G., and Moscarello, M. A. (2008) Myelin localization of peptidylarginine deiminases 2 and 4: comparison of PAD2 and PAD4 activities. *Laboratory investigation; a journal of technical methods and pathology* **88**, 354-364

44. Pritzker, L. B., Joshi, S., Gowan, J. J., Harauz, G., and Moscarello, M. A. (2000) Deimination of myelin basic protein. 1. Effect of deimination of arginyl residues of myelin basic protein on its structure and susceptibility to digestion by cathepsin D. *Biochemistry* **39**, 5374-5381

45. Tranquill, L. R., Cao, L., Ling, N. C., Kalbacher, H., Martin, R. M., and Whitaker, J. N. (2000) Enhanced T cell responsiveness to citrulline-containing myelin basic protein in multiple sclerosis patients. *Multiple sclerosis (Houndmills, Basingstoke, England)* **6**, 220-225

46. Mastronardi, F. G., Wood, D. D., Mei, J., Raijmakers, R., Tseveleki, V., Dosch, H. M., Probert, L., Casaccia-Bonnefil, P., and Moscarello, M. A. (2006) Increased citrullination of histone H3 in multiple sclerosis brain and animal models of demyelination: a role for tumor necrosis factor-induced peptidylarginine deiminase 4 translocation. *The Journal of neuroscience : the official journal of the Society for Neuroscience* **26**, 11387-11396

47. Asaga, H., Akiyama, K., Ohsawa, T., and Ishigami, A. (2002) Increased and type II-specific expression of peptidylarginine deiminase in activated microglia but not hyperplastic astrocytes following kainic acid-evoked neurodegeneration in the rat brain. *Neuroscience letters* **326**, 129-132

48. Asaga, H., and Ishigami, A. (2001) Protein deimination in the rat brain after kainate administration: citrulline-containing proteins as a novel marker of neurodegeneration. *Neuroscience letters* **299**, 5-8

49. Coudane, F., Mechin, M. C., Huchenq, A., Henry, J., Nachat, R., Ishigami, A., Adoue, V., Sebbag, M., Serre, G., and Simon, M. (2011) Deimination and expression of peptidylarginine deiminases during cutaneous wound healing in mice. *European journal of dermatology : EJD* **21**, 376-384

50. Barrett, T., Troup, D. B., Wilhite, S. E., Ledoux, P., Rudnev, D., Evangelista, C., Kim, I. F., Soboleva, A., Tomashevsky, M., Marshall, K. A., Phillippy, K. H., Sherman, P. M., Muertter, R. N., and Edgar, R. (2009) NCBI GEO: archive for high-throughput functional genomic data. *Nucleic acids research* **37**, D885-890

51. Hewitt, S. C., Deroo, B. J., Hansen, K., Collins, J., Grissom, S., Afshari, C. A., and Korach, K. S. (2003) Estrogen receptor-dependent genomic responses in the uterus mirror the biphasic physiological response to estrogen. *Molecular endocrinology (Baltimore, Md.)* **17**, 2070-2083

52. O'Brien, J. E., Peterson, T. J., Tong, M. H., Lee, E. J., Pfaff, L. E., Hewitt, S. C., Korach, K. S., Weiss, J., and Jameson, J. L. (2006) Estrogen-induced proliferation of uterine epithelial cells is independent of estrogen receptor alpha binding to classical estrogen response elements. *The Journal of biological chemistry* **281**, 26683-26692

53. Bourdeau, V., Deschenes, J., Metivier, R., Nagai, Y., Nguyen, D., Bretschneider, N., Gannon, F., White, J. H., and Mader, S. (2004) Genome-wide identification of high-affinity estrogen response elements in human and mouse. *Molecular endocrinology (Baltimore, Md.)* **18**, 1411-1427

54. Dong, S., Kojima, T., Shiraiwa, M., Mechin, M. C., Chavanas, S., Serre, G., Simon, M., Kawada, A., and Takahara, H. (2005) Regulation of the expression of peptidylarginine deiminase type II gene (PADI2) in human keratinocytes involves Sp1 and Sp3 transcription factors. *The Journal of investigative dermatology* **124**, 1026-1033

55. Tsuchida, M., Takahara, H., Minami, N., Arai, T., Kobayashi, Y., Tsujimoto, H., Fukazawa, C., and Sugawara, K. (1993) cDNA nucleotide sequence and primary structure of mouse uterine peptidylarginine deiminase. Detection of a 3'-untranslated nucleotide sequence common to the mRNA of transiently expressed genes and rapid turnover of this enzyme's mRNA in the estrous cycle. *European journal of biochemistry / FEBS* **215**, 677-685

56. Watanabe, K., and Senshu, T. (1989) Isolation and characterization of cDNA clones encoding rat skeletal muscle peptidylarginine deiminase. *The Journal of biological chemistry* **264**, 15255-15260

57. Watanabe, K., Akiyama, K., Hikichi, K., Ohtsuka, R., Okuyama, A., and Senshu, T. (1988) Combined biochemical and immunochemical comparison of peptidylarginine deiminases present in various tissues. *Biochimica et biophysica acta* **966**, 375-383

58. Senshu, T., Akiyama, K., Nagata, S., Watanabe, K., and Hikichi, K. (1989) Peptidylarginine deiminase in rat pituitary: sex difference, estrous cycle-related changes, and estrogen dependence. *Endocrinology* **124**, 2666-2670

59. Butcher, R. L., Collins, W. E., and Fugo, N. W. (1974) Plasma concentration of LH, FSH, prolactin, progesterone and estradiol-17beta throughout the 4-day estrous cycle of the rat. *Endocrinology* **94**, 1704-1708

60. Watanabe, K., Hikichi, K., Nagata, S., and Senshu, T. (1990) Estrous cycle dependent regulation of peptidylarginine deiminase transcripts in female rat pituitary. *Biochemical and biophysical research communications* **172**, 28-34

61. Nagata, S., and Senshu, T. (1990) Peptidylarginine deiminase in rat and mouse hemopoietic cells. *Experientia* **46**, 72-74

62. Nagata, S., Uehara, T., Inoue, K., and Senshu, T. (1992) Increased peptidylarginine deiminase expression during induction of prolactin biosynthesis in a growth-hormone-producing rat pituitary cell line, MtT/S. *Journal of cellular physiology* **150**, 426-432

63. Akiyama, K., Inoue, K., and Senshu, T. (1989) Immunocytochemical study of peptidylarginine deiminase: localization of its immunoreactivity in prolactin cells of female rat pituitaries. *Endocrinology* **125**, 1121-1127

64. Dong, S., Zhang, Z., and Takahara, H. (2007) Estrogen-enhanced peptidylarginine deiminase type IV gene (PADI4) expression in MCF-7 cells is mediated by estrogen receptor-alpha-promoted transfactors activator protein-1, nuclear factor-Y, and Sp1. *Molecular endocrinology (Baltimore, Md.)* **21**, 1617-1629

65. Takahara, H., Tsuchida, M., Kusubata, M., Akutsu, K., Tagami, S., and Sugawara, K. (1989) Peptidylarginine deiminase of the mouse. Distribution, properties, and immunocytochemical localization. *The Journal of biological chemistry* **264**, 13361-13368

66. Takahara, H., Kusubata, M., Tsuchida, M., Kohsaka, T., Tagami, S., and Sugawara, K. (1992) Expression of peptidylarginine deiminase in the uterine epithelial cells of mouse is dependent on estrogen. *The Journal of biological chemistry* **267**, 520-525

67. Rus'd, A. A., Ikejiri, Y., Ono, H., Yonekawa, T., Shiraiwa, M., Kawada, A., and Takahara, H. (1999) Molecular cloning of cDNAs of mouse peptidylarginine deiminase type I, type III and type IV, and the expression pattern of type I in mouse. *European journal of biochemistry / FEBS* **259**, 660-669

68. Esposito, G., Vitale, A. M., Leijten, F. P., Strik, A. M., Koonen-Reemst, A. M., Yurttas, P., Robben, T. J., Coonrod, S., and Gossen, J. A. (2007) Peptidylarginine deiminase (PAD) 6 is essential for oocyte cytoskeletal sheet formation and female fertility. *Molecular and cellular endocrinology* **273**, 25-31

69. Yurttas, P., Vitale, A. M., Fitzhenry, R. J., Cohen-Gould, L., Wu, W., Gossen, J. A., and Coonrod, S. A. (2008) Role for PADI6 and the cytoplasmic lattices in ribosomal storage in oocytes and translational control in the early mouse embryo. *Development* **135**, 2627-2636

70. Kan, R., Yurttas, P., Kim, B., Jin, M., Wo, L., Lee, B., Gosden, R., and Coonrod, S. A. (2011) Regulation of mouse oocyte microtubule and organelle dynamics by PADI6 and the cytoplasmic lattices. *Developmental biology* **350**, 311-322

71. Wang, L., Chang, X., Yuan, G., Zhao, Y., and Wang, P. (2010) Expression of peptidylarginine deiminase type 4 in ovarian tumors. *International journal of biological sciences* **6**, 454-464

72. King, A. E., and Critchley, H. O. (2010) Oestrogen and progesterone regulation of inflammatory processes in the human endometrium. *The Journal of steroid biochemistry and molecular biology* **120**, 116-126

73. Sentman, C. L., Meadows, S. K., Wira, C. R., and Eriksson, M. (2004) Recruitment of uterine NK cells: induction of CXC chemokine ligands 10 and 11 in human endometrium by estradiol and progesterone. *Journal of immunology (Baltimore, Md.: 1950)* **173**, 6760-6766

74. Loos, T., Mortier, A., Gouwy, M., Ronsse, I., Put, W., Lenaerts, J. P., Van Damme, J., and Proost, P. (2008) Citrullination of CXCL10 and CXCL11 by peptidylarginine deiminase: a naturally occurring posttranslational modification of chemokines and new dimension of immunoregulation. *Blood* **112**, 2648-2656

75. Espey, L. L. (1980) Ovulation as an inflammatory reaction--a hypothesis. *Biology of reproduction* **22**, 73-106

76. Jabbour, H. N., Sales, K. J., Catalano, R. D., and Norman, J. E. (2009) Inflammatory pathways in female reproductive health and disease. *Reproduction (Cambridge, England)* **138**, 903-919

CHAPTER THREE

ROLE OF PEPTIDYLARGININE DEIMINASE 2 (PADI2) IN MAMMARY TUMOR CELL MIGRATION AND INVASION

Reprinted from:

Horibata, S., Rogers, K., Sadegh, D., Anguish, L., Shah, P., Mohanan, S., Thompson, P.R., and Coonrod, S.A. Role of peptidylarginine deiminase 2 in tumor cell migration and invasion. *In Preparation*

Contributions:

Manuscript preparation: Horibata, S., Coonrod, S.A.

Conception and Design: Horibata, S., Coonrod, S.A.

Development of methodology: Horibata, S., Anguish, L.J., Coonrod, S.A.

BB-Cl-Amidine and Cl-Amidine: Provided by Thompson, P.R.

Acquisition of data:

Figure 3.1: Horibata, S.

Figure 3.2: Horibata, S. and Rogers, K.

Figure 3.3: Horibata, S.

Figure 3.4: Horibata, S.

Figure 3.5: Horibata, S.

Figure 3.6: Horibata, S.

Figure 3.7: Horibata, S., Sadegh, D., and Rogers, K.

Figure 3.8: Horibata, S., Mohanan, S., and Anguish, L.

Figure 3.9: Anguish, L. and Shah, P.

Figure 3.10: Horibata, S. and Anguish, L.

ABSTRACT

Introduction: Penetration of the basement membrane by cancer cells is a crucial first step in mammary tumor invasion. Using a mouse model of ductal carcinoma *in situ*, we previously found that inhibition of peptidylarginine deiminase 2 (PADI2) activity appears to suppress tumor cell migration across the basement membrane. The goal of this investigation was to gain insight into the mechanisms by which PADI2 mediates this process.

Method: For our study, we modulated PADI2 activity in mammary ductal carcinoma (MCF10DCIS.com) cells by lentiviral shRNA knockdown or PADI inhibition and explored the effects of these treatments on changes in cell migration and cell morphology. We also used these PADI2-modulated cells to test whether PADI2 may be required for EGF-induced cell migration. To test how PADI2 might promote tumor cell migration and invasion *in vivo*, we tested how PADI inhibition alters the expression of several cell migration mediators in MCF10DCIS.com xenograft tumors. Using a transgenic mouse model, we then tested the effects of PAD2 overexpression on mammary gland development. Additionally, we generated mammary gland organoids from the overexpressing mice to test the effect of PADI2 inhibition on EGF-induced ductal invasion.

Results: Our results find that PADI2 depletion or inhibition suppresses cell migration and alters the morphology of MCF10DCIS.com cells. Additionally, we find that PADI2 depletion suppresses the expression of the cytoskeletal regulatory proteins RhoA, Rac1, and Cdc42 and also promotes a mesenchymal to epithelial-like transition in tumor cells; with an associated increase in the cell adhesion marker, E-cadherin. *In vivo*, we find that PADI2 overexpression

causes mammary hyperbranching, a phenotype often observed during tumorigenesis. Additionally, our mammary gland organoid study found that inhibition of PADI2 activity suppresses EGF-induced ductal invasion.

Conclusion: Together, our work suggests that PADI2 plays a critical role in breast cancer cell migration and invasion. Our findings that EGF treatment increases protein citrullination and that PADI2 inhibition blocks EGF-induced cell migration, suggests that PADI2 likely functions within the EGF signaling pathway to mediate cell migration/invasion.

Key Words: Peptidylarginine deiminase 2 (PADI2); tumor cell migration; ductal invasion; mammary hyperbranching

INTRODUCTION

Cell migration is a highly complex process that is carried out by all cell types and is critical for various biological processes ranging from embryonic development to the immune responses (1-3). Cell migration is often dysregulated in cancer and plays an important role in metastasis and invasion (4,5). To migrate, cells modify their shape and stiffness by becoming polarized and elongated (6), forming protrusions and extensions which branch outwards to define the leading edge (7,8). These protrusions are functionally diverse and include lamelipodia, filopodia, spikes (early filopods), pseudopods, ruffles (early pseudopods), or invadopods (9). The newly formed leading edge establishes the formation of new adhesion sites (10). In addition to the formation of new adhesion sites at the leading edge, changes in the trailing edge are also required for cells to move forward. Cells lose contact with the previous adhesion site at the trailing edge and, when contraction of the actomyosin cytoskeleton occurs, it generates sufficient traction force to allow the cell body to move forward (4,11).

Given the critical role of cell migration in biological processes, it is not surprising that its dysregulation is associated with the progression of cancer. In normal breasts, there are two distinct cell layers that line the mammary duct. The basal layer of myoepithelial cells is bounded by a basement membrane that separates the mammary gland epithelium from the surrounding stromal tissues. Superficial to the basal layer are the luminal epithelial cells (12). In luminal breast cancers, the luminal epithelial cells proliferate uncontrollably and fill the mammary gland, thereby disrupting tissue architecture and eventually breaking the myoepithelial basement membrane allowing the cancer cells to migrate out from the mammary gland, thereby leading to invasive breast cancer **(Figure 3.1A)** (13). Although ductal carcinoma *in situ* (DCIS) is often benign, it is a major challenge to diagnose whether this non-invasive tumor will become invasive.

Figure 3.1: Schematic illustration of the progression of breast cancer. (A) Normal mammary duct is composed of two cell layers, luminal epithelial cells and myoepithelial cells that line the duct with the basement membrane. However, in invasive ductal carcinoma, the luminal epithelial cells will escape and migrate out from the basement membrane for metastasis. **(B)** Normal mammary epithelial cells have higher cell adhesive properties regulated by E-cadherin. In breast cancer cells, the cells are more migratory and their cellular movements are regulated by the Rho family to GTPases, RhoA, Rac, and Cdc42.

A.

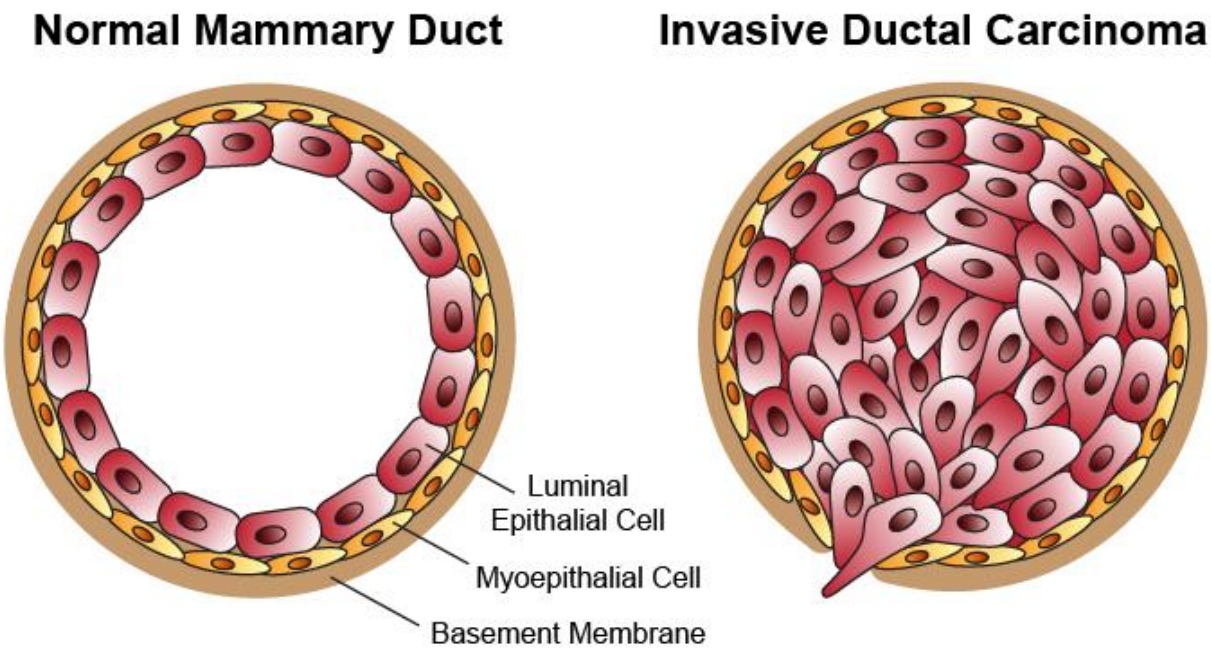
Normal Mammary Duct
Invasive Ductal Carcinoma
Luminal Epithalial Cell
Myoepithalial Cell
Basement Membrane

B.

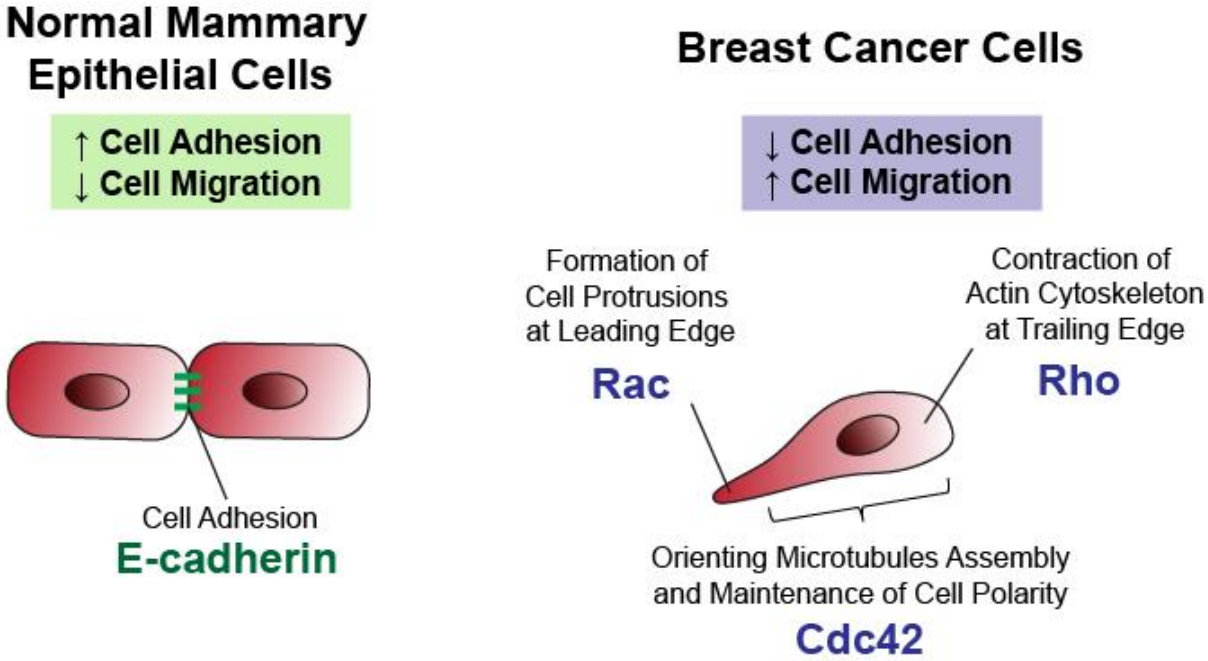
Normal Mammary Epithelial Cells
↑ Cell Adhesion
↓ Cell Migration
Cell Adhesion
E-cadherin
Breast Cancer Cells
↓ Cell Adhesion
↑ Cell Migration
Formation of Cell Protrusions at Leading Edge
Rac
Contraction of Actin Cytoskeleton at Trailing Edge
Rho
Orienting Microtubules Assembly and Maintenance of Cell Polarity
Cdc42

Therefore, markers that can predict the potential invasiveness of DCIS will greatly help women from undergoing life-threatening surgeries. When DCIS lesions become invasive, this is often accompanied by carcinoma cells undergoing epithelial-to-mesenchymal transition (EMT) (14,15). Cancer cells undergoing an EMT frequently downregulate E-cadherin leading to a loss of epithelial cell polarity and adhesiveness (16). Additionally, these tumor cells acquire mesenchymal cell characteristics that include increased cell motility and invasiveness. Multiple signaling pathways have been found to regulate the EMT including TGF-β, PI3K/AKT, and the transcription factors Snail, Slug, and Smad (15,17-19).

Initiation of cell migration is often mediated by growth factors and/or chemokines or by components of the extracellular matrix (ECM) (4). One of the main stimuli that can trigger cell migration in breast cancer cells is the epidermal growth factor (EGF), which can induce cell migration by activating a phosphatidyl-inositol 3-kinase (PI3K) signal transduction cascade leading to the activation of the Rho family of small GTPases (including Rho, Rac, and Cdc42) (7,20-23). These GTPases are regulated in a very specific manner in order to coordinate the proper movement of the cellular actin cytoskeleton (24). Rac localizes to the leading edge where it promotes the formation of cell protrusions via coordination of actin polymerization. On the other hand, Rho localizes to the trailing edge where it helps coordinate the contraction of the actin cytoskeleton. Lastly, Cdc42 is involved in orienting the microtubule assembly in the direction of cell movement (Figure 1B). It remains unclear which other protein factors could also play a role in Rho family-mediated cell migration.

Previously, we identified peptidylarginine deiminase 4 (PADI4) enzyme as a regulator of breast cancer cell migration (25). PADIs are a family of calcium-dependent enzyme that can post-translationally convert arginine residues into neutrally charged citrulline. This activity,

called either citrullination or deimination, can alter the target protein's tertiary structure or can modulate the target protein's ability to interact with other molecules (26). There are 5 PADI isozymes, PADI1-4, and 6, with each having a unique tissue distribution (27,28). Aside from PADI4, we recently also found that PADI2 localizes to mammary epithelial cells and is dysregulated in breast cancer (28-31). Furthermore, we also observed that the mammary duct basement membrane of MCF10DCIS.com xenograft tumor model treated with Cl-Amidine, a PADI inhibitor, restores the basement membrane integrity (30). In this study, we investigated the potential mechanisms by which PADI2 mediates tumor cell migration across the basement membrane, thereby enhancing tumor cell invasion.

RESULTS AND DISCUSSIONS

PADI2 depletion inhibits the migration of MCF10DCIS cells

To investigate whether PADI2 promotes the migration of breast cancer cells, we first generated PADI2-depleted ductal carcinoma *in situ* (MCF10DCIS.com) cells using the lentiviral shRNA knockdown system. We confirmed *PADI2* knockdown using quantitative real time PCR and found that the PADI2 shRNA line showed a 97% reduction in *PADI2* mRNA levels when compared to the scrambled shRNA cell line **(Figure 3.2A)**. Furthermore, immunoblot and immunofluorescent assays demonstrated that PADI2 protein levels were also reduced in the PADI2-depleted line **(Figure 3.2B and 3.2C)**. Additionally, IIF analysis we found that global levels of citrullinated proteins were reduced in the PADI2-depleted line compared to the shRNA control line **(Figure 3.2D)**.

We then test the effects of *PADI2* depletion on cell migration. Using a wound healing assay, we found that depletion of *PADI2* in MCF10DCIS.com cells inhibited cell migration, with

Figure 3.2: Depletion of PADI2 suppresses cell migration in MCF10DCIS.com cells. (A) Total RNA was isolated from MCF10DCIS.com cells infected with scrambled-shRNA and PADI2-shRNA lentiviruses. Their *PADI2* mRNA levels were determined by qRT-PCR (SYBR) using scrambled-shRNA as a reference and β-actin normalization. Data were analyzed using the $2^{-\Delta\Delta C(t)}$ method and are expressed as the mean ± SD from three independent experiments (* $p < 0.05$). **(B)** The whole cell lysates of MCF10DCIS scrambled-shRNA and PADI2-shRNA cells were immunoblotted with PADI2. The blot was also proved with β-actin antibody to determine equal loading. **(C)** Immunofluorescent assay was performed on scrambled-shRNA and PADI2-shRNA cells probed with PADI2 antibody, **(D)** pan-citrulline antibody and DAPI (nuclei). Scale bars = (C) 50 μm and (D) 25 μm. **(E)** Relative average areas of wound closure from the wound healing assays were calculated using ImageJ and normalizing to scrambled-shRNA (** $p < 0.05$). **(F)** A wound healing assays were performed on MCF10DCIS.com scrambled-shRNA and PADI2-shRNA cells. The cells were fixed using 4% paraformaldehyde 24 hours after striking the wound (24 hr.). The cells were then visualized and imaged using the light microscopy to determine the extent of the wound closure. The widths of the initial wounds are indicated by the lines. The cells were also fixed immediately after striking the wound (0 hr.) to indicate the size of the initial wounds. The images on the right are the enlarged images of the boxed images.

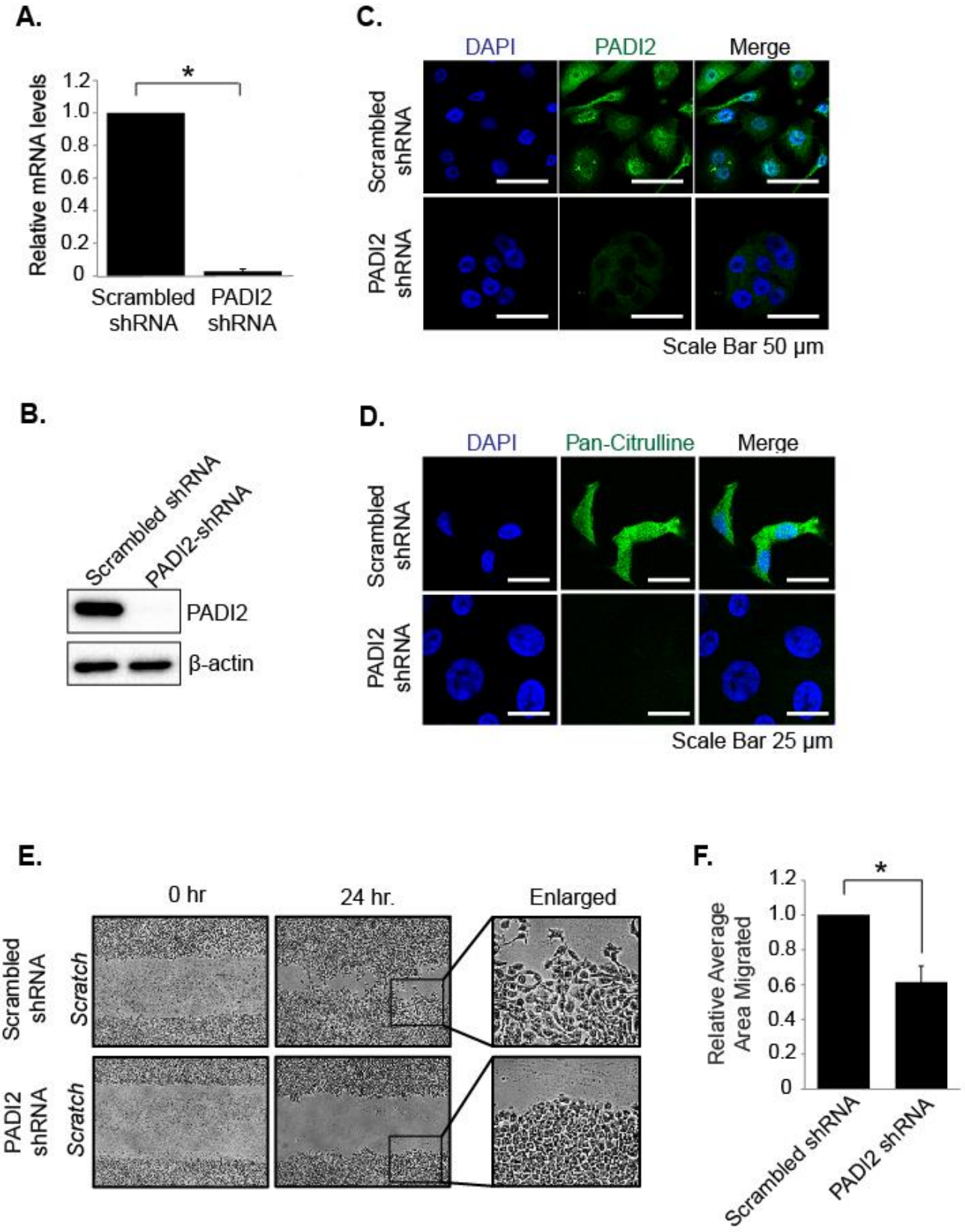
A.
Relative mRNA levels
1.2
1.0
0.8
0.6
0.4
0.2
0
*
Scrambled shRNA
PADI2 shRNA
B.
Scrambled shRNA
PADI2-shRNA
PADI2
β-actin
C.
DAPI
PADI2
Merge
Scrambled shRNA
PADI2 shRNA
Scale Bar 50 μm
D.
DAPI
Pan-Citrulline
Merge
Scrambled shRNA
PADI2 shRNA
Scale Bar 25 μm
E.
0 hr
24 hr.
Enlarged
Scrambled shRNA
Scratch
PADI2 shRNA
Scratch
F.
Relative Average Area Migrated
1.2
1.0
0.8
0.6
0.4
0.2
0
*
Scrambled shRNA
PADI2 shRNA

a 39% reduction in migration in the PADI2-depleted cells compared to the scrambled shRNA cell line **(Figure 3.2E and 3.2F)**. Interestingly, in addition to inhibiting cell migration, we found that *PADI2* depleted cells appeared to be more rounded and tightly packed when compared to the control group which contained elongated cells that had frequently appeared to migrate independently into the wound **(Figure 3.2F)**. This observation mirrors the initial step of metastasis where epithelial cells lose their cell-cell adhesion and gain mesenchymal properties to become more migratory (16).

To confirm whether the migratory phenotype seen in Figure 2C was caused by cell movement and not cell proliferation, we tracked the movement of single cells using time-lapse imaging. Results show that the *PADI2*-depleted cells appeared to be actively dividing, however, the resulting daughter cells displayed diminished mobility **(Figure 3.3A)**. On the other hand, the scrambled cells were more migratory and more dynamic in cell shape.

We further analyzed 20 scrambled and 20 *PADI2* knockdown cells during the course of 19 hours and tracked the distance travelled away from the point of origin. Strikingly, most of the *PADI2* depleted cells remained stationary, while the scrambled cells actively migrated away from the point of origin **(Figure 3.3B)**. Using the Tracking Tool^{TM} Pro v2.0, we quantified the accumulated distance travelled by these cells and found that the scrambled cells had an average total distance travelled of 577.0 μm whereas the *PADI2* depleted cells only travelled 139.1 μm **(Figure 3.3C)**. Furthermore, we found the average velocity of the scrambled cells to be 0.5 μm/min, with the maximum velocity of 1.3 μm/min. In contrast, the *PADI2* depleted cells had an average velocity of 0.1 μm/min, with the maximum velocity of 0.3 μm/min **(Figure 3.3D)**. This represents a 5-fold reduction in average velocity in the *PADI2* depleted cells compared to the

Figure 3.3: Single cell migration is impaired in PADI2 depleted MCF10DCIS.com cells. (A) Images of MCF10DCIS scrambled-shRNA and PADI2-shRNA cells taken at times 0, 3, 6, 9, 12, and 15 hours at the same location using the wide-field microscope with built-in incubation chamber. The arrow indicates the directional movement of the cells. Scale bar = 50 μm. **(B)** Graphical representation tracking the movement of individual cells (n=20) of scrambled-shRNA and PADI2-shRNA cells in culture. The line shows the trails of the cell movement and the black circle shows the final location of the movement of the cells away from the point of origin shown as white dot. The graph was generated using the Tracking Tool™ Pro v2.0. **(C)** Graph depicts average velocity and **(D)** accumulated distance travelled of single cell movement of scrambled-shRNA and PADI2-shRNA cells.

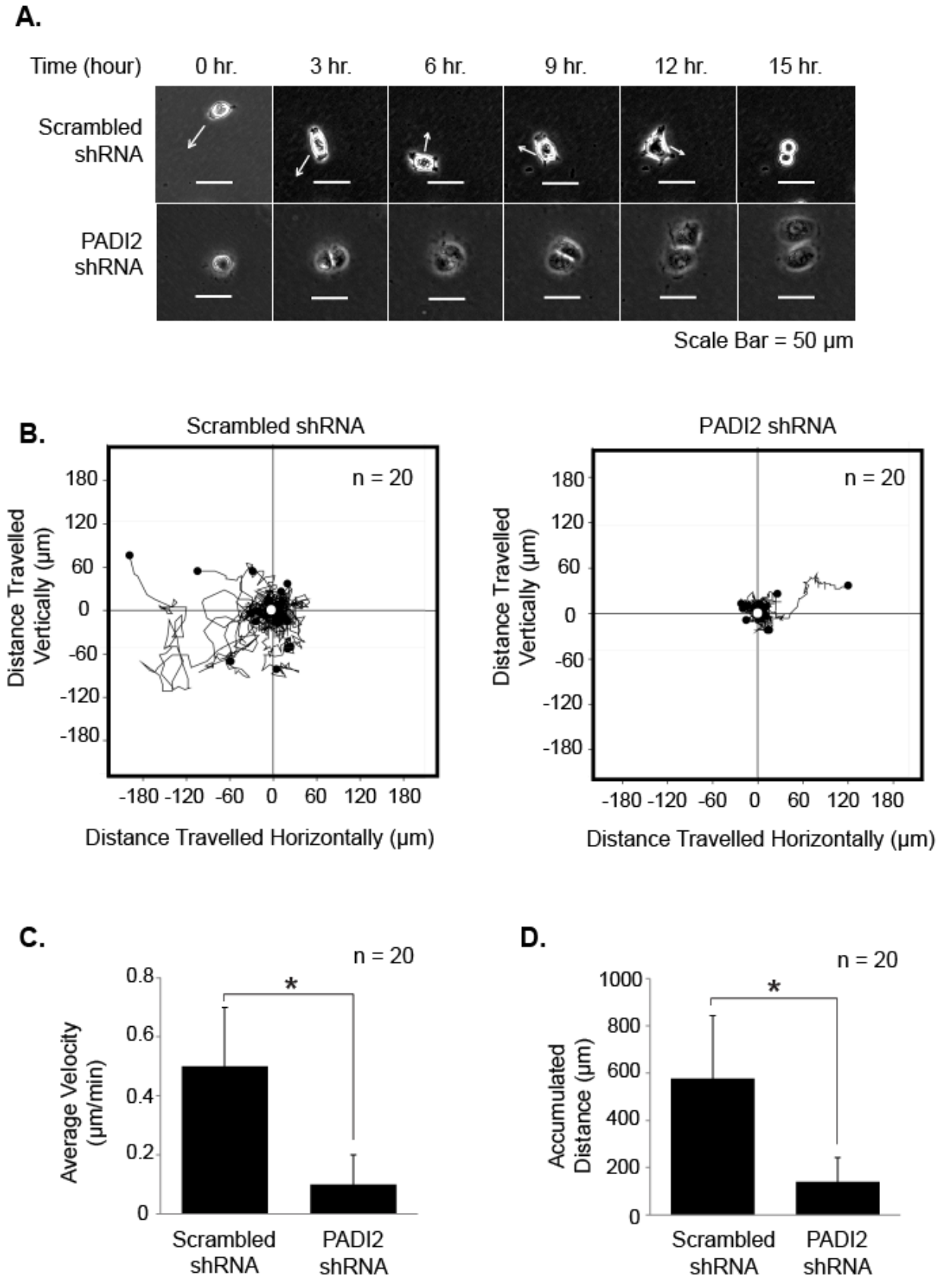
A.
Time (hour)
0 hr.
3 hr.
6 hr.
9 hr.
12 hr.
15 hr.
Scrambled shRNA
PADI2 shRNA
Scale Bar = 50 μm
B.
Scrambled shRNA
PADI2 shRNA
n = 20
Distance Travelled Vertically (μm)
Distance Travelled Horizontally (μm)
180
120
60
0
-60
-120
-180
C.
Average Velocity (μm/min)
0.8
0.6
0.4
0.2
0
*
D.
Accumulated Distance (μm)
1000
800
600
400
200
Scrambled shRNA
PADI2 shRNA

scrambled cells. These results suggest that PADI2 plays an important role in regulating cell migration.

Depletion of PADI2 reduces cell protrusion and downregulates cytoskeletal markers

Cells migrate by altering their shape and stiffness leading to a polarized and elongated phenotype (6). We next tested whether PADI2 depletion can alter the morphological changes that are required for cell migration. We found that *PADI2* depleted cells are less elongated and appeared flatter in shape and more tightly adhered to the underlying plate (extracellular matrix) **(Figure 3.4A, *white arrows*)**. Moreover, we found that *PADI2* depleted cells were predominantly grouped together rather than in single cells, again, suggesting that these cells may be more adherent. In contrast, the scrambled cells were elongated in shape with membrane ruffling at the edge of the cell protrusions **(Figure 3.4A, *black arrows*)**. In addition, we observed cells in the control group with up to five protrusions, thus highlighting their dynamic movement. Furthermore, we found enlarged nuclei in single, isolated *PADI2* depleted cells compared to scrambled cell **(Figure 3.4A and Figure 3.1D)**. However, when the cells were grouped or adhered to other cells, the nuclei of *PADI2* depleted cells were smaller in size.

Next, we tested whether the distinct changes in cell morphology caused by *PADI2* depletion was associated with cytoskeletal changes. More specifically, we tested for expression levels of the Rho family of GTPases, RhoA, Rac1, and Cdc42, as these actin cytoskeleton markers are known to regulate cell migration (24). Interestingly, we found a reduction in *RHOA*, *RAC*, and *CDC42* transcripts levels in the PADI2 depleted cells compared to the control cells. We found that there was a significant decrease in *RHOA* (38.0%), *RAC* (32.1%), and *CDC42* (30.3%) transcript levels in the *PADI2* depleted line compared to the control line (Figure 4B).

Figure 3.4: Depletion of PADI2 alters cell morphology of MCF10DCIS.com cells. (A) Representative images of scrambled-shRNA and PADI2-shRNA cells in culture. Scale bar = 200 μm. The square frames on the left images are enlarged on the middle and right images. The middle images show the morphology of cells when there are multiple cells growing together; images on right are the images depicting images of a single cell. The black arrow indicates the cell protrusion and membrane ruffling in the scrambled-shRNA cells. The white arrow shows the flat-like structure of the cytoplasmic region of the PADI2-shRNA cells. **(B)** Total RNA was isolated from scrambled-shRNA and PADI2-shRNA cells. Their *RHOA, RAC1, CDC42* mRNA levels were determined by qRT-PCR (SYBR) using scrambled-shRNA as a reference and β-actin normalization. Data were analyzed using the $2^{-\Delta\Delta C(t)}$ method and are expressed as the mean ± SD from three independent experiments (* $p < 0.05$). **(C)** The whole cell lysates of MCF10DCIS scrambled-shRNA and PADI2-shRNA cells were immunoblotted with RhoA, Rac1, and Cdc42. The blot was also proved with β-actin antibody to determine equal loading.

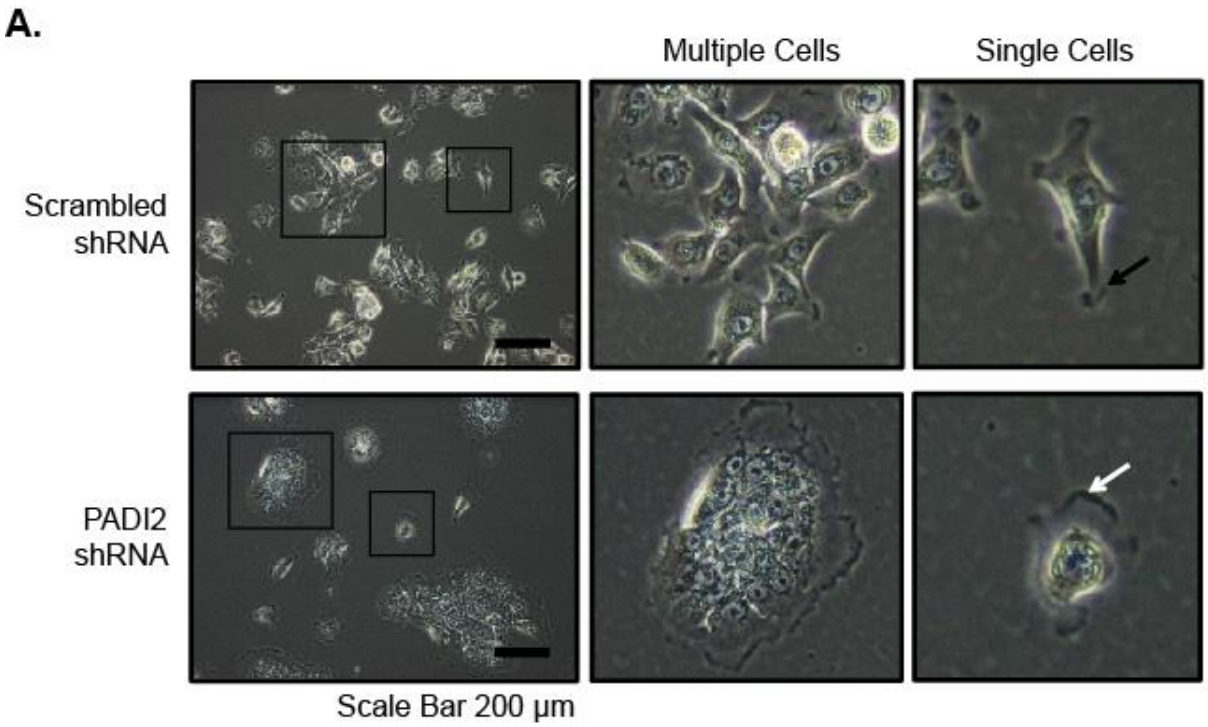
A.
Multiple Cells
Single Cells
Scrambled shRNA
PADI2 shRNA
Scale Bar 200 µm

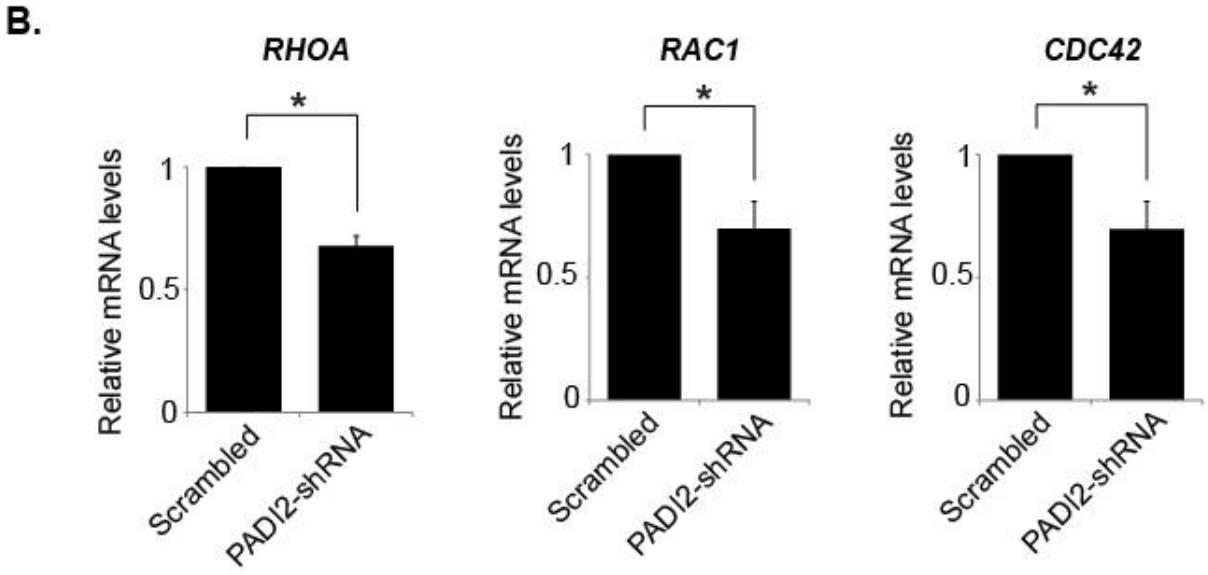
B.
RHOA
RAC1
CDC42
Relative mRNA levels
1
0.5
0
*
Scrambled
PADI2-shRNA

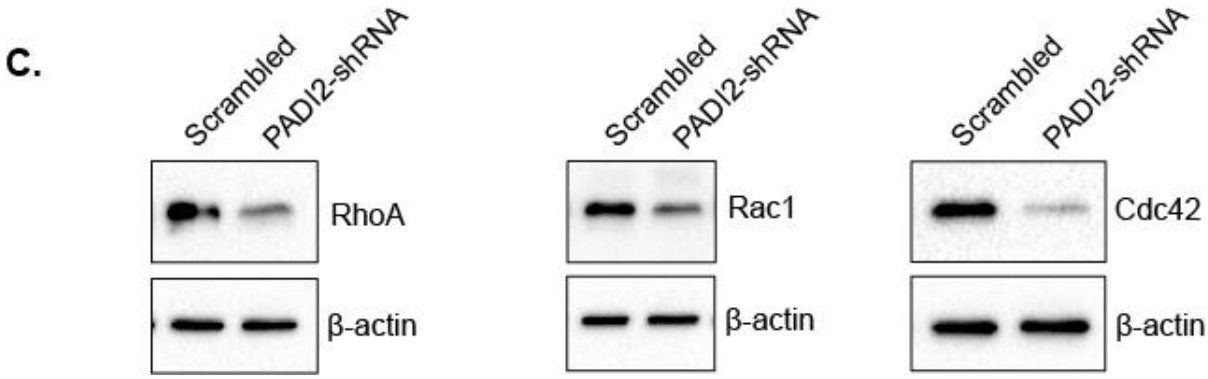
C.
Scrambled
PADI2-shRNA
RhoA
Rac1
Cdc42
β-actin

Furthermore, immunoblot assays confirmed our mRNA findings **(Figure 3.4C)**. Collectively, these results suggest that PADI2 promotes cell migration by modulating the cytoskeletal machinery that is required for cell motility.

Cell adhesion increases upon PADI2 depletion

Aside from changes in cell morphology, we also observed changes in the adhesive properties of the *PADI2* depleted cells. During the time course of the wound healing assay, we found that scrambled cells migrated into the wound following the initial scratch as described previously. Surprisingly, however, following wounding, the *PADI2* depleted cells appeared to contract away from the wound first before eventually filling the vacated area up to the point of the scratch **(Figure 3.5A)**. We next investigated the adhesive properties of single cells. In the PADI2 depleted cells, we found that, over time, independent cells would adhere to each other eventually forming cell clusters. In contrast, we found that the control cells would often detached from each and migrate independently **(Figure 3.5B)**. These observations suggested that PADI2 depletion may lead to the upregulation of cell-cell adhesion molecules, such as E-cadherin. We tested this hypothesis and found that depletion of PADI2 upregulates the expression of E-cadherin by approximately 5-fold **(Figure 3.5C)**. Together, these findings suggest that depletion of PADI2 suppresses cell migration by promoting the upregulation of molecules that are involved in cell-cell adhesion.

PADI2 may function within the EGF signaling pathway to regulate cell migration.

EGF signaling plays an important role in cancer cell polarization and migration. Therefore, we tested whether EGF may regulate PADI2 expression and activity and whether modulation of

Figure 3.5: Enhanced adhesion observed in PADI2-shRNA cells. (A) A scratch assays were performed on scrambled-shRNA and PADI2-shRNA cells. The cells were visualized and imaged using the wide-field microscope with built-in incubation chamber at time 0, 12, and 24 hours to determine the extent of the wound closure. The widths of the initial wounds are indicated by the lines. Arrow indicates the directional movement of the migrating cells. Scale bar = 200 μm. **(B)** Images of 2 to 3 scrambled-shRNA and PADI2-shRNA cells are taken at times 0, 6, and 12 hours using the wide-field microscope with built-in incubation chamber. Scale bar = 50 μm. **(C)** The whole cell lysates of scrambled-shRNA and PADI2-shRNA cells were immunoblotted with E-cadherin. The blot was also proved with β-actin antibody to determine equal loading. The intensity of the band was measured using ImageJ and is normalized to the scrambled-shRNA.

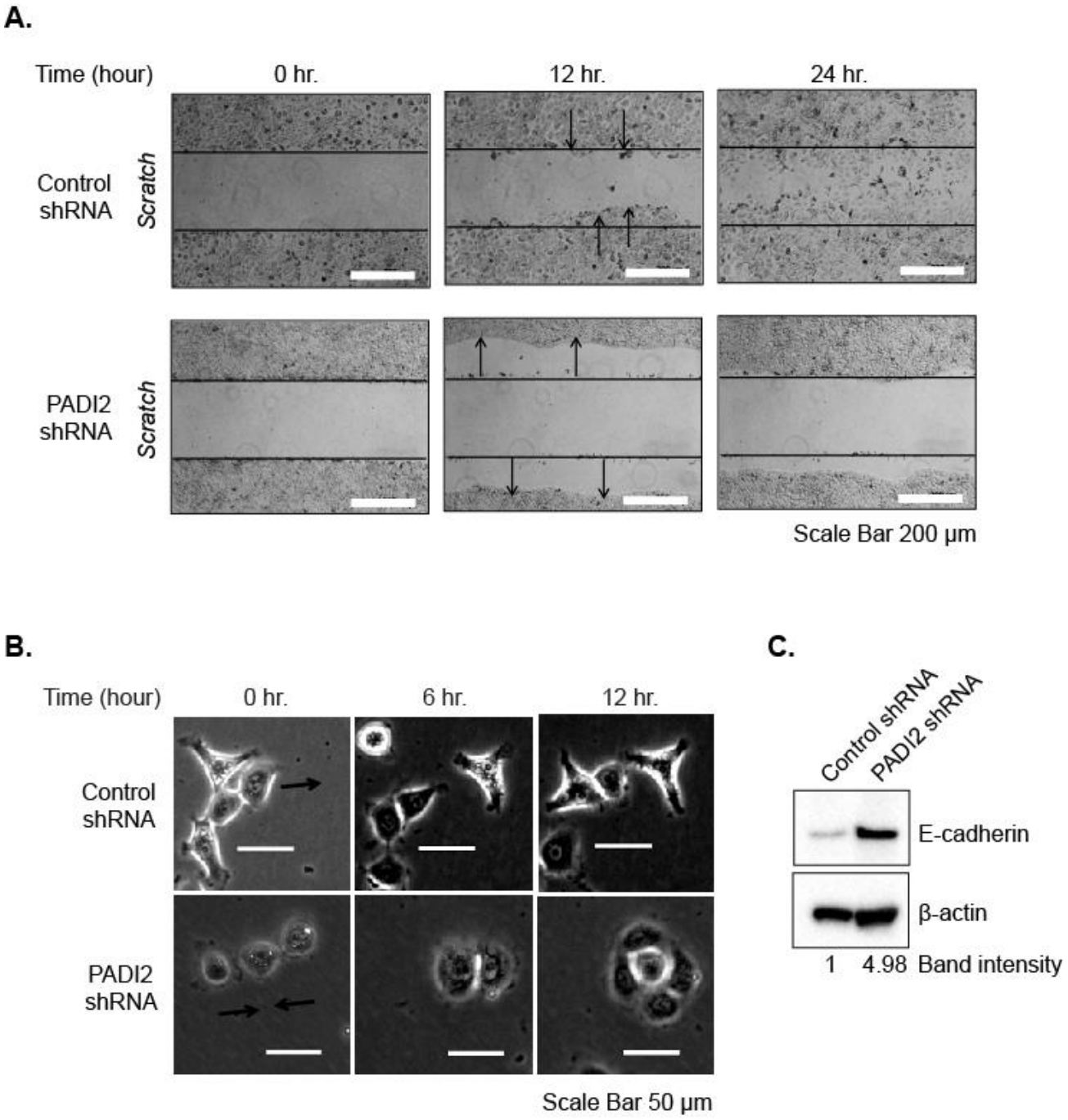
A.
Time (hour)
0 hr.
12 hr.
24 hr.
Control shRNA
Scratch
PADI2 shRNA
Scratch
Scale Bar 200 μm
B.
Time (hour)
0 hr.
6 hr.
12 hr.
Control shRNA
PADI2 shRNA
Scale Bar 50 μm
C.
Control shRNA
PADI2 shRNA
E-cadherin
β-actin
1
4.98
Band intensity

PADI2 activity may affect EGF-induced cell migration. We first tested the ability of EGF to induce cell migration in MCF10DCIS.com cells and observed robust enhancement of cell migration into the wound **(Figure 3.6A)** following EGF treatment, thus confirming that EGF promotes the migration of MCF10DCIS.com cells **(Figure 3.6B)**. We tested the effect of EGF treatment on PADI2 expression and activity. Immunofluorescent analysis found that treating MCF10DCIS.com cells with EGF (for 1 hour) appeared to increased PADI2 expression levels and also strongly increased levels of protein citrullination in these cells **(Figure 3.6C)**. Together, these data suggest that EGF-induced cell migration may be regulated by PADI2.

BB-Cl-Amidine suppresses EGF-induced cell migration

Since EGF stimulation appears to upregulate PADI2 expression and activity, we tested whether EGF-induced cell migration can be inhibited by targeting PADI2. Results show that the PADI inhibitor, BB-Cl-Amidine (32), suppressed EGF-induced migration of MCF10DCIS cells **(Figure 3.7A)**. Importantly, analysis of individual cells found that BB-Cl-Amidine treatment promoted the conversion of MCF10DCIS cells from an elongated fibroblast-like migratory phenotype to a more epithelial-like adherent phenotype which is similar to that of the PADI2 depleted cells **(Figure 3.7B)**.

We then tested whether BB-Cl-Amidine treatment increased the expression of the cell-cell adhesion molecule E-cadherin (*CDH1*) in MCF10DCIS.com cells. We found that MCF10DCIS.com cells expressed significantly higher levels of *CDH1* mRNA levels in the presence of BB-Cl-Amidine **(Figure 3.7C)**. Indirect immunofluorescence analysis supported our PCR results as we found that E-cadherin levels appeared to be higher in the BB-Cl-Amidine

Figure 3.6: Enhanced activity and expression of PADI2 observed in EGF treated MCF10DCIS.com cells. (A) A scratch assays were performed on serum-deprived MCF10DCIS.com cells treated without (*Untreated*) or with EGF. The MCF10DCIS.com cells were fixed 24 hours after striking the wound. The cells were then visualized using light microcopy to determine the extent of wound closure. **(B)** Serum-deprived MCF10DCIS.com cells were treated without (*Untreated*) or with EGF for 1 hour, and then immunofluorescent assays were performed on the cells using DAPI (nucleus), PADI2 antibody, and **(C)** pan-citrulline antibody. Scale bar = 50 μm.

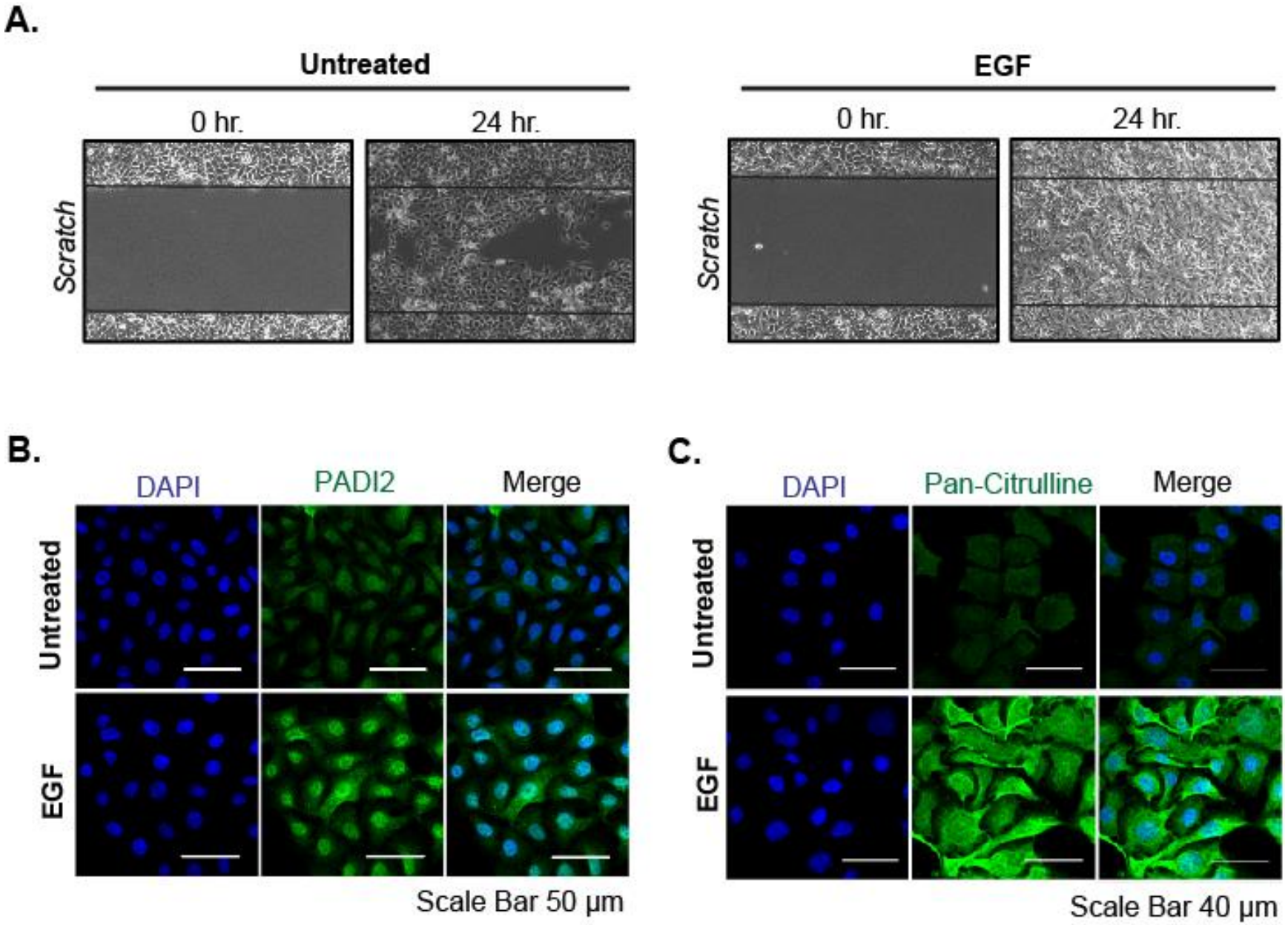
A.
Untreated
EGF
0 hr.
24 hr.
Scratch
B.
DAPI
PADI2
Merge
Untreated
EGF
Scale Bar 50 µm
C.
DAPI
Pan-Citrulline
Merge
Untreated
EGF
Scale Bar 40 µm

Figure 3.7: BB-Cl-Amidine treatment suppresses cell migration and enhances cell adhesion in MCF10DCIS.com cells. **(A)** A scratch assays were performed on serum-deprived MCF10DCIS.com cells treated without (*Untreated*), with EGF, with EGF and BB-Cl-Amidine, or with BB-Cl-Amidine alone. The MCF10DCIS.com cells were pre-treated with BB-Cl-Amidine for 23 hours and then EGF was added for 1 hour. This gives a total of 24 hours BB-Cl-Amidine treatment and 1 hour of EGF treatment. The cells were fixed using 4% paraformaldehyde 24 hours after striking the wound (24 hr.). The cells were then visualized and imaged using the light microscopy to determine the extent of the wound closure. The widths of the initial wounds are indicated by the lines. The cells were also fixed immediately after striking the wound (0 hr.) to indicate the size of the initial wounds. **(B)** MCF10DCIS.com cells were treated either with DMSO or 2 μM BB-Cl-Amidine. 1 hour after treatment, the cells were imaged using the light microscopy. Scale bar = 100 μm. **(C)** Total RNA was isolated from MCF10DCIS.com cells treated with either 0 (DMSO), 1, or 2 μM Tamoxifen. Their *CDH1* mRNA levels were determined by qRT-PCR (SYBR) using DMSO treated control cells as a reference and β-actin normalization. Data were analyzed using the $2^{-\Delta\Delta C(t)}$ method and are expressed as the mean ± SD from three independent experiments (* $p < 0.05$). **(D)** An immunofluorecent assay was performed on serum-deprived MCF10DCIS cells treated without (*Untreated*), with EGF, with EGF and BB-Cl-Amidine, or with BB-Cl-Amidine alone using an E-cadherin antibody and DAPI staining. The MCF10DCIS cells were pre-treated with BB-Cl-Amidine for 23 hours and then EGF was added for 1 hour. This gives a total of 24 hours BB-Cl-Amidine treatment and 1 hour of EGF treatment. Scale bar = 50 μm.

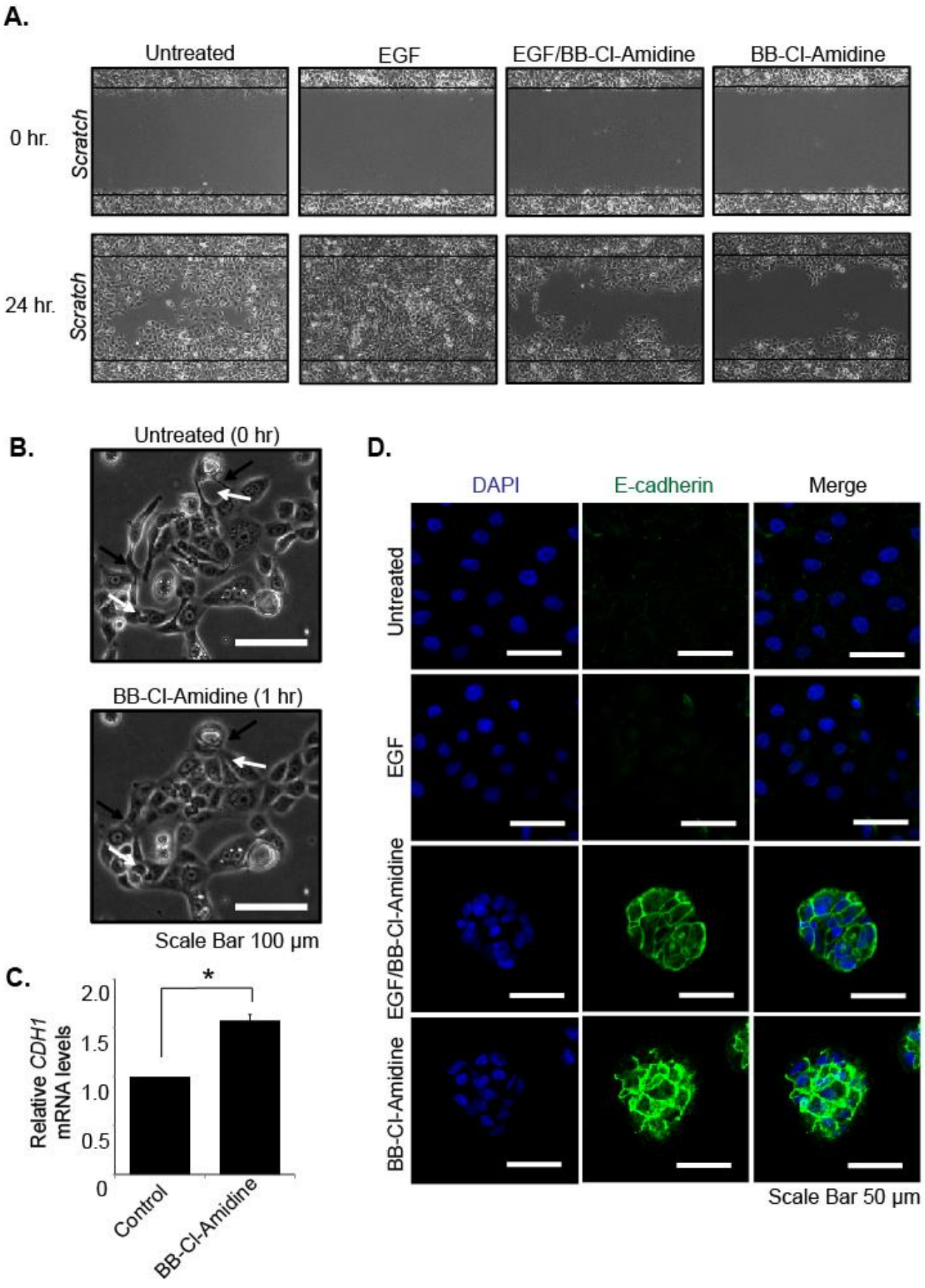
A.
Untreated
EGF
EGF/BB-Cl-Amidine
BB-Cl-Amidine
0 hr.
24 hr.
Scratch
Scratch
B.
Untreated (0 hr)
BB-Cl-Amidine (1 hr)
Scale Bar 100 µm
C.
Relative CDH1 mRNA levels
2.0
1.5
1.0
0.5
0
*
Control
BB-Cl-Amidine
D.
DAPI
E-cadherin
Merge
Untreated
EGF
EGF/BB-Cl-Amidine
BB-Cl-Amidine
Scale Bar 50 µm

treated cells **(Figure 3.7D)**. The increase was also observed in cells treated with BB-Cl-Amidine in the presence of EGF. As seen by the DAPI staining, the cells are in closer proximity to each other in the presence of BB-Cl-Amidine, further suggesting increased adhesion when PADI2 is depleted. These results suggest that one mechanism by which PADI2 activity promotes cell migration is by downregulating the expression of cell-cell adhesion molecules in an EGF-dependent manner.

Cl-Amidine treatment increases in vivo E-cadherin and GSK3β expression levels

Previously, we generated a DCIS mouse xenograft model and tested the effects of the first-generation PADI inhibitor, Cl-Amidine, on tumor growth (30). In this model system we consistently found that tumor cells in the Cl-amidine treated mice appeared to be less invasive and that the basement membranes of the ducts within the treated tumors were more intact **(Figure 3.8A)**. Therefore, we used this model system to test whether PADI inhibition may suppress tumor cell migration in vivo by promoting the upregulation of E-cadherin in the tumor cells.

Results show that E-cadherin expression appears to be strongly upregulated in the Cl-Amidine treated group compared to the control group **(Figure 3.8B)**. This suggests that Cl-Amidine treatment maintained the epithelial-like state of the cells and suppressed tumor cells from migrating out from the mammary duct. Interestingly, In addition to E-cadherin, we also observed a striking upregulation of GSK3β expression in Cl-Amidine treated DCIS xenograft mice **(Figure 3.8C)**. GSK3β is known to play an important role in suppressing the EMT via its role in promoting E-cadherin expression, thus it is possible that PADI2 functions upstream of the GSK3β signaling pathway to regulate E-cadherin expression **(Figure 3.8D)** (33).

Figure 3.8: Cl-Amidine treatment increases E-cadherin and GSK3β expressions in MCF10DCIS.com xenograft model. (A) PAS staining of representative mammary tissue sections of MCF10DCIS xenograft mice treated without (PBS) or with Cl-Amidine (50 mg/kg/day) for 2 weeks. To generate the MCF10DCIS.com xenograft, MCF10DCIS.com cells (1×10^6) were injected subcutaneously into female nude (nu/nu) mice. When the tumor volume is approximately 200 mm^3, mice were treated without (PBS) or with Cl-Amidine (50 mg/kg/day) for 2 weeks. The treatment was performed with intraperitoneal injections. After 2 weeks, the mice were sacrificed and the PAS stained sections were prepared and imaged using the bright field optics of the Axiophot inverted microscope. Scale bar = 200 μm. **(B)** Immunofluorescent images of mouse mammary tissue sections of MCF10DCIS.com xenograft mice treated without (PBS) or with Cl-Amidine (50 mg/kg/day) for 2 weeks stained with DAPI (nucleus) and E-cadherin antibody. Scale bar = 50 μm. **(C)** Immunohistochemistry images of mouse mammary tissue sections of MCF10DCIS.com xenograft mice treated without (PBS) or with Cl-Amidine (50 mg/kg/day) for 2 weeks. Samples were stained with GSK3β antibody using citrate for unmasking and DAB as a substrate and counterstained with hematoxylin. Scale bar = 100 μm. **(D)** Schematic diagram of the proposed signaling pathways of PADI2.

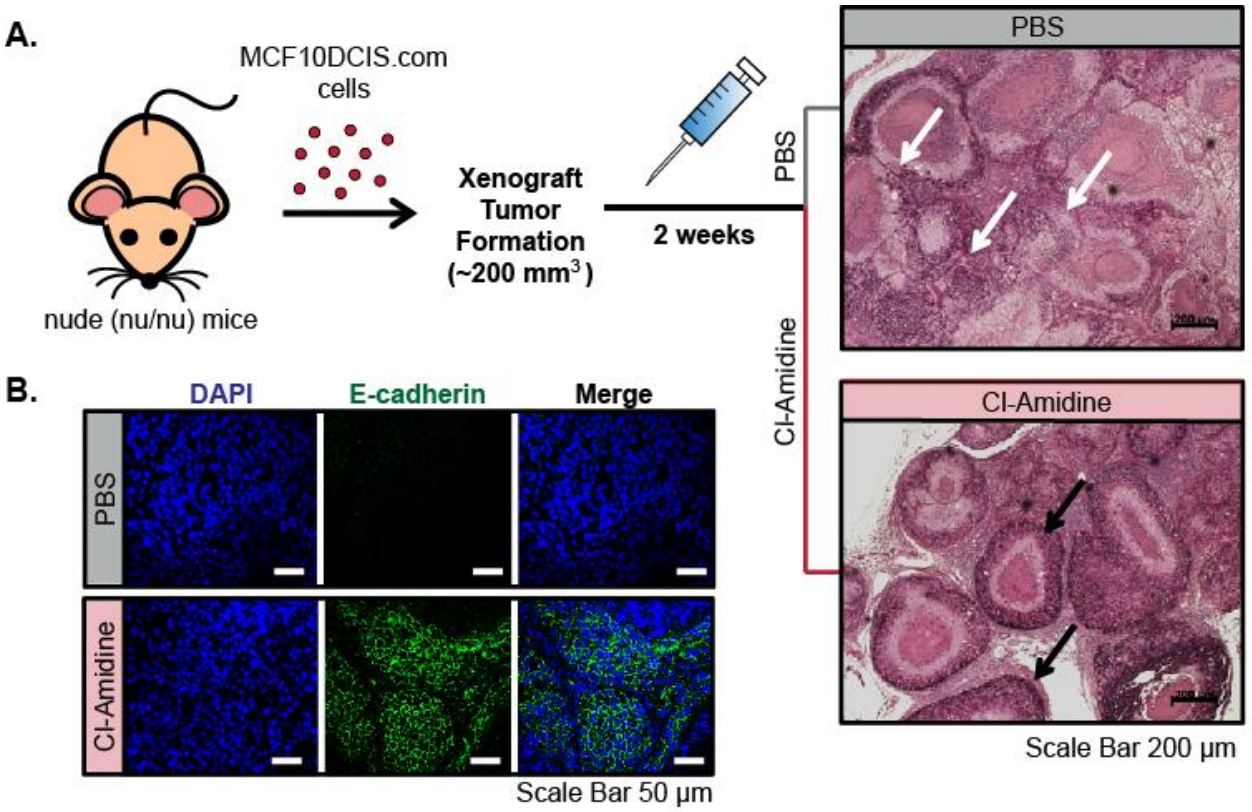
A.
MCF10DCIS.com cells
nude (nu/nu) mice
Xenograft Tumor Formation (~200 mm3)
2 weeks
PBS
Cl-Amidine
PBS
Cl-Amidine
B.
DAPI
E-cadherin
Merge
PBS
Cl-Amidine
Scale Bar 50 µm
Scale Bar 200 µm

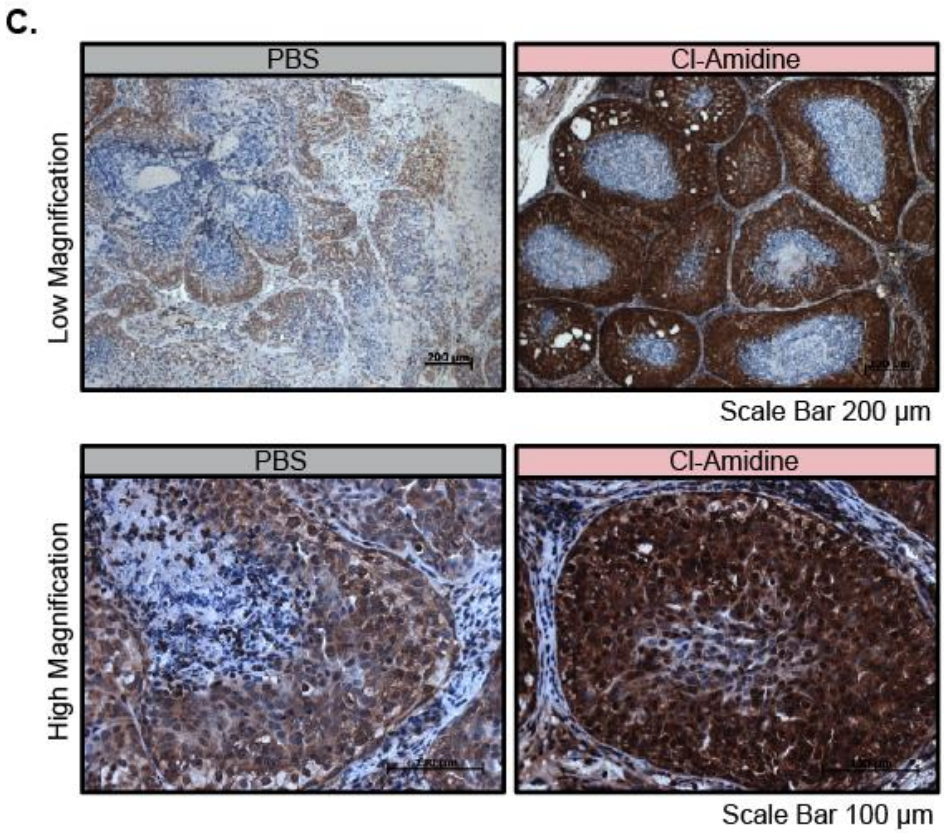
C.
Low Magnification
High Magnification
PBS
Cl-Amidine
Scale Bar 200 µm
Scale Bar 100 µm

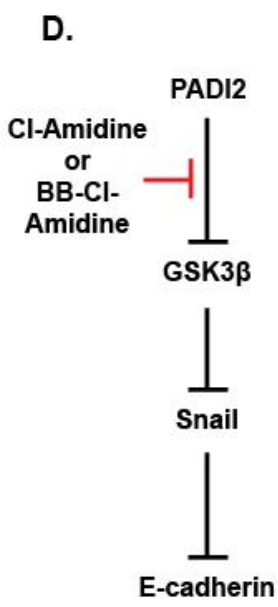
D.
PADI2
Cl-Amidine or BB-Cl-Amidine
GSK3β
Snail
E-cadherin

PADI2 overexpression enhances mammary branching

EGF and its receptor EGFR are known to play critical roles in mammary gland morphogenesis during early development (34-36). Given the observed links between PADI2 and EGF signaling, we tested whether overexpression of PADI2 in the mammary gland may affect mammary gland development. At 8 weeks of age, we found a 1.7 fold increase in ductal branching in the PADI2 overexpressed mice compared to the wild-type controls **(Figure 3.9A)**. Histological evaluation of the mammary tree in adult females finds that the epithelial cells are hyperplastic in nature with poorly formed ductal structures **(Figure 3.9B)**. Together, these data PADI2 suggest that PADI2 plays an important role in mammary gland morphogenesis during development.

BB-Cl-Amidine suppresses ductal invasion in an *ex vivo* model of mammary gland development.

We next utilized a three-dimensional organoid culture system to investigate the effect of PADI2 inhibition on mammary gland morphogenesis *in vivo* **(Figure 3.10A)**. We first induced ductal morphogenesis using EGF and found a robust increase in the ductal elongation compared to the control organoid **(Figure 3.10B)**. We found that when the organoids were treated with 0.5 μM BB-Cl-Amidine, there was a striking reduction in EGF-induced ductal elongation **(Figure 3.10B)** with 5 μM BB-Cl-Amidine completely blocking ductal elongation **(Figure 3.10B)**.

Figure 3.9: Mammary Gland Development in 8 weeks old female wild type versus MMTV-PADI2 mice in diestrus. (A) Alveolar bud branches of 8 weeks old female wild type FVB and MMTV-PADI2 mice in diestrus (n=3) were quantified (20x). Panels show representative images of the alveolar tree stained with carmine-alum in wild type and MMTV-PADI2 mice. **(B)** Fomalin-fixed- paraffin embedded samples of mammary gland stained with H&E at 5x (low magnification) and 20x (high magnification). Note the normal appearance of acini in WT mice showing typical epithelial layer and lumen. In MMTV-PADI2 mice the acini are less organized, more frequent and the lumen appears to be indistinct.

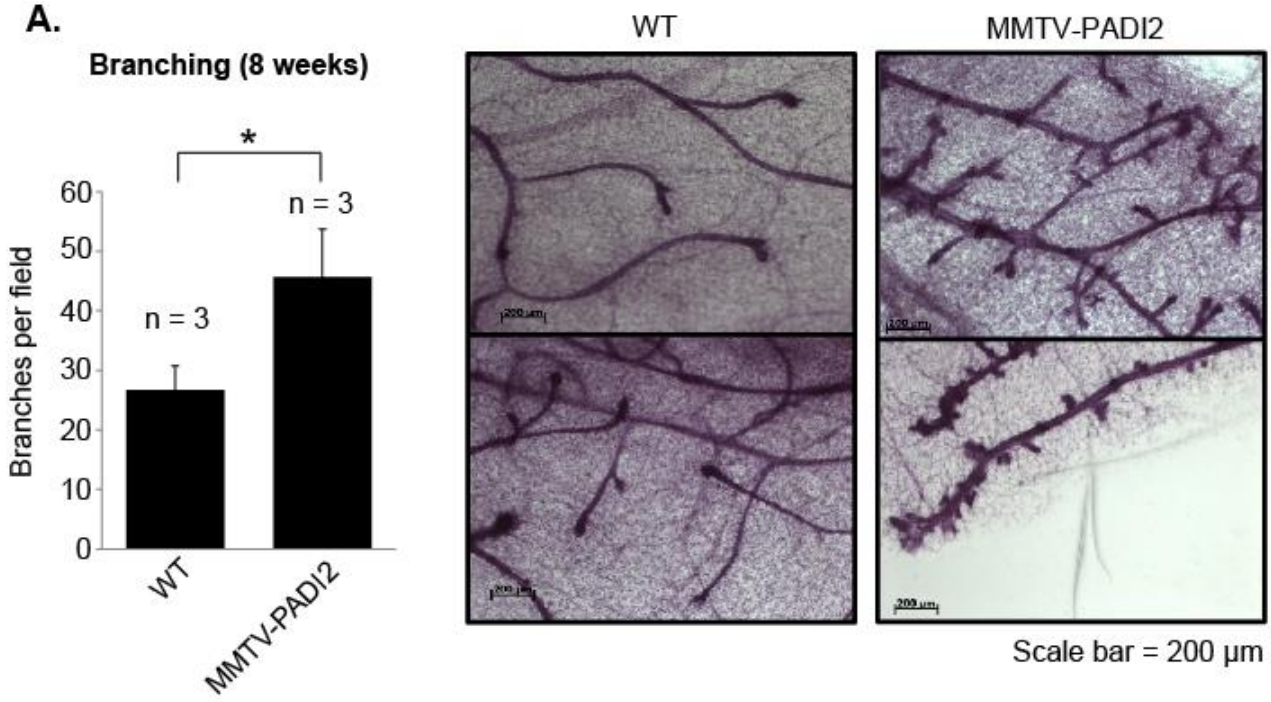
A.
Branching (8 weeks)
*
n = 3
n = 3
Branches per field
60
50
40
30
20
10
0
WT
MMTV-PADI2
WT
MMTV-PADI2
Scale bar = 200 µm

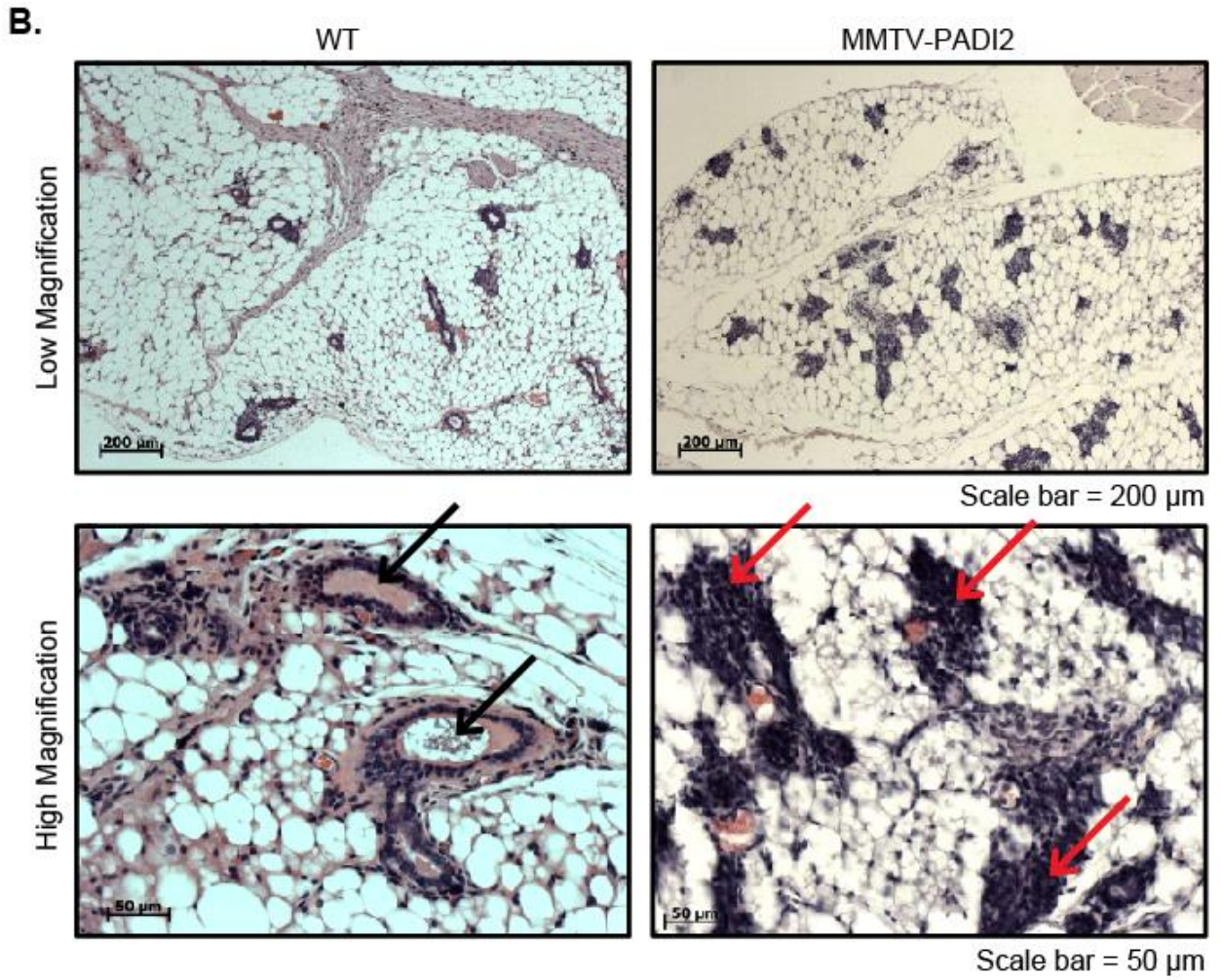
B.
WT
MMTV-PADI2
Low Magnification
200 µm
200 µm
Scale bar = 200 µm
High Magnification
50 µm
50 µm
Scale bar = 50 µm

Figure 3.10: EGF induces while BB-Cl-Amidine inhibits ductal invasion and elongation in primary mouse mammary organoids. (A) Schematic diagram depicting the preparation of primary mouse mammary organoid samples from 8 weeks old female FVB mice (n=3). **(B)** Collected mammary organoids were cultured in matrigel and were treated with either control (DMSO), EGF, EGF with 0.5 μM BB-Cl-Amidine, or EGF with 5 μM BB-Cl-Amidine. After 6 days of culture, the samples were imaged using Zeiss Axio Observer inverted microscope.

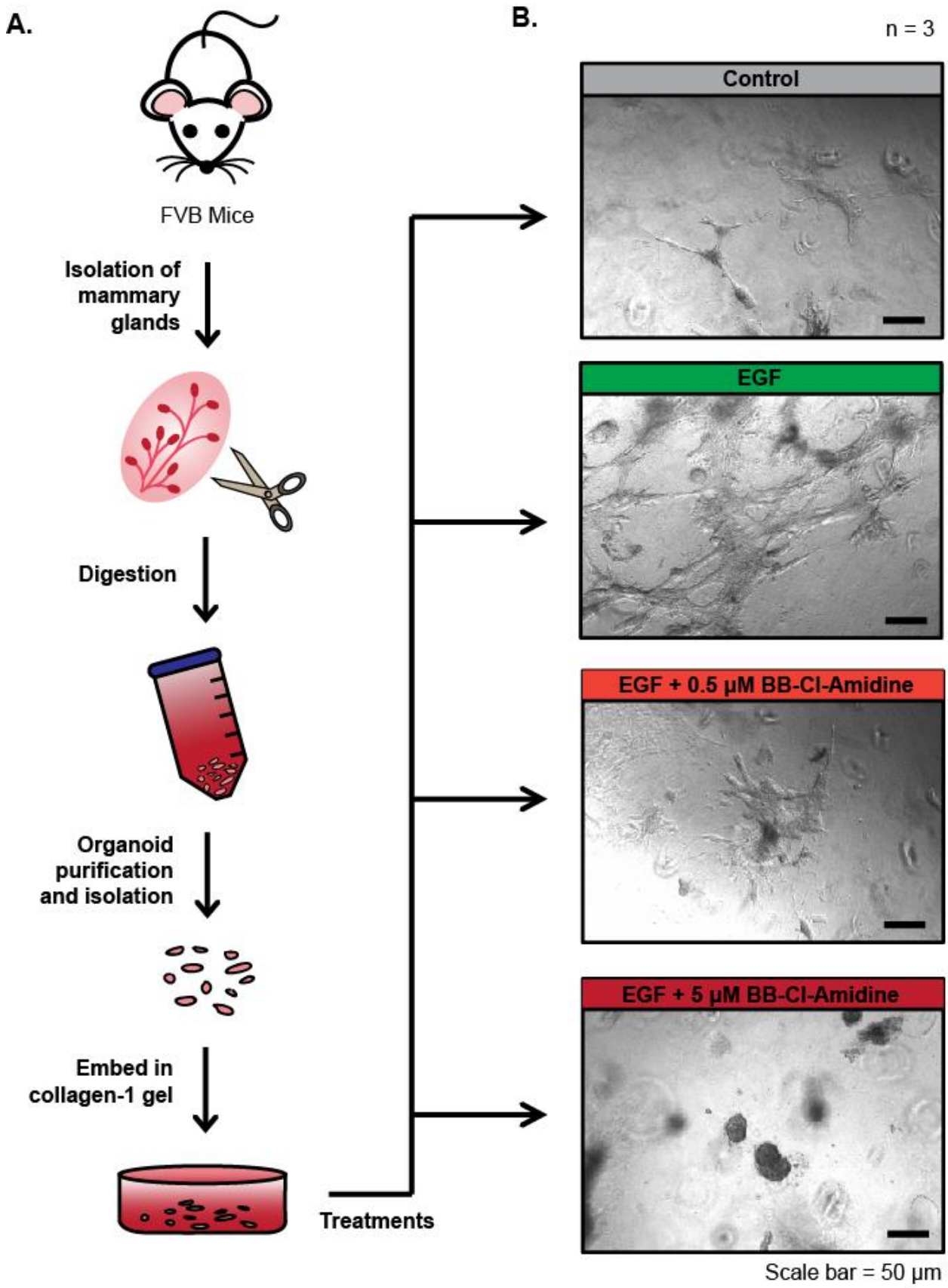
A.
FVB Mice
Isolation of mammary glands
Digestion
Organoid purification and isolation
Embed in collagen-1 gel
Treatments
B.
n = 3
Control
EGF
EGF + 0.5 µM BB-Cl-Amidine
EGF + 5 µM BB-Cl-Amidine
Scale bar = 50 µm

CONCLUSIONS

In this study, we perform *in vitro* and *in vivo* assays to test the involvement of PADI2 in cellular migration observed during mammary tumorigenesis. We find that PADI2 depletion or inhibition suppresses cell migration and alters the morphology of MCF10DCIS.com cells. In addition, we find that PADI2 depletion suppresses the expression of the cytoskeletal regulatory proteins RhoA, Rac1, and Cdc42. This results in changes in cell morphology from a mesenchymal-like structure to epithelial-like structure. In addition, the PADI2 depleted cells acquire higher adhesive properties via induction of E-cadherin expression, often found in non-migratory cells. Depletion of PADI2 activity via the use of inhibitor, BB-Cl-Amidine, greatly suppressed the migratory ability of the MCF10DCIS.com cells and enhanced E-cadherin expression even in the presence of EGF. *In vivo*, PADI2 overexpression resulted in mammary hyperbranching and enhanced infiltration of epithelial cells into the alveoli of the mammary gland. Our *ex vivo* organoid study found that PAD2 inhibition suppresses EGF inducted ductal invasion. Together, these results support the hypothesis that PADI2 plays a critical role in mammary development and mammary cancer progression.

MATERIALS AND METHODS

Materials

The following antibodies were used: anti-PADI2 (12110-1-AP, Proteintech), anti-E-cadherin (ab15148, Abcam), anti-RhoA (2117, Cell Signaling), anti-Rac1 (05-389, Millipore), anti-Cdc42 (07-1466, Millipore), anti-GSK3β (ab18893; Abcam), anti-pan-Citrulline (07-377, Millipore), and anti-β-actin (ab8227, Abcam) antibodies. BB-Cl-Amidine and Cl-Amidine were generous gifts from Dr. Paul Thompson (University of Massachusetts Medical School).

Cell Culture and Lentivirus Generation

MCF10DCIS.com cells were obtained from Dr. Fred Miller (Barbara Ann Karmanos Cancer Institute, Detroit, MI, USA). Generation of MCF10DCIS.com cells has been described (37). Cells were cultured in DMSO/F-12 medium containing 5% house serum and 1% penicillin streptomycin. Scrambled control shRNA and PADI2 shRNA of MCF10DCIS.com cells were grown in the described MCF10DCIS.com media containing 2μg/ml of puromycin. MCF10DCIS.com cells were stably transduced with lentivirus expressing either shRNA scrambled control or PADI2 shRNA. Mission shRNA lentivirus plasmids for control shRNA (SHC002) and PADI2 shRNA (TRCN0000051447; NM_007365.1-995s1c1) from Sigma were used. The lentiviruses were generated and transduced according to the manufacturer's instructions (Sigma). Selection of the stable clones was accomplished via treatment with 2 μg/ml of puromycin for at least 2 weeks.

Immunoblot Analysis

Whole cell lysates were resolved by SDS-PAGE followed by transfer to PVDF membrane. The membranes were incubated overnight with primary antibodies diluted in TBST overnight in 4 °C using the following antibody concentrations: anti-PADI2 (1:1000), anti-E-cadherin (1:1000), anti-RhoA (1:1000), anti-Rac1 (1:1000), and anti-Cdc42 (1:1000) antibodies. To ensure equal loading, membranes were probed with anti-β-actin (1:6000) antibody. The primary antibodies were detected with HRP-conjugated secondary antibodies and were exposed to ECL reagents.

RNA Isolation and Quantitative Real-Time PCR

RNA was purified using RNeasy Kit (Qiagen) and reverse-transcribed using High Capacity RNA-to-cDNA kit (Applied Biosystems) according to the manufacturer's protocol. Real-time quantitative PCR analysis was performed using primers described in McElwee et al. (38) and Zhang et al. (39): *PADI2* Forward (5'-TCTCAGGCCTGGTCTCCA-3') and Reverse (5'-AAGATGGGAGTCAGGGGAAT-3'); E-cadherin (*CDH1*) Forward (5'-TGGAGGAATTCTTGCTTTGC-3') and Reverse (5'- CGCTCTCCTCCGAAGAAAC-3'); β-actin (*ACTB*) Forward (5'- CCAACCGCGAGAAGATGA-3') and Reverse (5'-CCAGAGGCGTACAGGGATAG-3'); RhoA (*RHOA*) Forward (5'-CCAAATGTGCCCATCATCCTAGTTG-3') and Reverse (5'-TCCGTCTTTGGTCTTTGCTGAACAC-3'); Rac1 (*RAC1*) Forward (5'-CAATGCGTTCCCTGGAGAGTACA-3') and Reverse (5'-ACGTCTGTTTGCGGGTAGGAGAG-3'); Cdc42 (*CDC42*) Forward (5'-TAACTCACCACTGTCCAAAGACTCC-3') and Reverse (5'-CCTCATCAAACACATTCTTCAGACC-3') and Power SYBR Green PCR Master Mix (Applied Bioystems). The samples were normalized to β-actin.

Immunofluorescence (IF) and Immunohistochemistry (IHC)

Cells were fixed with 4% paraformaldehyde for 15 minutes and were permeabilized and blocked with PBS containing 0.1% Triton X-100 and 10% BSA. Cells were incubated overnight with indicated primary antibodies in 1:100 dilutions in 4 °C. Cells were rinsed with PBS and were incubated with secondary antibody diluted in PBS containing DAPI (1:50,000) for 1 hour. Cells were washed with PBS and mounted using gold antifade mounting reagent. IF and IHC of tissue sections were prepared using a standard protocol as described previously (40).

Cell Migration (scratch or wound healing assays)

MCF10DCIS.com cells expressing scrambled shRNA or PADI2 shRNA were grown to confluence. A wound was generated on a cover slip using a pipette tip and the culture media were changed to remove detached cells. Eighteen or twenty-four hours later, the cells were fixed for 12 minutes with 4% paraformaldehyde, washed with PBS, and visualized by light microscopy. When examining the effect of EGF or BB-Cl-Amidine on cell migration, the MCF10DCIS.com cells were grown to confluence, and a wound was struck and the detached cells were removed. New media containing the following treatments were added: control (DMSO), EGF (100 ng/ml), BB-Cl-Amidine (0.5 μM), or both EGF (100 ng/ml) and BB-Cl-Amidine (0.5 μM). For live cell-imaging of cell migration, after the wound was struck and the detached cells were removed, the cells were imaged every 10 minutes over the duration of 24 hours.

Live cell imaging to track single or multi cell migration assay

Scrambled shRNA and PADI2 shRNA MCF10DCIS.com cells were plated lightly in tissue culture flask and cultured overnight in cell culture incubator. Once the cells adhered to the bottom of the flask, the flask containing the cells was transferred to the Zeiss Axio Observer inverted microscope with built-in incubator. The Axiovision software was used to image the cells every 10 minutes for the duration of 15 hours.

Generation of MCF10DCIS.com xenograft mice

MCF10DCIS.com xenograft mice were generated and treated with PBS or Cl-Amidine (50 mg/kg/day) using the protocol described previously (30).

Mammary Gland Development and PADI2 in vivo

Wild type (FVB) and PADI2 overexpressing (MMTV-PADI2) 8 week old female mice were used to examine differences in mammary gland development under the influence of increased PADI2 expression *in vivo*. The derivation of MMTV-PADI2 mice has been described previously (38). The estrous cycle of mice was determined by vaginal flushes and cytological examination and only those in diestrous were used for mammary harvest. Mice were sacrificed by CO_2 inhalation and both mammary glands were removed as described by Plante et al. (41). One gland was fixed in 10% neutral buffered formalin, processed and embedded in paraffin for sectioning. Five micron sections were stained with hematoxalin and eosin (H&E). The other gland was fixed in Carnoy's, stained with carmine alum and whole mounted on a slide (41) for measurement of ductal elongation and alveolar branching. Images at 5x and 20x were obtained of H&E stained slides using Axiovision software on a Zeiss Axio Observer inverted microscope equipped with an Axiocam color CCD camera. To measure branching, whole mounts were imaged at 0.8x and 5x and branching was quantified on images using ImageJ software by counting the number of branching points (nodes) in three different and defined areas of 250 X 150 pixels for each tissue sample. All experimental procedures using mice followed recommended guidelines and were approved by the Institutional Animal Care and Use Committee at Cornell University.

Ductal Invasion and Elongation using Primary Mouse Mammary Organoids

Primary mouse mammary organoids were prepared using the protocol described in (42). 8 weeks mice were sacrificed and mammary glands were isolated. Isolated mammary glands were cut and digested using digestion buffer (2 g/l trypsin, 2 g/l collagenase type-iv, 5 % (v/v) FBS, 5 µg/ml insulin in DMEM/F12 medium) and incubated on shaker at 37°C rotating at 100 rpm for 30 minutes. The centrifuged samples have 3 layers; the top layer (fat layer), middle layer (digestion buffer), and bottom layer (organoid). Organoids are collected, purified, and enriched. After organoid collection, the organoids are embedded in matrigel containing 8 wells-tissue slide chambers. 24 hours later, the samples were treated either with DMSO Control, EGF (10ng/ml), EGF + 0.5 uM BB-Cl-Amidine, or 5 uM BB-Cl-Amidine. The media containing the treatments were replaced every 3 days. The samples were imaged using Zeiss Axio Observer inverted microscope after 6 days.

REFERENCES

1. Cyster, J. G. (2005) Chemokines, sphingosine-1-phosphate, and cell migration in secondary lymphoid organs. *Annu Rev Immunol* **23**, 127-159

2. Luster, A. D., Alon, R., and von Andrian, U. H. (2005) Immune cell migration in inflammation: present and future therapeutic targets. *Nat Immunol* **6**, 1182-1190

3. Aman, A., and Piotrowski, T. (2010) Cell migration during morphogenesis. *Dev Biol* **341**, 20-33

4. Friedl, P., and Wolf, K. (2003) Tumour-cell invasion and migration: diversity and escape mechanisms. *Nat Rev Cancer* **3**, 362-374

5. Yamaguchi, H., Wyckoff, J., and Condeelis, J. (2005) Cell migration in tumors. *Curr Opin Cell Biol* **17**, 559-564

6. Lauffenburger, D. A., and Horwitz, A. F. (1996) Cell migration: a physically integrated molecular process. *Cell* **84**, 359-369

7. Raftopoulou, M., and Hall, A. (2004) Cell migration: Rho GTPases lead the way. *Dev Biol* **265**, 23-32

8. Rohatgi, R., Ma, L., Miki, H., Lopez, M., Kirchhausen, T., Takenawa, T., and Kirschner, M. W. (1999) The interaction between N-WASP and the Arp2/3 complex links Cdc42-dependent signals to actin assembly. *Cell* **97**, 221-231

9. Adams, J. C. (2001) Cell-matrix contact structures. *Cell Mol Life Sci* **58**, 371-392

10. Parsons, J. T., Horwitz, A. R., and Schwartz, M. A. (2010) Cell adhesion: integrating cytoskeletal dynamics and cellular tension. *Nat Rev Mol Cell Biol* **11**, 633-643

11. Burridge, K., and Chrzanowska-Wodnicka, M. (1996) Focal adhesions, contractility, and signaling. *Annu Rev Cell Dev Biol* **12**, 463-518

12. Gudjonsson, T., Adriance, M. C., Sternlicht, M. D., Petersen, O. W., and Bissell, M. J. (2005) Myoepithelial cells: their origin and function in breast morphogenesis and neoplasia. *J Mammary Gland Biol Neoplasia* **10**, 261-272

13. Vargo-Gogola, T., and Rosen, J. M. (2007) Modelling breast cancer: one size does not fit all. *Nat Rev Cancer* **7**, 659-672

14. Foroni, C., Broggini, M., Generali, D., and Damia, G. (2012) Epithelial-mesenchymal transition and breast cancer: role, molecular mechanisms and clinical impact. *Cancer Treat Rev* **38**, 689-697

15. Thiery, J. P., Acloque, H., Huang, R. Y., and Nieto, M. A. (2009) Epithelial-mesenchymal transitions in development and disease. *Cell* **139**, 871-890

16. Onder, T. T., Gupta, P. B., Mani, S. A., Yang, J., Lander, E. S., and Weinberg, R. A. (2008) Loss of E-cadherin promotes metastasis via multiple downstream transcriptional pathways. *Cancer Res* **68**, 3645-3654

17. Vincent, T., Neve, E. P., Johnson, J. R., Kukalev, A., Rojo, F., Albanell, J., Pietras, K., Virtanen, I., Philipson, L., Leopold, P. L., Crystal, R. G., de Herreros, A. G., Moustakas, A., Pettersson, R. F., and Fuxe, J. (2009) A SNAIL1-SMAD3/4 transcriptional repressor complex promotes TGF-beta mediated epithelial-mesenchymal transition. *Nat Cell Biol* **11**, 943-950

18. Wang, H., Quah, S. Y., Dong, J. M., Manser, E., Tang, J. P., and Zeng, Q. (2007) PRL-3 down-regulates PTEN expression and signals through PI3K to promote epithelial-mesenchymal transition. *Cancer Res* **67**, 2922-2926

19. Fuxe, J., Vincent, T., and Garcia de Herreros, A. (2010) Transcriptional crosstalk between TGF-beta and stem cell pathways in tumor cell invasion: role of EMT promoting Smad complexes. *Cell Cycle* **9**, 2363-2374

20. Stephens, L., Ellson, C., and Hawkins, P. (2002) Roles of PI3Ks in leukocyte chemotaxis and phagocytosis. *Curr Opin Cell Biol* **14**, 203-213

21. Kraynov, V. S., Chamberlain, C., Bokoch, G. M., Schwartz, M. A., Slabaugh, S., and Hahn, K. M. (2000) Localized Rac activation dynamics visualized in living cells. *Science* **290**, 333-337

22. Ridley, A. J. (2001) Rho GTPases and cell migration. *J Cell Sci* **114**, 2713-2722

23. Nobes, C. D., and Hall, A. (1995) Rho, rac, and cdc42 GTPases regulate the assembly of multimolecular focal complexes associated with actin stress fibers, lamellipodia, and filopodia. *Cell* **81**, 53-62

24. Jaffe, A. B., and Hall, A. (2005) Rho GTPases: biochemistry and biology. *Annu Rev Cell Dev Biol* **21**, 247-269

25. Stadler, S. C., Vincent, C. T., Fedorov, V. D., Patsialou, A., Cherrington, B. D., Wakshlag, J. J., Mohanan, S., Zee, B. M., Zhang, X., Garcia, B. A., Condeelis, J. S., Brown, A. M., Coonrod, S. A., and Allis, C. D. (2013) Dysregulation of PAD4-mediated citrullination of nuclear GSK3beta activates TGF-beta signaling and induces epithelial-to-mesenchymal transition in breast cancer cells. *Proc Natl Acad Sci U S A* **110**, 11851-11856

26. Vossenaar, E. R., Zendman, A. J., van Venrooij, W. J., and Pruijn, G. J. (2003) PAD, a growing family of citrullinating enzymes: genes, features and involvement in disease. *Bioessays* **25**, 1106-1118

27. Senshu, T., Akiyama, K., Kan, S., Asaga, H., Ishigami, A., and Manabe, M. (1995) Detection of deiminated proteins in rat skin: probing with a monospecific antibody after modification of citrulline residues. *J Invest Dermatol* **105**, 163-169

28. Horibata, S., Coonrod, S. A., and Cherrington, B. D. (2012) Role for peptidylarginine deiminase enzymes in disease and female reproduction. *J Reprod Dev* **58**, 274-282

29. Mohanan, S., Cherrington, B. D., Horibata, S., McElwee, J. L., Thompson, P. R., and Coonrod, S. A. (2012) Potential role of peptidylarginine deiminase enzymes and protein citrullination in cancer pathogenesis. *Biochem Res Int* **2012**, 895343

30. McElwee, J. L., Mohanan, S., Griffith, O. L., Breuer, H. C., Anguish, L. J., Cherrington, B. D., Palmer, A. M., Howe, L. R., Subramanian, V., Causey, C. P., Thompson, P. R., Gray, J. W., and Coonrod, S. A. (2012) Identification of PADI2 as a potential breast cancer biomarker and therapeutic target. *BMC Cancer* **12**, 500

31. Cherrington, B. D., Zhang, X., McElwee, J. L., Morency, E., Anguish, L. J., and Coonrod, S. A. (2012) Potential role for PAD2 in gene regulation in breast cancer cells. *PLoS One* **7**, e41242

32. Knight, J. S., Subramanian, V., O'Dell, A. A., Yalavarthi, S., Zhao, W., Smith, C. K., Hodgin, J. B., Thompson, P. R., and Kaplan, M. J. (2015) Peptidylarginine deiminase inhibition disrupts NET formation and protects against kidney, skin and vascular disease in lupus-prone MRL/lpr mice. *Ann Rheum Dis* **74**, 2199-2206

33. Doble, B. W., and Woodgett, J. R. (2007) Role of glycogen synthase kinase-3 in cell fate and epithelial-mesenchymal transitions. *Cells Tissues Organs* **185**, 73-84

34. Bray, K., Gillette, M., Young, J., Loughran, E., Hwang, M., Sears, J. C., and Vargo-Gogola, T. (2013) Cdc42 overexpression induces hyperbranching in the developing mammary gland by enhancing cell migration. *Breast Cancer Res* **15**, R91

35. Troyer, K. L., and Lee, D. C. (2001) Regulation of mouse mammary gland development and tumorigenesis by the ERBB signaling network. *J Mammary Gland Biol Neoplasia* **6**, 7-21

36. Sebastian, J., Richards, R. G., Walker, M. P., Wiesen, J. F., Werb, Z., Derynck, R., Hom, Y. K., Cunha, G. R., and DiAugustine, R. P. (1998) Activation and function of the epidermal growth factor receptor and erbB-2 during mammary gland morphogenesis. *Cell Growth Differ* **9**, 777-785

37. Miller, F. R., Soule, H. D., Tait, L., Pauley, R. J., Wolman, S. R., Dawson, P. J., and Heppner, G. H. (1993) Xenograft model of progressive human proliferative breast disease. *J Natl Cancer Inst* **85**, 1725-1732

38. McElwee, J. L., Mohanan, S., Horibata, S., Sams, K. L., Anguish, L. J., McLean, D., Cvitas, I., Wakshlag, J. J., and Coonrod, S. A. (2014) PAD2 overexpression in transgenic mice promotes spontaneous skin neoplasia. *Cancer Res* **74**, 6306-6317

39. Zhang, Y., Zhang, H., Yuan, X., and Gu, X. (2007) Differential effects of phenylalanine on Rac1, Cdc42, and RhoA expression and activity in cultured cortical neurons. *Pediatr Res* **62**, 8-13

40. Cherrington, B. D., Morency, E., Struble, A. M., Coonrod, S. A., and Wakshlag, J. J. (2010) Potential role for peptidylarginine deiminase 2 (PAD2) in citrullination of canine mammary epithelial cell histones. *PLoS One* **5**, e11768

41. Plante, I., Stewart, M. K., and Laird, D. W. (2011) Evaluation of mammary gland development and function in mouse models. *J Vis Exp*

42. Lo, A. T., Mori, H., Mott, J., and Bissell, M. J. (2012) Constructing three-dimensional models to study mammary gland branching morphogenesis and functional differentiation. *J Mammary Gland Biol Neoplasia* **17**, 103-110

CHAPTER FOUR

UTILIZATION OF THE SOFT AGAR COLONY FORMATION ASSAY TO IDENTIFY INHIBITORS OF TUMORIGENICITY IN BREAST CANCER CELLS

* Reprinted from Horibata, S., Vo, T.V., Venkataraman, S., Thompson, P.R. and Coonrod, S.A. 2015. Utilization of the soft agar colony formation assay to identify inhibitors of tumorigenicity in breast cancer cells. J. Vis. Exp. e52727.

Contributions:

Manuscript preparation: Horibata, S.

Conception and Design: Horibata, S.

Edits: Vo, T.V. and Coonrod, S.A.

Video: Horibata, S.

BB-Cl-Amidine was provided by Venkataraman, S. and Thompson, P.R.

Figure 4.1: Venkataraman, S.

Figure 4.2: Horibata, S.

Figure 4.3: Horibata, S.

Figure 4.4: Horibata, S.

ABSTRACT

Given the inherent difficulties in investigating the mechanisms of tumor progression *in vivo*, cell-based assays such as the soft agar colony formation assay (hereafter called soft agar assay), which measures the ability of cells to proliferate in semi-solid matrices, remain a hallmark of cancer research. A key advantage of this technique over conventional 2D monolayer or 3D spheroid cell culture assays is the close mimicry of the 3D cellular environment to that seen *in vivo.* Importantly, the soft agar assay also provides an ideal tool to rigorously test the effects of novel compounds or treatment conditions on cell proliferation and migration. Additionally, this assay enables the quantitative assessment of cell transformation potential within the context of genetic perturbations. We recently identified peptidylarginine deiminase 2 (PAD2) as a potential breast cancer biomarker and therapeutic target. Here we highlight the utility of the soft agar assay for preclinical anti-cancer studies by testing the effects of the PAD inhibitor, BB-Cl-Amidine (BB-CLA), on the tumorigenicity of human ductal carcinoma *in situ* (MCF10DCIS) cells.

INTRODUCTION

Both non-transformed (normal) and transformed cells can readily proliferate in a 2D monolayer culture. This form of adherent cell growth is quite dissimilar from that which occurs *in vivo* where, in the absence of mitogenic stimulation, cells do not often rapidly divide within their microenvironment. The soft agar assay on the other hand is distinct from 2D culture systems because it quantifies tumorigenicity by measuring a cell's ability to proliferate and form colonies in suspension within a semi-solid agarose gel (1). In this setting, non-transformed cells are unable to rapidly propagate in the absence of anchorage to the extracellular matrix (ECM) and undergo apoptosis; a process known as anoikis. In contrast, cells that have undergone malignant transformation lose their anchorage dependence due to activation of signaling pathways such as phosphatidylinositol 3-kinase (PI3K)/Akt and Rac/Cdc42/PAK. Therefore, these cells are able to grow and form colonies within the semi-solid soft agar matrix (2).

A common use of the soft agar assay is to test whether specific compounds, such as PAD inhibitors, are able to suppress tumor growth *in vitro*. In general, colony count or colony sizes are quantitative read-outs from the assay that can be compared between control and treatment groups to assess differences in cellular tumorigenicity. Therefore, if one finds that colony formation is inversely correlated with increasing drug concentration, then a conclusion could be drawn that the drug is an effective inhibitor of tumorigenicity *in vitro*. On the other hand, if the drug does not affect colony formation, the drug is either not at the appropriate dosage or it is not an effective tumorigenic inhibitor. In addition to testing the anti-tumor effects of specific compounds, the requirement of a specific gene for tumorigenesis can be also tested by determining whether overexpression of the gene transcript in a normal cell line promotes

transformation or whether suppression of the transcript in a tumorigenic cell line reduces colony formation.

PADs are calcium-dependent enzymes that post-translationally modify proteins by converting positively charged arginine residues into neutrally charged citrulline in a process known as citrullination or deimination (3-5). We have recently found that peptidylarginine deiminase 2 (PAD2) may function as a novel breast cancer biomarker and that PAD inhibitors represent candidate therapies for early stage breast cancers (6). For example, we have previously demonstrated that a "pan-PAD" inhibitor, Cl-amidine, suppresses the proliferation of breast cancer cells using 2D monolayers and that the inhibitor suppressed the growth of 3D tumor spheroids (6). In this report, we extend these studies, and highlight the utility of the soft agar assay, by testing the efficacy of a new PAD inhibitor, BB-CLA (**Figure 4.1**), in suppressing the growth of MCF10DCIS breast cancer colonies (7). We note that we used MCF10DCIS cells for this experiment because they are oncogenic derivatives of non-transformed human MCF10A cells and because they contain high steady state levels of PAD2 protein (8). We hypothesize that PAD2 enzymatic activity plays a key role in the tumorigenicity of this cell line and that BB-CLA-mediated inhibition of PAD2 activity will suppress cancer progression.

Figure 4.1: Chemical structure of BB-Cl-Amidine.

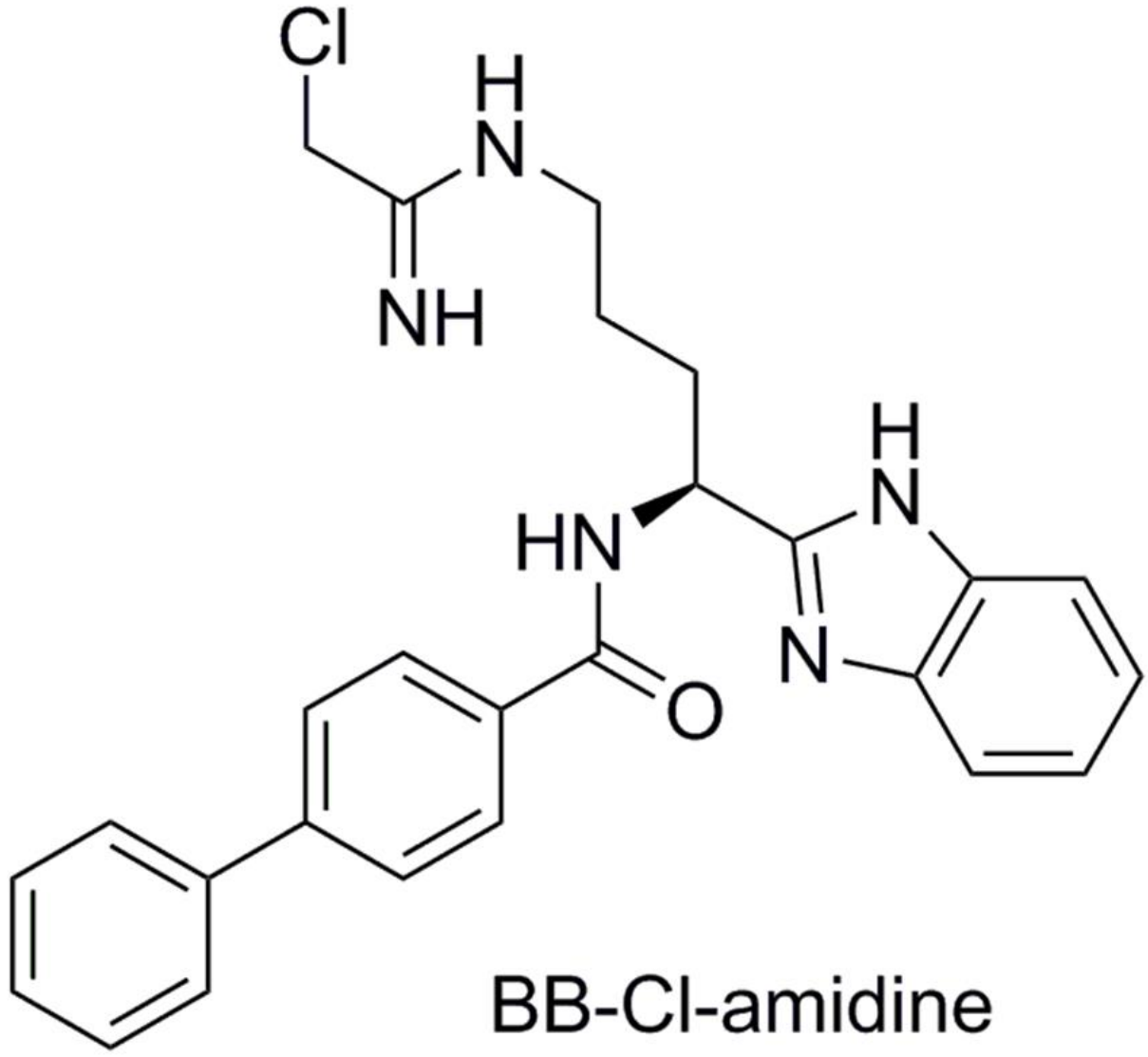

BB-Cl-amidine

Chemical Formula: $C_{26}H_{26}ClN_5O$

Molecular Weight: 459.98

PROTOCOL

1. **Preparation of 3% 2-Hydroxyethyl Agarose**

1.1) Into a clean, dry 100 mL glass bottle, add 0.9 g of 2-hydroxyethyl agarose (Agarose VII from Sigma) followed by 30 mL of distilled water.

1.2) Microwave the mixture for 15 sec and gently swirl. Repeat this step at least three more times until the agarose powder fully dissolves.

1.3) Autoclave the solution-containing bottle for 15 min.

1.4) Allow the agarose solution to cool down to room temperature before further use. The solution can then be stored at room temperature.

2. **Preparation of the bottom layer: 0.6% agarose gel**

2.1) Pre-warm several 5 mL and 10 mL pipettes in a 37 °C incubator. This is to prevent your agarose from solidifying in the pipette when handling.

2.2) Partially loosen the bottle lid and microwave the pre-made 3% 2-hydroxyethyl agarose solution for 15 sec. Then, gently swirl the solution and microwave for another 15 sec. CAUTION: Be careful when swirling the agarose solution because the solution rises up when exposed to air and can spill over.

2.3) If there is residual solid gel in the bottle, microwave for a few more seconds.

2.4) Keep the bottle containing the agarose solution in a 45 °C water bath during the next steps to prevent the agarose solution from solidifying prematurely.

2.5) Warm MCF10DCIS media in a 37 °C water bath. MCF10DCIS media consists of DMEM/F12, 5% horse serum, 5% penicillin streptomycin.

2.6) Transfer 3 mL of the 3% agarose solution using the pre-warmed pipettes into a sterile 50 mL conical tube.

2.7) Immediately add 12 mL of warm MCF10DCIS media and gently invert the conical tube to mix the agarose with the media. Try not to form any bubbles as it will interfere with the colony counting later.

2.8) Gently add 2 mL of this mixture into each well of a 6-well culture plate without forming any air bubbles.

2.9) Incubate the 6-well culture plate horizontally on a flat surface at 4 °C for 1 hour to allow the mixture to solidify.

2.10) After the mixture solidifies, place the plate into a 37 °C incubator for 30 min. The bottom layer is now ready for use.

3. **Preparation of the cell-containing layer: 0.3% agarose gel**

3.1) Trypsinize MCF10DCIS cells and dilute them to a cell concentration of 4×10^4 /mL. The cell concentration can be anywhere from 5×10^2 /mL to 1×10^4 /mL depending on the cell proliferation rate and colony size of the cell line.

3.2) Take 2 mL of the 3% agarose using pre-warmed pipettes and transfer into a sterile 50 mL conical tube.

3.3) Immediately add 8 mL of MCF10DCIS media to the conical tube and gently invert to mix the agarose with the media. Avoid forming any bubbles.

3.4) Take 2 mL of the MCF10DCIS cells (4×10^4 /mL) and treat with BB-CLA (0 µM (DMSO) or 1 µM).

3.5) In a 1:1 dilution, mix the cells with the 0.3% agarose.

3.6) Take 1 mL of the cell-agarose mixture and gently add onto the bottom layer of the 6-well culture plate.

3.7) Place the 6-well culture plate horizontally on a flat surface at 4 °C for at least 15 min to allow the top layer to solidify.

3.8) After the mixture solidifies, place the plate into a 37 °C incubator for a week before adding the feeding layer.

4. **Preparation of the feeder layer: 0.3% agarose gel**

4.1) Microwave the pre-made 3% 2-Hydroxyethyl agarose solution for 15 sec. Gently swirl the solution and microwave for another 15 sec.

4.2) Equilibrate the agarose solution bottle in a 45 °C water bath.

4.3) Warm the MCF10DCIS media in a 37 °C water bath.

4.4) Mix 1 mL of 3% agarose solution with 9 mL of warm MCF10DCIS media into a 50 mL conical tube and gently invert to mix the agarose with the media. Avoid forming air bubbles.

4.5) Treat the mixture with BB-CLA (0 μM (DMSO) or 1 μM).

4.6) Gently add 1 mL of this mixture (without forming bubbles) into each well of the 6-well culture plate containing the bottom and soft layers.

4.7) Place the 6-well culture plate horizontally on a flat surface at 4 °C for at least 15 min to allow the mixture to solidify.

4.8) After the feeder layer solidifies, place the plate into a 37 °C incubator.

4.9) Repeat this feeding procedure weekly by overlaying 1 mL of 0.3% agarose/medium/treatment solution onto the existing feeder layer to replenish the cells with new media until colony formation is observed. Note: Agar in the soft and feeder layers is

very soft and, therefore, the added nutrients from the feeder layer will readily diffuse into the cell-containing layer to reach the cells.

5. **Data collection**

5.1) After 2.5 weeks of cell growth in the soft agar (2 to 4 weeks depending on the cells), count the number of colonies in each well using a light microscope. To facilitate quantification, print a grid onto a transparency and attach the grid to the 6-well plate to help you locate where the cells are during counting. In addition, colony size will vary, so predefine a reference colony size to determine which colonies will be scored. For example, colony sizes of 70 μm or larger will be included in the data analysis.

5.2) Store the samples at 4 °C to prevent further colony formation and for future counting. Seal the 6-well culture plate with parafilm to prevent the gels from drying out.

RESULTS

The soft agar colony formation assay can be used for a broad range of applications documenting the tumorigenicity of cancer cells. A major advantage of this technique is that the semi-solid matrix selectively favors the growth of cells that can proliferate in an anchorage-independent manner. This trait is mainly exhibited by cancer cells but not by normal cells. In our laboratory, we primarily use this technique to test the efficacy of tumor growth inhibition by drugs and to test for the effect of overexpression or depletion of our genes of interest, including PAD genes, on the tumorigenicity of breast cancer cells. Here, we assessed the effect of BB-CLA on tumorigenic inhibition of PAD2-overexpressing MCF10DCIS cells (**Figure 4.2**).

Figure 4.2: Schematic overview of the protocol for the soft agar colony formation assay.

Each well of the 6-well culture plates was first coated with 0.6% agarose gel (bottom layer). A 0.3% agarose gel mixture containing the MCF10DCIS cells and either the BB-CLA inhibitor (1 μM) or DMSO (control) was then layered on top of the 0.6% gel. Once a week, the 0.3% agarose gel mixture (containing BB-CLA) was added on top of the soft layer. After 2 to 4 weeks, colony formation was observed and counted for data analysis.

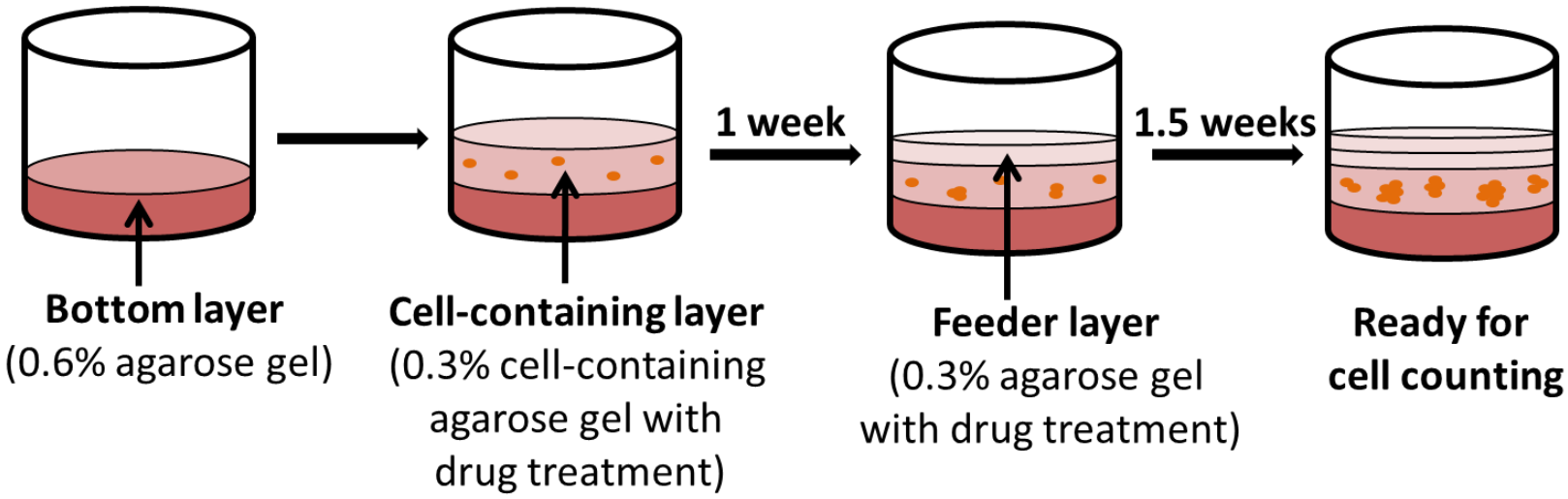
1 week
1.5 weeks
Bottom layer
(0.6% agarose gel)
Cell-containing layer
(0.3% cell-containing agarose gel with drug treatment)
Feeder layer
(0.3% agarose gel with drug treatment)
Ready for cell counting

Our results demonstrate that BB-CLA significantly inhibits the formation of MCF10DCIS cell-derived colonies. **Figure 4.3.** shows that, in the presence of a PAD inhibitor, there was a reduction in both colony formation and colony size when compared to the DMSO control. [Note: BB-CLA was dissolved in DMSO and thus, DMSO was used as a control.] The size of colonies for BB-CLA treated MCF10DCIS cells were predominantly within the range of 20 to 100 μm while the size of colonies for the DMSO control exhibited a greater range of 70 to 150 μm after 2.5 weeks of growth.

Colonies larger than 70 μm were counted and analyzed (**Figure 4.4**). There was an average of 3,536 colonies in the DMSO control whereas only 1,967 colonies were seen in the BB-CLA treated group after 2.5 weeks of soft agar culture. This represents a 44% decrease in the average colony formation in the presence of 1 μM BB-CLA, indicating a significant tumorigenic inhibition of breast cancer cells (MCF10DCIS cells) by the PAD inhibitor.

Figure 4.3: Images of colony formation in BB-CLA-treated MCF10DCIS cells.

MCF10DCIS cells were grown in soft agar in the presence (1 μM BB-CLA) or absence of BB-CLA (0 μM DMSO). After 2.5 weeks, colonies were imaged using Olympus CKX41 inverted microscope for low magnification images and Zeiss Axiopot light microscope for high magnification images.

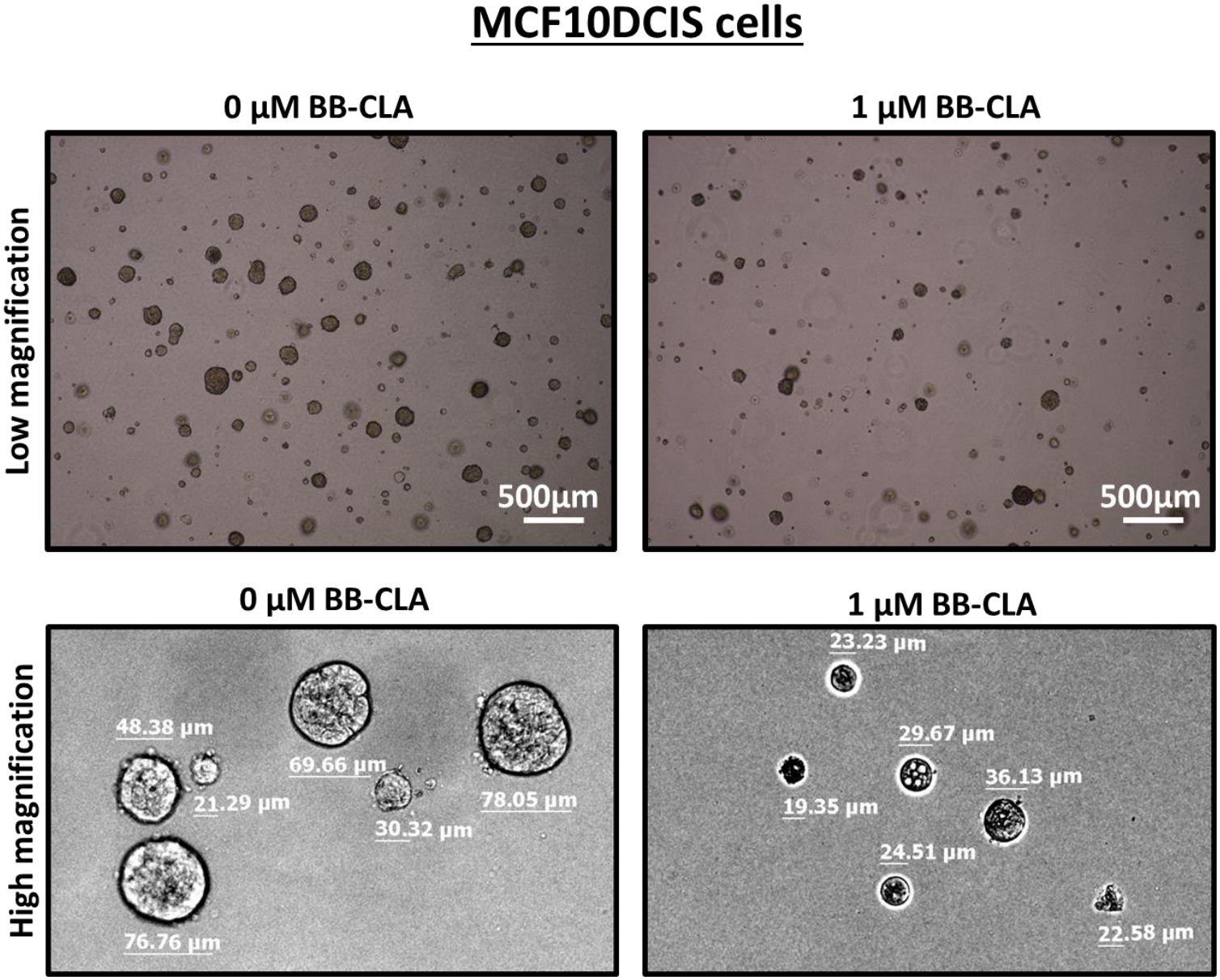
MCF10DCIS cells
0 µM BB-CLA
1 µM BB-CLA
Low magnification
500µm
500µm
0 µM BB-CLA
1 µM BB-CLA
High magnification
48.38 µm
21.29 µm
69.66 µm
30.32 µm
78.05 µm
76.76 µm
23.23 µm
29.67 µm
19.35 µm
36.13 µm
24.51 µm
22.58 µm

Figure 4.4: Quantification of MCF10DCIS colony number after BB-CLA treatment.

MCF10DCIS cells were grown in soft agar at different concentrations of BB-CLA (0 μM (DMSO), or 1 μM BB-CLA). After 2.5 weeks, individual colonies larger than 70 μm were counted and quantified.

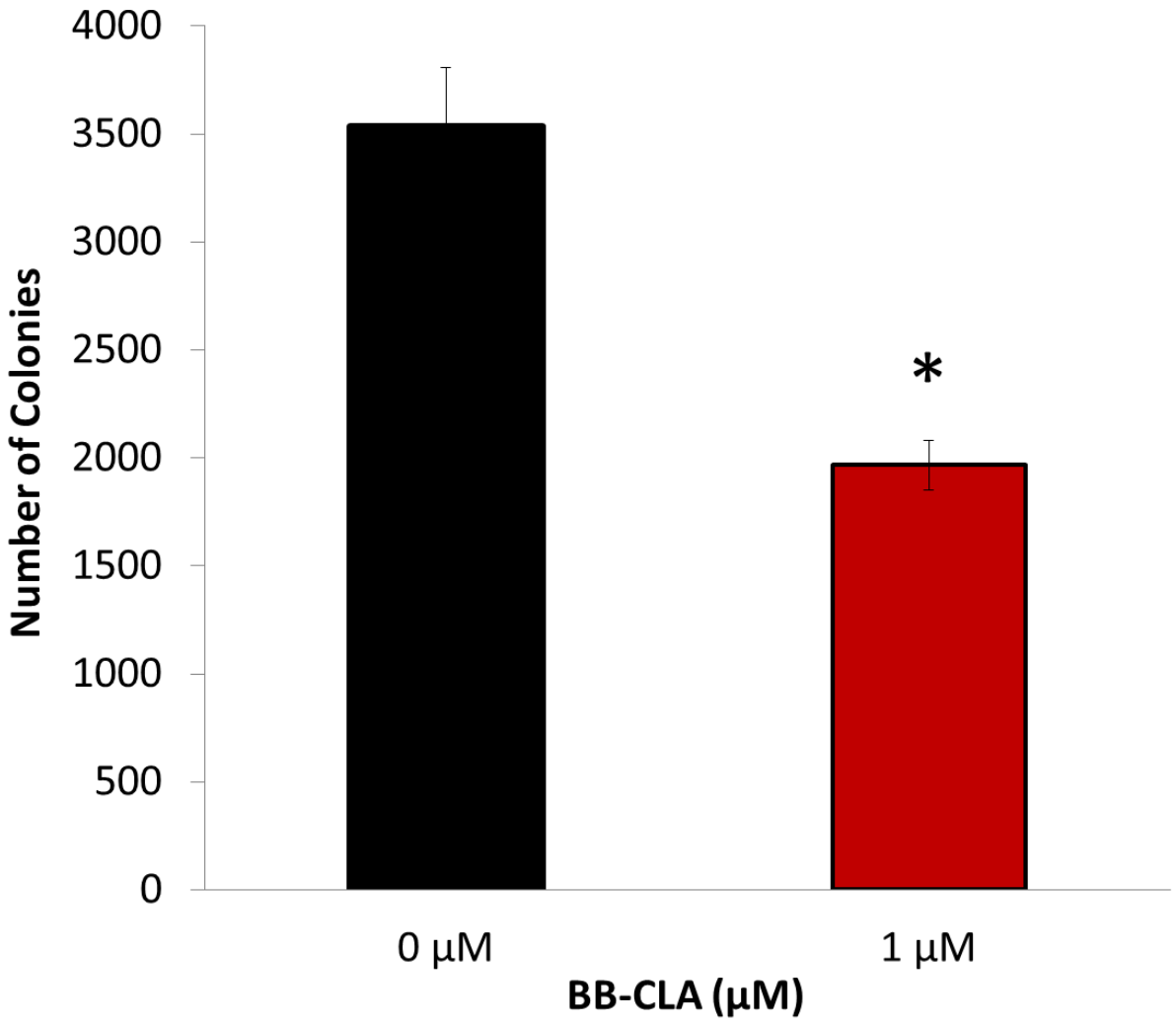
4000
3500
3000
2500
2000
1500
1000
500
0
Number of Colonies
*
0 µM
1 µM
BB-CLA (µM)

DISCUSSION

The rate of colony formation in soft agar varies depending on the cell type (9). Therefore, the number of cells to start with should be optimized and adjusted accordingly. A suggested starting range is between 5×10^2 to 1×10^4 cells. In addition, colony size varies depending on the growth rate of each cell. Therefore, a predefined a cut-off for colony size is needed to annotate individual colonies for downstream quantitative analyses. Here, colonies larger than 70 μm were quantified to avoid inclusion of non-proliferating cells derived from the initial plating.

For optimal growth, when making the 3D agarose gels, it is advisable to use the same cell culture medium normally used for 2D cell cultures. This is because changing medium often times alters the cells growth rate, thus necessitating additional passaging to allow the cells to adapt to the new medium. For example, MCF10DCIS cells can be grown optimally in RPMI-1640, DMEM, or DMEM/F12 media. However, when MCF10DCIS culture media is changed from RPMI-1640 to DMEM/F12, there is a noticeable reduction in cell proliferation rate. Additionally, care should be taken to maintain serum concentrations at a constant level because, without serum, colony formation will be inhibited (10). Furthermore, after the agarose is microwaved, allow the bottle to equilibrate in a 45 °C water bath before mixing with media containing cells to prevent overheating the cells. Given that agarose solidifies rapidly at room temperature, we also recommend that all pipettes and 6-well culture plates are preheated in a 37 °C incubator before adding agarose solution to prevent premature solidification while handling.

While the soft agar colony formation technique is a valuable tool for measuring tumorigenicity in a range of cancer cell lines, some lines do not grow in soft agar. Another potential drawback of the method is that viable cells cannot be recovered once they are plated

into the soft agar. Furthermore, this technique can be time consuming and difficult when testing a large number of samples. However, technological advances have helped to overcome some of these limitations. The conventional soft agar assay (as documented in this manuscript) typically uses 6-well culture plates or 6mm culture dishes. With automated plate readers, however, multiple samples can be processed in 384-well plates (11). For example, investigators pre-loaded tumor cells with dyes such as alamarBlue and tetrazolium dyes and colonies are quantified using plate reader, thus obviating the need to manually count colony number (11). This high-throughput capability is, therefore, amenable for large scale cancer drug screens.

In sum, the soft agar assay is a valuable pre-clinical technique that can be used to assess the tumorigenicity of a wide-range of cancer cells (breast, prostate, ovarian, and others) with regards to their sensitivity to drugs, hormones, heat, hypoxia, and a multitude of other treatment conditions. The assay continues to provide a straightforward and informative tool for cancer researchers who wish to better understand the mechanisms of cancer progression and test the anti-tumor potential of new cancer therapies.

REFERENCES

1. Hamburger, A. W., and Salmon, S. E. (1977) Primary bioassay of human tumor stem cells. *Science* **197**, 461-463

2. Wang, L. H. (2004) Molecular signaling regulating anchorage-independent growth of cancer cells. *Mt Sinai J Med* **71**, 361-367

3. Vossenaar, E. R., Zendman, A. J., van Venrooij, W. J., and Pruijn, G. J. (2003) PAD, a growing family of citrullinating enzymes: genes, features and involvement in disease. *Bioessays* **25**, 1106-1118

4. Horibata, S., Coonrod, S. A., and Cherrington, B. D. (2012) Role for peptidylarginine deiminase enzymes in disease and female reproduction. *J Reprod Dev* **58**, 274-282

5. Mohanan, S., Cherrington, B. D., Horibata, S., McElwee, J. L., Thompson, P. R., and Coonrod, S. A. (2012) Potential role of peptidylarginine deiminase enzymes and protein citrullination in cancer pathogenesis. *Biochem Res Int* **2012**, 895343

6. McElwee, J. L., Mohanan, S., Griffith, O. L., Breuer, H. C., Anguish, L. J., Cherrington, B. D., Palmer, A. M., Howe, L. R., Subramanian, V., Causey, C. P., Thompson, P. R., Gray, J. W., and Coonrod, S. A. (2012) Identification of PADI2 as a potential breast cancer biomarker and therapeutic target. *BMC Cancer* **12**, 500

7. Knight, J. S., Subramanian, V., O'Dell, A. A., Yalavarthi, S., Zhao, W., Smith, C. K., Hodgin, J. B., Thompson, P. R., and Kaplan, M. J. (2015) Peptidylarginine deiminase inhibition disrupts NET formation and protects against kidney, skin and vascular disease in lupus-prone MRL/lpr mice. *Ann Rheum Dis* **74**, 2199-2206

8. Miller, F. R., Santner, S. J., Tait, L., and Dawson, P. J. (2000) MCF10DCIS.com xenograft model of human comedo ductal carcinoma in situ. *J Natl Cancer Inst* **92**, 1185-1186

9. Fan, D., Morgan, L. R., Schneider, C., Blank, H., and Fan, S. (1985) Cooperative evaluation of human tumor chemosensitivity in the soft-agar assay and its clinical correlations. *J Cancer Res Clin Oncol* **109**, 23-28

10. Hamburger, A. W., White, C. P., Dunn, F. E., Citron, M. L., and Hummel, S. (1983) Modulation of human tumor colony growth in soft agar by serum. *Int J Cell Cloning* **1**, 216-229

11. Anderson, S. N., Towne, D. L., Burns, D. J., and Warrior, U. (2007) A high-throughput soft agar assay for identification of anticancer compound. *J Biomol Screen* **12**, 938-945

CHAPTER FIVE

PADI2 AS A POTENTIAL THERAPEUTIC TARGET IN HER2/ERBB2-POSITIVE BREAST CANCER

Reprinted from:

McElwee, J.L., Horibata, S., Zhang, X., Chen, J.I., McLean, D., Anguish, L.J., Thompson, P.R., and Coonrod, S.A. PADI2 as a potential therapeutic target in HER2/ERBB2-positive breast cancer. (*In preparation*)

Contributions:

Manuscript preparation: McElwee, J.L.

Conception and Design: Horibata, S., McElwee, J.L., Coonrod, S.A.

Development of methodology: Horibata, S., McElwee, J.L., Anguish, L.J., Coonrod, S.A.

Acquisition of data:

Figure 5.1: McElwee, J.L.

Figure 5.2: Zhang, X. and Horibata, S.

Figure 5.3: Horibata, S.

Figure 5.4: Horibata, S.

Figure 5.5: (A) Thompson, P.R., (B) McElwee, J.L., (C) Mclean,D., (D) Horibata, S.

Figure 5.6: Anguish, L.J.

Figure 5.7: McElwee, J.L., and Chen, J.I.

Figure 5.8: Horibata, S.

ABSTRACT

Introduction: We have recently reported that the expression of peptidylarginine deiminase 2 (PADI2) is correlated with HER2 expression in breast cancer cell lines and appears to play a role in the proliferation of mammary tumors *in vitro* and *in vivo*; however, the functional relationship between these two genes has yet to be investigated. The goals of this study were to examine the role of PADI2 in HER2-positive breast cancer, and to validate our next generation PADI inhibitor in the treatment of these tumors.

Methods: Using molecular genetics approaches, we looked to find whether PADI2 functions upstream or downstream of HER2. Lentiviral transduction of MCF10DCIS and BT474 cells was used to examine the role of PADI2 knockdown on HER2 signaling and cellular malignancy. Chromatin-immunoprecipitation (ChIP) was performed to identify whether PADI2 binds the HER2 promoter and/or upstream intronic ERE. Lastly, we used our next-generation PADI inhibitor, BB-Cl-amidine, to examine the role of PADI2 signaling in HER2-positive breast cancer cell lines.

Results: Our study suggests that PADI2 appears to play an important role in HER2-signaling and may form an oncogenic positive-feedback loop with HER2. First, we show using MCF10DCIS and BT474 cells stably knocked-downed for PADI2, that HER2 expression levels are decreased. Next, we show that PADI2 binds the HER2 promoter and its intronic ERE, and that reduced levels of PADI2 are concomitant with reduced levels of citrullinated H3R26 (H3Cit26). Interestingly, we also show that increased HER2 signaling can upregulate PADI2

expression. Lastly, we found that the next-generation PADI inhibitor, BB-Cl-amidine, has a synergistic effect with lapatinib (HER2 inhibitor).

Conclusion: Taken together, these results suggest a role for PADI2 in HER2+ breast cancers, and that the PADI inhibitor, BB-Cl-amidine, represents a potential novel therapy for the treatment of patients with HER2-positive mammary tumors.

Key words: Peptidylarginine deiminase, PAD2/PADI2, HER2/ERBB2, Breast Cancer, BB-Cl-amidine, Citrullination, Histone H3 Arginine 26

INTRODUCTION

Breast cancer is the most frequently diagnosed cancer in women, with over 1 million new cases in the world each year (1). Approximately 75% of breast cancers are ER-positive, with anywhere between 15-20% of breast cancers positive for HER2 amplification or overexpression (2). Between ER and HER2, the majority of breast cancers express at least one or both of these markers. While there are drugs targeting both of these signaling pathways, about ~30% of patients with ER-positive breast cancers fail to respond to treatments such as tamoxifen; in addition, the majority of those patients that do initially respond develop resistance over time (3). Interestingly, the most commonly documented mechanism of resistance to tamoxifen occurs via EGFR and HER2 overexpression (4-6). The same problem exists for patients with HER2-positive tumors, as greater than 60% of patients fail to respond to trastuzumab monotherapy, with initial responders developing resistance within 1 year (7,8). In addition, a significant portion of those patients treated with trastuzumab must discontinue treatment because of cardiotoxic side effects, owing to the role of HER2 receptor signaling in the heart (9). This has highlighted the critical need to discover and validate novel targets for both ER-positive and HER2-positive tumors, so that additional treatments may be used in combination with, or in the place of, current therapies to overcome issues with *de novo* and acquired resistance.

Recently, in addition to genetic mutations, numerous studies have found that epigenetics plays a direct role in the etiology of breast cancer (10-12). The PADIs are a family of posttranslational modification enzymes that convert positively charged arginine residues on substrate proteins to neutrally charged citrulline, and this activity is alternatively called citrullination or deimination. Protein citrullination has recently been implicated in many diseases, including cancer (13-19). PADI2 has historically been defined as a cytoplasmic protein;

however, recent evidence from our lab shows that PADI2 can localize to the nucleus and directly bind chromatin to influence target gene expression (13,14,16). In the canine mammary gland, PADI2 expression in epithelial tissue was found to vary across the estrous cycle and to correlate with citrullinated histone levels, potentially indicating a role in gene expression. Recent evidence from our lab supports this prediction, as Zhang et al. have shown that PADI2 catalyzed citrullination of histone H3 arginine 26 (H3R26) facilitates ER target gene activation (16). PADI2-mediated citrullination of histone H3R26 likely facilitates transcriptional activation by creating open, permissive, chromatin architecture around the EREs of E2-induced genes. Following this, we established a new line of evidence demonstrating that PADI2 plays a role in the oncogenic progression of breast cancer using the MCF10AT model. Furthermore, we showed using RNA-seq, that *PADI2* is highly correlated with *HER2/ERBB2* overexpression across 57 breast cancer cell lines. We concluded this study with the first preclinical evidence showing that the PADI inhibitor, Cl-amidine, could be utilized as a therapeutic agent for the treatment of tumors *in vivo*.

These findings led to additional questions, mainly, what was the functional relationship between PADI2 and HER2 in breast cancer. In this study, we present an additional role for PADI2 in the expression of the HER2 oncogene. Interestingly, PADI2 appears to function both upstream and downstream of HER2, potentially indicating a role in an oncogenic positive-feedback loop with HER2. Since our previous evidence suggested that PADI2 could act as an ER co-activator via the citrullination of H3R26, we were curious whether PADI2 regulates *HER2* expression using the same mechanism. Using both *PADI2* shRNA and our next-generation PADI inhibitor BB-Cl-amidine, we show that the reduction of PADI2, as well as the inhibition of PADI2-mediated citrullination of H3R26 (BB-Cl-amidine), leads to decreased expression of

HER2. Conversely, HER2 regulation of *PADI2* gene expression is most likely downstream of PI3K signaling. Lastly, we validate our next-generation PADI inhibitor, BB-Cl-amidine, in the treatment of breast cancer cells.

Taken together, these results suggest an enhanced role for PADI2 in HER2 expressing breast cancers. Given the role of PADI2 in ER- and HER2-positive tumors, PADI2 inhibitors may have therapeutic value for over 85% of all breast cancers, thus potentially benefiting a large majority of patients.

RESULTS

Knockdown of PADI2 reduces HER2/ERBB2 expression levels

The coordinated increase in *PADI2* and *HER2* expression levels suggested a direct relationship, and given our previously established role for PADI2 as an ER co-activator, we wanted to assess the potential effect of PADI2 on HER2 signaling. Using lentiviral delivery of shRNA targeting PADI2 (or scrambled control), we generated two different breast cancer cell lines that stably knocked-downed *PADI2* expression. We first targeted the MCF10DCIS cell line, which we previously described as having high PADI2 expression levels *in vitro* and *in vivo*. This cell line is part of the MCF10AT model of breast cancer progression, and faithfully recapitulates highly invasive human comedo-like ductal carcinoma *in situ* tumors (20). We found that when we knocked-down *PADI2* in MCF10DCIS cells, HER2 expression levels were reduced at both the protein and mRNA levels (**Figure 5.1A and 5.1B**). Interestingly, we also saw a slight reduction in the activated form of HER2/ERBB2, indicated by phosphorylation at tyrosine-1248 (pERBB2). We have previously shown, along with others, that MCF10DCIS cells have upregulated HER2/ERBB2 expression levels (when compared to their isogenic parental cell line,

Figure 5.1: *PADI2* depletion leads to decreased HER2/ERBB2 expression at both protein and mRNA levels. (**A**) Western blot analyses of PADI2, ERBB2, and phosphorylated ERBB2 protein levels (pERBB2-Y1248) in MCF10DCIS (DCIS) or BT474 cells stably expressing a scrambled control shRNA (SC) or shRNA directed against *PADI2* (P2KD). Equal loading was determined by probing the membrane with β-actin antibody. (**B**) Relative *PADI2* and *ERBB2* mRNA levels in MCF10DCIS and BT474 P2KD cell lines compared to scrambled control. *PADI2* and *ERBB2* mRNA levels were determined by qPCR (TaqMan) using scrambled control (SC) cells as the reference and with *GAPDH* normalization. Expression levels were analyzed using the $2^{-\Delta\Delta C(t)}$ method, and data are expressed as the mean ± SD from three independent experiments (* $p < 0.05$).

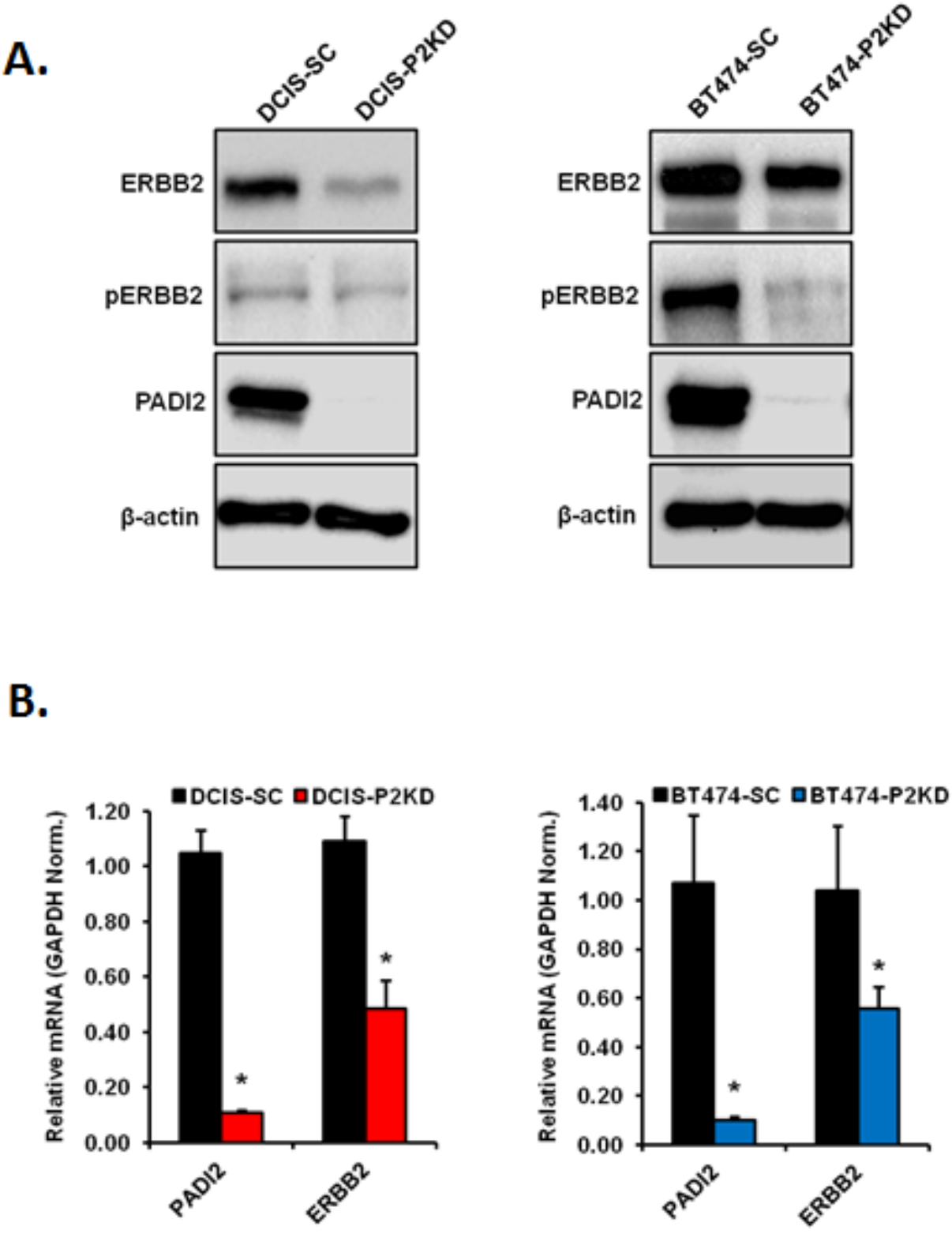
A.
DCIS-SC
DCIS-P2KD
ERBB2
pERBB2
PADI2
β-actin
BT474-SC
BT474-P2KD
ERBB2
pERBB2
PADI2
β-actin
B.
DCIS-SC
DCIS-P2KD
Relative mRNA (GAPDH Norm.)
1.20
1.00
0.80
0.60
0.40
0.20
0.00
*
*
PADI2
ERBB2
BT474-SC
BT474-P2KD
Relative mRNA (GAPDH Norm.)
1.40
1.20
1.00
0.80
0.60
0.40
0.20
0.00
*
*
PADI2
ERBB2

MCF10A) (15,21,22), but we wanted to compare whether we see this same effect in the HER2-amplified BT474 cell line. This cell line was chosen due to its high levels of HER2/ERBB2 and PADI2 expression. Again, we see the same effect on HER2 /ERBB2 expression when we knockdown PADI2, with the effect on pERBB2 levels more pronounced in BT474 than MCF10DCIS (**Figure 5.1A and 5.1B**). The reduction in activated HER2/ERBB2 in both cell lines could potentially be a byproduct of the decreased HER2/ERBB2 protein levels; however, we cannot rule out additional mechanisms.

PADI2 binds the HER2/ERBB2 promoter and downstream ERE and potentially acts as a co-activator of HER2 signaling

Given our previously findings linking PADI2 and histone H3 arginine (H3R26) citrullination (H3Cit26) with ER-target gene expression, and our results here showing PADI2 knockdown leads to decreased HER2 expression levels, we predicted that PADI2 might directly regulate HER2 via the same mechanism. To test this hypothesis, we used chromatin immunoprecipitation (ChIP) to assay PADI2 binding to the *HER2/ERBB2* promoter and downstream estrogen response element (ERE) in both MCF10DCIS and BT474 cells. Results show that the strong association of PADI2 with ETS elements at the *HER2/ERBB2* promoter, in addition to the recently identified downstream intronic ERE, is lost upon PADI2 knockdown in both the MCF10DCIS (**Figure 5.2A**) and BT474 (**Figure 5.2B**) cell lines. Furthermore, we also found a sharp reduction in the H3Cit26 modification at both of these sites in PADI2-depleted (PADI2-KD) cell lines, suggesting that PADI2-catalyzed H3Cit26 modification may regulate *HER2/ERBB2* expression.

Figure 5.2: PADI2 and H3Cit26 bind the *HER2/ERBB2* promoter and intronic ERE in MCF10DCIS and BT474 cells. Chromatin-immunoprecipitation (ChIP) qPCR was used to analyze the binding of PADI2 and citrullinated H3R26 (H3Cit26) to the *HER2/ERBB2* promoter and/or downstream ERE in MCF10DCIS (a) and BT474 (b) cells. ChIP-qPCR data are presented as % input for MCF10DCIS and signal/background for BT474. Error bars indicate ± SEM of three independent experiments.

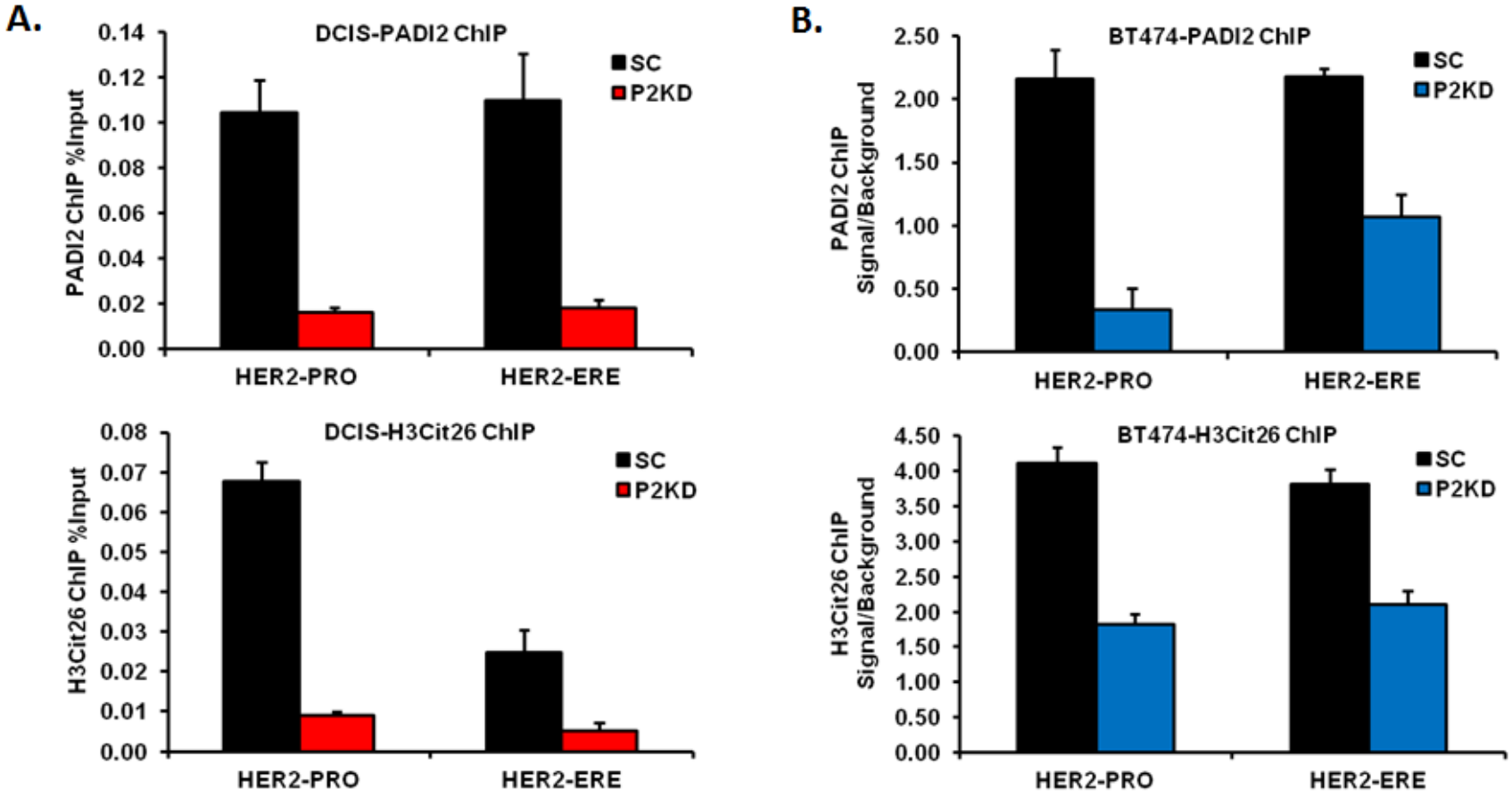
A.
DCIS-PADI2 ChIP
PADI2 ChIP %Input
0.14
0.12
0.10
0.08
0.06
0.04
0.02
0.00
SC
P2KD
HER2-PRO
HER2-ERE
DCIS-H3Cit26 ChIP
H3Cit26 ChIP %Input
0.08
0.07
0.06
0.05
0.04
0.03
0.02
0.01
0.00
SC
P2KD
HER2-PRO
HER2-ERE
B.
BT474-PADI2 ChIP
PADI2 ChIP Signal/Background
2.50
2.00
1.50
1.00
0.50
0.00
SC
P2KD
HER2-PRO
HER2-ERE
BT474-H3Cit26 ChIP
H3Cit26 ChIP Signal/Background
4.50
4.00
3.50
3.00
2.50
2.00
1.50
1.00
0.50
0.00
SC
P2KD
HER2-PRO
HER2-ERE

PADI2 expression levels correlate with cellular malignancy

Next, we tested to see what effects the knockdown of PADI2 has on cellular malignancy. We tested the ability of our PADI2 knocked-down MCF10DCIS cells to form colonies in soft-agar. The ability of cells to grow under anchorage-independent conditions is a hallmark of malignant transformation. We show that both the size (**Figure 5.3A**) and number (**Figure 5.3B**) of colonies are severely reduced in the PADI2-KD (DCIS-P2KD) cells, when compared to scrambled control shRNA cells (DCIS-SC). However, we did not see any effect on anchorage-independent growth of BT474-P2KD cells (data not shown). In addition, we assayed the focus-forming activity for both MCF10DCIS (**Figure 5.3C**) and BT474 (**Figure 5.3D**) cells, with both showing a marked reduction in PADI2-KD cell lines compared to the scrambled control. Conversely, we tested the ability of PADI2 overexpression to enhance malignancy in MCF10AT cells lines. While we do not see any significant difference in the number of colonies grown on soft-agar, the MCF10AT-PADI2 cells have larger colonies (**Figure 5.4A and 5.4B**). We also found a slight increase in HER2/ERBB2 expression in the stably overexpressing MCF10AT-PADI2 cells, when compared to the control empty vector cells (MCF10AT-empty) (**Figure 5.4C**).

Inhibition of PADI2 activity reduces HER2/ERBB2 associated oncogenic signaling and cellular malignancy

To investigate whether PADI2 expression is important for HER2 gene expression and downstream signaling, we next tested the pharmacological inhibition of PADI2 on breast cancer cells *in vitro.* We have recently developed a next-generation PADI inhibitor, biphenyl-benzimidazole-Cl-amidine (BB-Cl-amidine), which has increased cellular permeability, stability,

Figure 5.3: *PADI2* knockdown (KD) decreases cellular malignancy in breast cancer cells. (a) MCF10DCIS cells stably overexpressing shRNA for *PADI2* or scrambled control were plated at a density of 5,000 cells/ml in medium containing 0.3% agarose onto media containing 0.6% agarose in 6-well dishes. Cultures were fed once a week and colonies counted (b) after 3-weeks of growth. The data shown in (b) are expressed as the mean ± SD from three independent experiments (* $p < 0.05$). MCF10DCIS (c) and BT474 (d) cells stably expressing scrambled or *PADI2* shRNA were grown for 1-week, fixed with 4% PFA, and stained with crystal violet for subsequent analysis of focus formation.

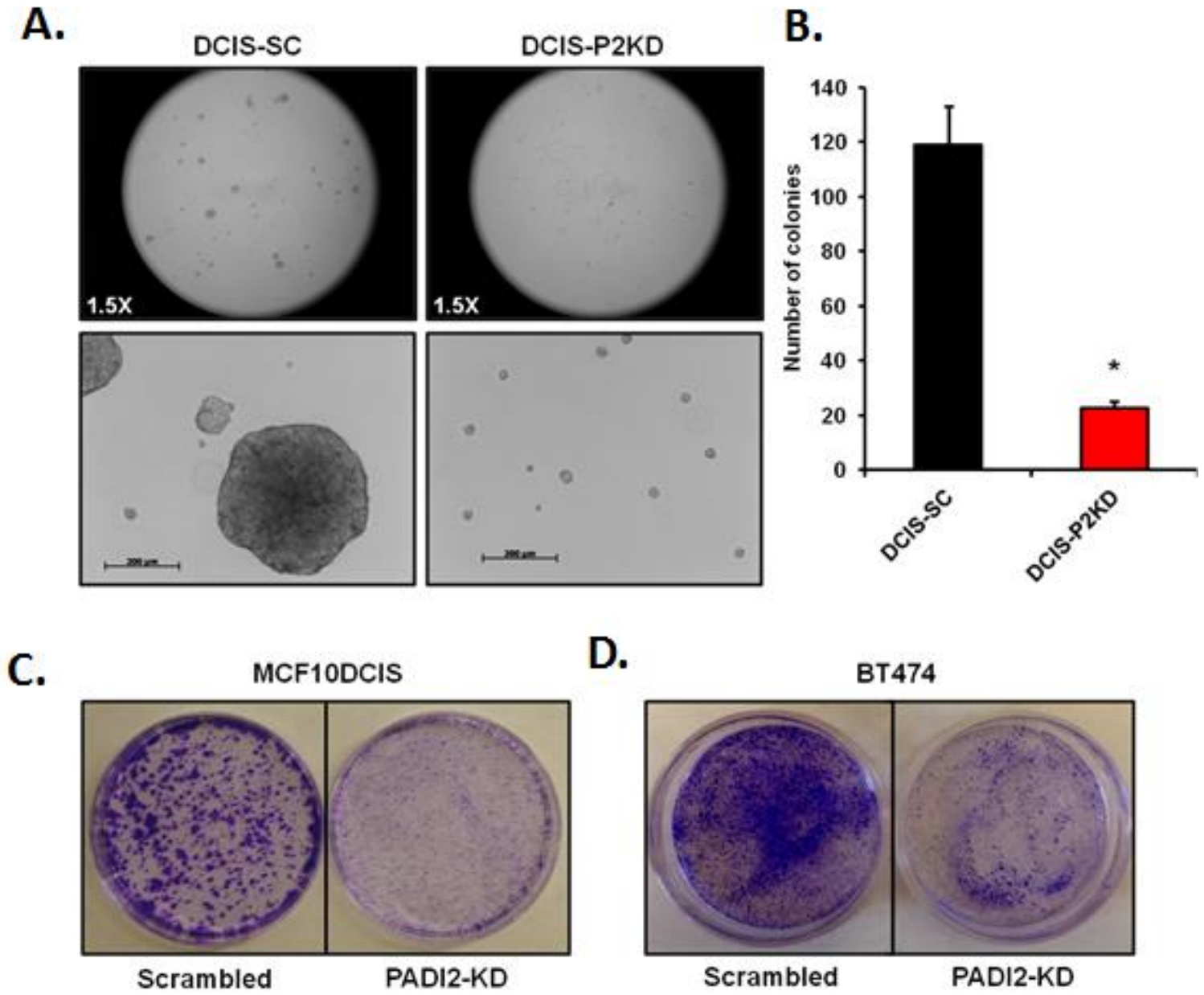
A.
DCIS-SC
DCIS-P2KD
1.5X
1.5X
B.
Number of colonies
140
120
100
80
60
40
20
0
*
DCIS-SC
DCIS-P2KD
C.
MCF10DCIS
Scrambled
PADI2-KD
D.
BT474
Scrambled
PADI2-KD

Figure 5.4: Stable overexpression of PADI2 in premalignant MCF10AT cells leads to increased colony size in anchorage-independent growth. (a) MCF10AT cells stably overexpressing FLAG-tagged PADI2 (pcDNA3.1-FLAG-PADI2) or an empty vector control were plated at a density of 5,000 cells/ml in medium containing 0.3% agarose onto media containing 0.6% agarose in 6-well dishes. Cultures were fed once a week and colonies counted (b) after 3-weeks of growth. The data shown in (b) are expressed as the mean ± SD from three independent experiments (* $p < 0.05$). (c) Western blot of PADI2 and ERBB2 protein levels in MCF10AT cells overexpressing PADI2 or empty vector. (β-actin = loading control).

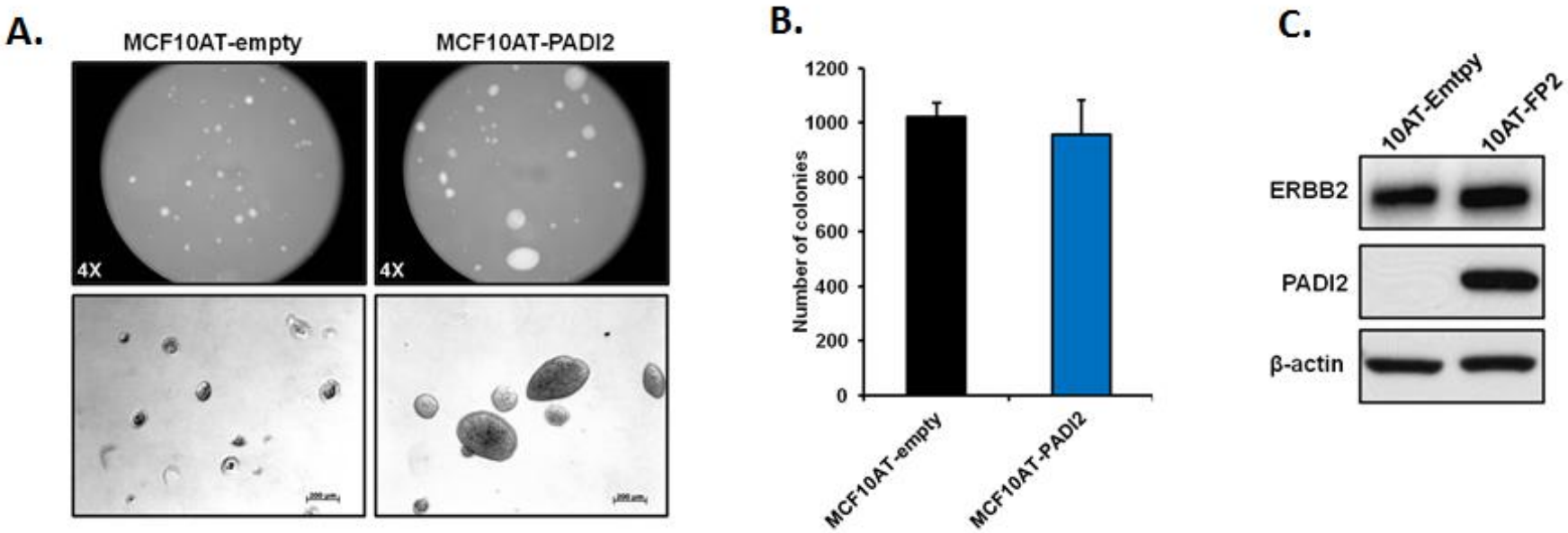
A.
MCF10AT-empty
MCF10AT-PADI2
4X
4X
B.
Number of colonies
1200
1000
800
600
400
200
0
MCF10AT-empty
MCF10AT-PADI2
C.
10AT-Emtpy
10AT-FP2
ERBB2
PADI2
β-actin

and potency compared to first-generation Cl-amidine. BB-Cl-amidine is a derivative of Cl-amidine (**Figure 5.5A**), and has much of the same properties, including the ability to bind irreversibly to the active site of PADIs, thereby blocking activity *in vitro* and *in vivo* (23). BB-Cl-amidine functions as a "pan-PADI" inhibitor as it blocks the activity of all PADIs, though PADI2 has been shown to be the predominant isozyme expressed in both MCF10DCIS and BT474 cells (McElwee et al. (15) and data not shown). We found that BB-Cl-amidine reduces HER2/ERBB2 and EGFR, along with both of their tyrosine phosphorylated activated forms (pERBB2-Y1248 and pEGFR-Y1173) (**Figure 5.5B**). As expected, we also see a dose-dependent reduction in both ER and AIB1 levels (**Figure 5.5B**). This reduction in protein expression is concomitant with a reduction in gene expression (**Figure 5.5C**). Both MCF10DCIS and BT474 cells show a dose-dependent decrease in focus formation when treated with BB-Cl-amidine (**Figure 5.5D**). To investigate whether there was an increase in apoptosis in the treated MCF10DCIS and BT474 cells, we examined the cells by flow-cytometry for activated caspase-3 levels. Results show a dose-dependent reduction in cellular proliferation (**Figure 5.6A**), as well as the induction of activated caspase-3 (**Figure 5.6B**), upon treatment with BB-Cl-amidine in both breast cancer cell lines. Conversely, we do not see any adverse effects on growth or apoptosis in two normal cell lines, CHO-KI and NIH-3T3. Taken together, these results suggest that BB-Cl-amidine blocks the growth of MCF10DCIS and BT474 cells by inducing cell cycle arrest and apoptosis. This prediction is supported by our previous finding that Cl-amidine drives apoptosis in lymphocytic cell lines (17), and can reduce tumor growth *in vitro* and *in vivo*, ultimately leading to S-phase induced apoptosis (15). Importantly, the lack of an apoptotic effect on CHO-K1 and NIH-3T3 cells suggests that BB-Cl-amidine may primarily target tumor cells for killing. Consistent with this possibility is the fact that our first-generation PADI inhibitor, Cl-

Figure 5.5: BB-Cl-amidine leads to decreased malignancy of breast cancer cells and dose-dependent reduction in the expression of genes involved in ER-signaling and tamoxifen resistance pathways. (A) The chemical structure of next-generation PADI inhibitor, biphenyl-benzimidazole-Cl-amidine (BB-CLA); BB-CLA has increased cellular permeability, stability, and potency compared to first-generation Cl-amidine. (B) Western blot analysis of proteins involved in ER-signaling and tamoxifen resistance in BT474 cells after treatment of cells for 24h with vehicle (DMSO) or increasing doses of BB-Cl-amidine (500 nM, 1.25 μM, 2.5 μM, and 5.0 μM). Whole-cell lysates were analyzed by western blot for the indicated proteins, including active forms of ERBB2 (phosphorylated -ERBB2, Y1248) and EGFR (phosphorylated-EGFR, Y1173), with β-actin serving as a loading control. (C) Total RNA was isolated after 24h of treatment and analyzed for *ERBB2*, *EGFR*, *AIB1*, *PADI2*, and *ESR1* mRNA expression using qPCR (TaqMan). Values represent the averages of three independent experiments (* $p < 0.05$) using DMSO treated cells as the reference and with *GAPDH* normalization. (D) MCF10DCIS and BT474 cells were treated with increasing doses of BB-Cl-amidine over the course of 1-week, with replacement of media and drug every 3 days. Cells were fixed with 4% PFA and stained with crystal violet for subsequent analysis.

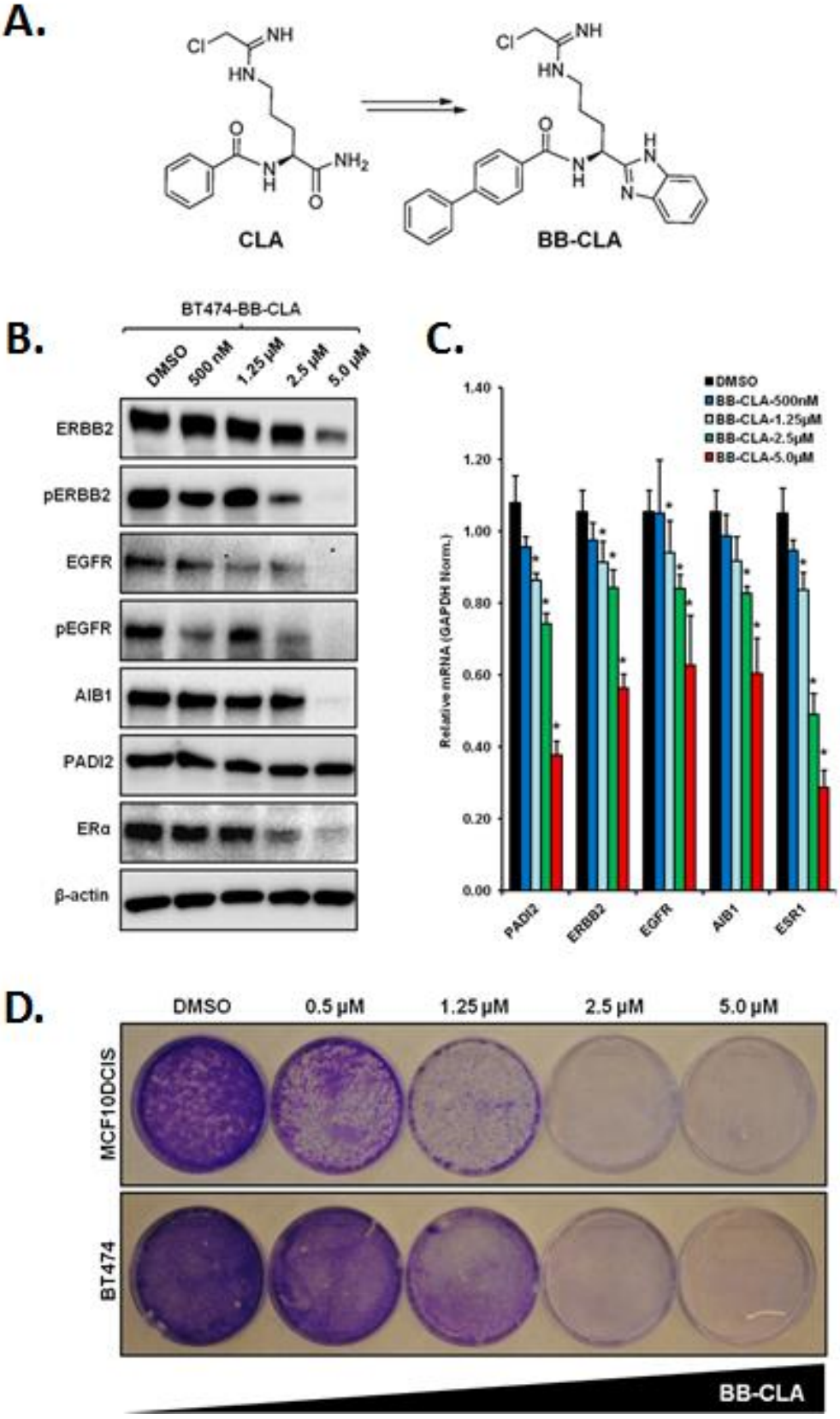
A.
CLA
BB-CLA
B.
BT474-BB-CLA
DMSO
500 nM
1.25 μM
2.5 μM
5.0 μM
ERBB2
pERBB2
EGFR
pEGFR
AIB1
PADI2
ERα
β-actin
C.
DMSO
BB-CLA-500nM
BB-CLA-1.25μM
BB-CLA-2.5μM
BB-CLA-5.0μM
Relative mRNA (GAPDH Norm.)
1.40
1.20
1.00
0.80
0.60
0.40
0.20
0.00
PADI2
ERBB2
EGFR
AIB1
ESR1
D.
DMSO
0.5 μM
1.25 μM
2.5 μM
5.0 μM
MCF10DCIS
BT474
BB-CLA

Figure 5.6: BB-Cl-amidine treatment leads to a decrease in cellular proliferation and increased apoptosis in BT474 and MCF10DCIS breast cancer cell lines, with no significant negative effects on growth seen in normal CHO-K1 or NIH-3T3 cells. (a) BT474 and MCF10DCIS cells were treated with increasing concentrations of BB-Cl-amidine or vehicle (DMSO, 0.6125μM, 1.25 μM, 2.5 μM, and 5.0 μM) and analyzed by flow-cytometry for proliferation (a) and apoptosis (b). (a) Cell counts (DAPI) show a dose-dependent decrease in growth of BT474 and MCF10DCIS cells after 48h of BB-Cl-amidine compared to DMSO treatment. Normal cell lines, CHO-KI and NIH-3T3, were largely unaffected by treatment. (b) BT474 and MCF10DCIS cells show increased apoptosis upon treatment with BB-Cl-amidine, compared to normal cells (CHO-KI and NIH-3T3). Data represent cell number and percent apoptotic cells (cleaved Caspase-3 positive) after 48h of treatment and are expressed as the mean ± SD from three independent experiments (* $p < 0.05$).

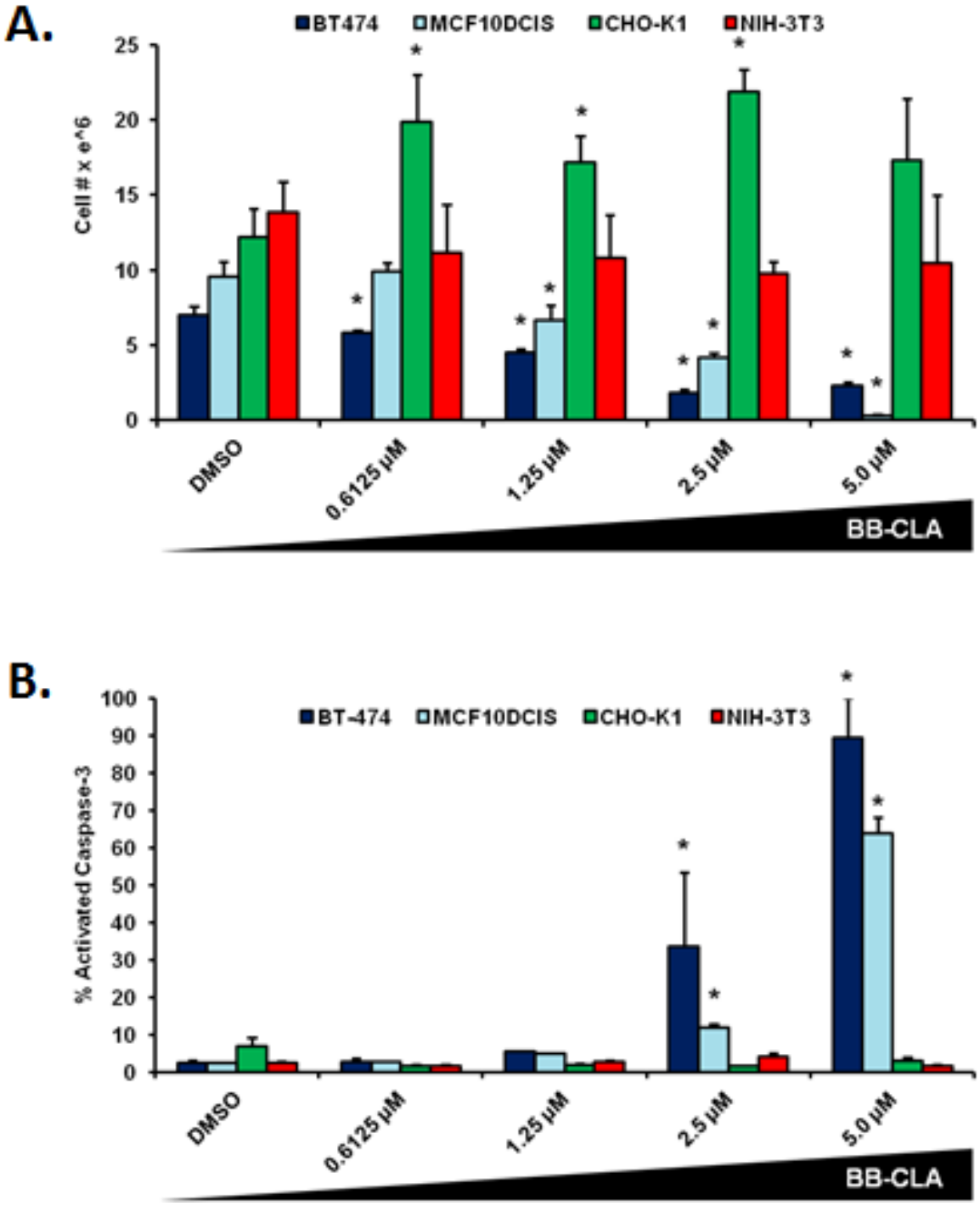
A.
BT474
MCF10DCIS
CHO-K1
NIH-3T3
Cell # x e^6
25
20
15
10
5
0
DMSO
0.6125 µM
1.25 µM
2.5 µM
5.0 µM
BB-CLA
B.
BT-474
MCF10DCIS
CHO-K1
NIH-3T3
% Activated Caspase-3
100
90
80
70
60
50
40
30
20
10
0
DMSO
0.6125 µM
1.25 µM
2.5 µM
5.0 µM
BB-CLA

amidine, did not affect the growth of "normal" MCF10A cells (15), in addition to non-tumorigenic NIH3T3 cells and HL60 granulocytes (24).

HER2/ERBB2 upregulates PADI2 expression through PI3K pathway signaling

Interestingly, we find that PADI2 appears to be both upstream and downstream of HER2/ERBB2 signaling. Overexpression of HER2/ERBB2 in MCF10A cells upregulates PADI2 expression (**Figure 5.7A**). Furthermore, using siRNA to transiently knockdown *HER2/ERBB2*, we show that in BT474 cells, reduced *HER2/ERBB2* leads to a decrease in *PADI2* expression (**Figure 5.7B**). Signaling downstream of HER2/ERBB2 is known to occur through either the MAPK or PI3K pathway. To determine which signaling pathway may affect PADI2 expression, we treated BT474 cells with inhibitors for both the PI3K and MAPK pathways. We found that PADI2 signaling is reduced when PI3K pathway inhibitors (LY294002-PI3K, triciribine-Akt, and rapamycin-mTOR) were used (**Figure 5.7C**), while the MAPK pathway inhibitor (PD98059-MEK1) had no effect, indicating that PADI2 expression is downstream of the PI3K-AKT-mTOR axis.

PADI inhibitor BB-Cl-amidine enhances HER2/ERBB2 and PI3K pathway inhibitors

As we previously noted here, BB-Cl-amidine treatment leads to a marked reduction in activated HER2/ERBB2 and EGFR. This potentially suggests that PADI2 may act directly on proteins, and that reducing PADI2-mediated citrullination might have an effect on these proteins phosphorylation levels. To test this, we treated BT474 cells with BB-Cl-amidine and the same PI3K pathway inhibitors, along with lapatinib, as well as combinations of the two. Interestingly, we found that BB-Cl-amidine reduces both phospho-AKT (serine-473) and phospho-MAPK

Figure 5.7: PADI2 expression is downstream of HER2/ERBB2 signaling via the PI3K-ATK-mTOR pathway, and BB-Cl-amidine can reduce activation of both PI3K and MAPK signaling. (A) MCF10A cells stably overexpressing HER2 (10A-HER2) or GFP (10A-GFP) were analyzed by western blot for ERBB2 and PADI2 expression. β-actin was used as a loading control for both blots. (B) Bt474 cells were transfected with siRNA targeting *PADI2* and *ERBB2*, or control non-targeting siRNA, for 72h. Western blot analyses of siRNA treated BT474 cells for ERBB2 and PADI2 protein expression with β-actin serving as a loading control. (C) Western blot analysis of protein expression in BT474 cells treated with the following small molecule inhibitors: AG1478 (EGFR, 10 μM), lapatinib ([LAP] EGFR/HER2, 1 μM), LY294002 (PI3K, 20 μM), triciribine (Akt, 1 μM), rapamycin (mTOR, 100 nM), and PD98059 (MAPK/MEK, 20 μM). Antibodies against ERBB2/pERBB2 (Y1248), PADI2, phospho-AKT (S473), and phospho-MAPK (T202/Y204) were used, with β-actin serving as a loading control. (D) BT474 cells were treated for 48h with BB-Cl-amidine, BB-Cl-amidine and lapatinib together, or with a combination of BB-Cl-amidine plus PI3K pathway inhibitors (LY294002, triciribine, and rapamycin). Whole-cell lysates were probed for ERBB2/pERBB2 (Y1248), AKT/pAKT (S473), and MAPK/pMAPK (T202/Y204), with β-actin serving as a loading control.

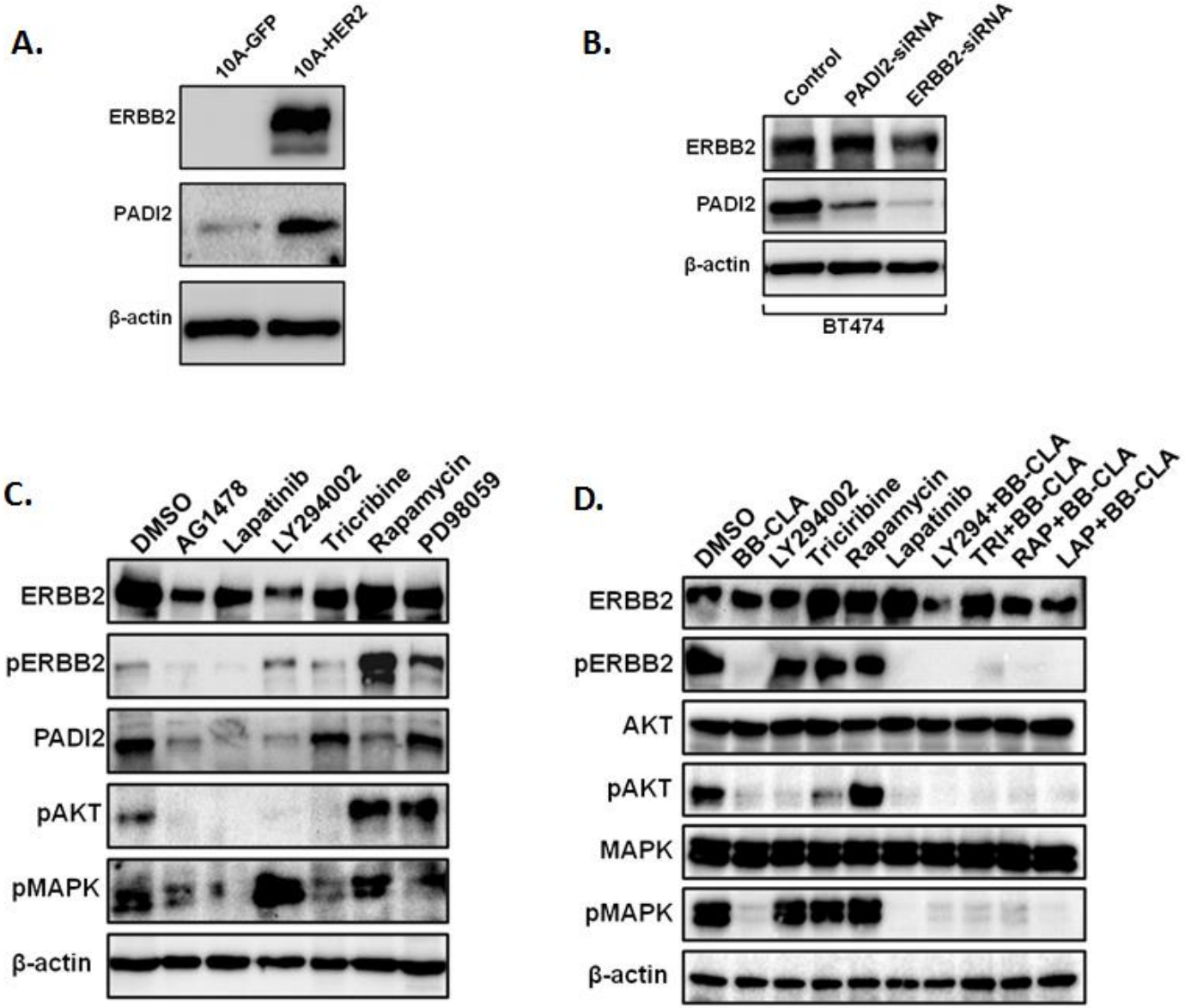
A.
10A-GFP
10A-HER2
ERBB2
PADI2
β-actin
B.
Control
PADI2-siRNA
ERBB2-siRNA
ERBB2
PADI2
β-actin
BT474
C.
DMSO
AG1478
Lapatinib
LY294002
Tricribine
Rapamycin
PD98059
ERBB2
pERBB2
PADI2
pAKT
pMAPK
β-actin
D.
DMSO
BB-CLA
LY294002
Triciribine
Rapamycin
Lapatinib
LY294+BB-CLA
TRI+BB-CLA
RAP+BB-CLA
LAP+BB-CLA
ERBB2
pERBB2
AKT
pAKT
MAPK
pMAPK
β-actin

(threonine-202/ tyrosine-204) levels (**Figure 5.7D**). Furthermore, we found that increasing levels of lapatinib along with a low-dose of BB-Cl-amidine (500 nM), had synergistic effects and greatly reduced cellular proliferation of BT474 cells (**Figure 5.8A**). However, we did not see the same effect on the MCF10DCIS cells (**Figure 5.8B**). This was not surprising, as MCF10DCIS cells have been reported to be resistant to lapatinib treatment due to an activating mutation in the PIK3CA gene (H1047R) (25,26). The following results establish a novel role for any PADI inhibitor, and potentially indicate an enhanced role for this small molecule in the treatment of breast cancers. Future studies might examine whether PADI2 knockdown might have any effect on the lapatinib resistance of MCF10DCIS cells.

DISCUSSIONS

Our previous work has established a role for PADI2 as an epigenetic regulator of ER-target gene expression in mammary tumorigenesis (16), in addition to establishing a correlation between PADI2 and HER2/ERBB2 expression across 57 breast cancer cell lines (15). The work presented here looks to expand on both of these studies, and to establish a role for PADI2 in the expression of the HER2 oncogene. We set out to explore the functional relationship between PADI2 and HER2, i.e. whether PADI2 enhances HER2 expression or vice-versa. Interestingly, PADI2 appears to function both upstream and downstream of HER2, potentially indicating a role in an oncogenic positive-feedback loop with HER2. Previous evidence from our lab has shown that PADI2 can act as an ER co-activator via the citrullination of H3R26 (16), so we were curious to see if PADI2 regulates *HER2* expression using the same mechanism. Interestingly, a recent report by Hurtado et al. has found that ER can regulate HER2/ERBB2 expression by binding to an estrogen response element (ERE) within intron 4 of the HER2/ERBB2 gene (27).

Figure 5.8: BB-Cl-amidine has a synergistic effect with lapatinib in the treatment of BT474, but not MCF10DCIS breast cancer cells. BT474 (a) or MCF10DCIS (b) cells were treated with increasing concentrations of BB-Cl-amidine or lapatinib alone, or with a combination of BB-Cl-amidine (0.5 μM) and increasing concentrations of lapatinib. BT474 cells were treated over the course of 3-weeks, and MCF10DCIS cells 1-week, with new media and drug added every 3d. Cells were fixed with 4% PFA and stained with crystal violet for subsequent analysis of focus formation.

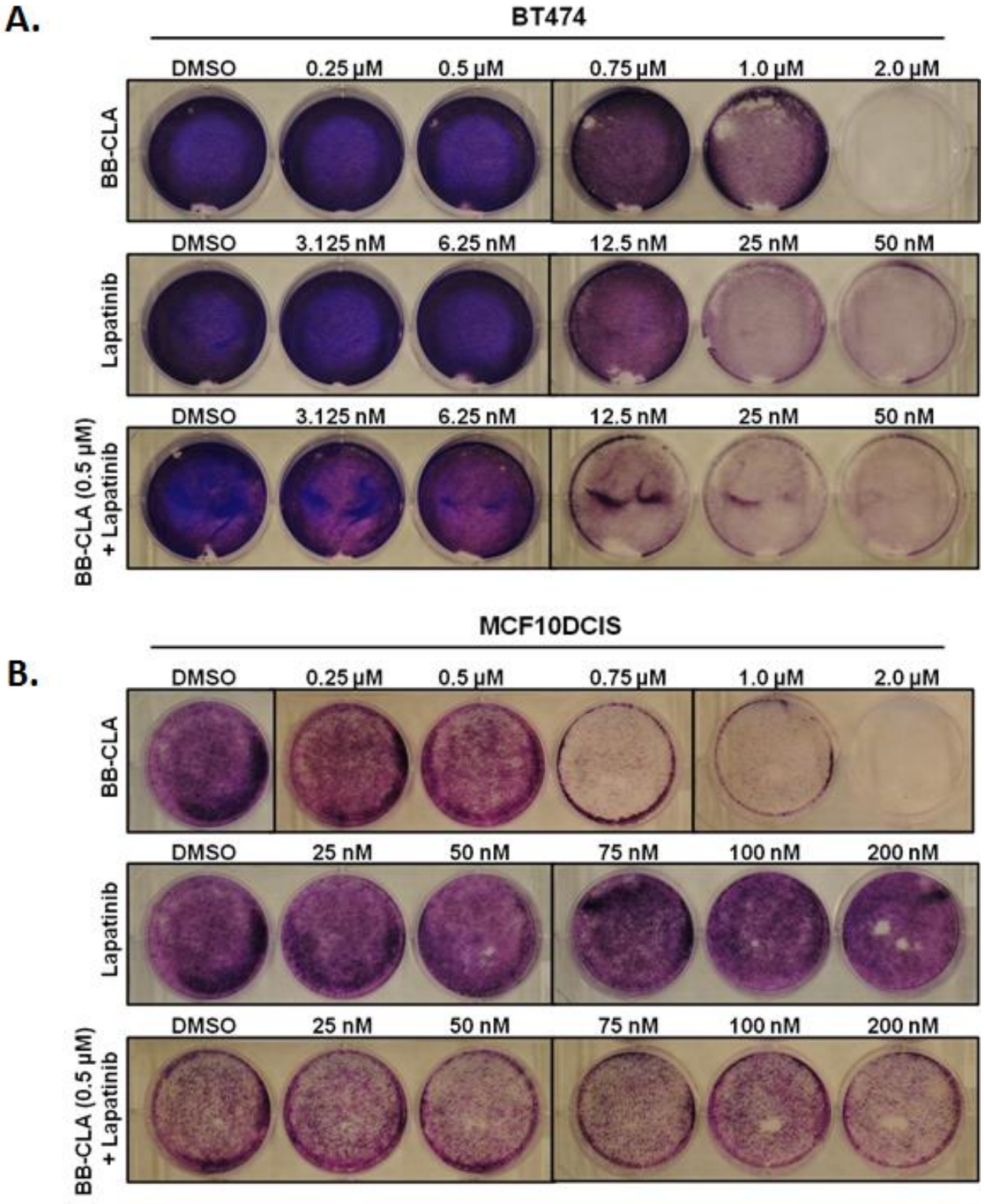
A.
BT474
DMSO
0.25 µM
0.5 µM
0.75 µM
1.0 µM
2.0 µM
BB-CLA
DMSO
3.125 nM
6.25 nM
12.5 nM
25 nM
50 nM
Lapatinib
DMSO
3.125 nM
6.25 nM
12.5 nM
25 nM
50 nM
BB-CLA (0.5 µM) + Lapatinib
B.
MCF10DCIS
DMSO
0.25 µM
0.5 µM
0.75 µM
1.0 µM
2.0 µM
BB-CLA
DMSO
25 nM
50 nM
75 nM
100 nM
200 nM
Lapatinib
DMSO
25 nM
50 nM
75 nM
100 nM
200 nM
BB-CLA (0.5 µM) + Lapatinib

Therefore, it is possible that, similar to other ER target genes, PADI2 regulates HER2/ERBB2 expression by functioning as an ER co-factor. We show here that PADI2 strongly binds the *HER2* proximal promoter), in addition to the recently characterized ERE. In the presence of the PADI inhibitor, BB-Cl-amidine, we see a dose-dependent reduction in HER2 protein and mRNA. We also see the reduction of HER2 protein and mRNA in cells that were stably transfected with shRNA for *PADI2*. Furthermore, there was also a concomitant reduction in the growth and malignant progression of these cells upon inhibition or shRNA knockdown of PADI2. It is interesting to speculate how PADI2 can function both as an ER and HER2 cofactor, especially with regard to mammary tumorigenesis. Previous evidence suggests that histone acetylation and phosphorylation play key roles in inducing HER2 expression (28), and we have previously shown that histone citrullination enhances histone acetylation and vice-versa (29). Therefore, provided with what we know about PADI2 as a co-activator of ER target genes, we can hypothesize that HER2 gene expression might work in the same fashion. Finally, we also provide evidence that PADI2 functions in a positive-feedback loop with HER2/ERBB2. We found using inhibitors for MAPK and PI3K pathways, that HER2/ERBB2 induces PADI2 expression downstream of PI3K-AKT-mTOR signaling. Interestingly, we also note that using the PADI2 inhibitor BB-Cl-amidine, along with lapatinib, had synergistic inhibitory effects on the growth and malignant nature of tumor cells *in vitro*. Currently, PI3K-AKT and mTOR inhibitors are effective therapies for the treatment of breast cancer, but they are often plagued by acquired resistance through the upregulation of receptor tyrosine kinase (RTK) activation via MAPK-ERK signaling (30). Surprisingly, we showed that BB-Cl-amidine treatment can reduce both pMAPK and pAKT, in addition to pERBB2; thus, relieving the RTK-activation seen when cells are treated with the mTOR inhibitor rapamycin.

CONCLUSIONS

Taken together, these results suggest an enhanced role for PADI2 in HER2 expressing breast cancers, and that the PADI inhibitor, BB-Cl-amidine, represents a potential novel therapy for the treatment of patients with HER2-positive mammary tumors.

MATERIALS AND METHODS

Cell culture and treatment with BB-Cl-amidine and small-molecule inhibitors

Cell lines from the MCF10AT breast cancer progression model used were the non-tumorigenic MCF10A, MCF10AT1kC1.2 (MCF10AT), and MCF10DCIS.com (MCF10DCIS) cells, and were obtained from Dr. Fred Miller (Barbara Ann Karmanos Cancer Institute, Detroit, MI, USA). This biological system has been extensively reviewed (31,32) and culture conditions described (33-35). The BT474, SKBR3, CHO-K1, and NIH-3T3 cell lines were obtained from ATCC and cultured according to manufacturer's directions. MCF10A cells overexpressing GFP or HER2 were a generous gift of Dr. Zachary Hartman, MD Anderson Cancer Center, and have been previously described elsewhere (36,37). All cells were maintained in a humidified atmosphere of 5% CO_2 at 37^o C. For the experimental treatment of cell lines with inhibitors, cells were seeded in 6-well plates (2×10^4) and treated with select inhibitors: LY294002 (#9901, Cell Signaling), PD98059 (#9900, Cell Signaling), AG1478 (#658548, Calbiochem), Triciribine (#124012, Calbiochem), Rapamycin (R0395, Sigma), Lapatinib (SC-202205, Santa Cruz), and BB-Cl-amidine, which was a generous gift of Dr. Paul Thompson (The Scripps Research Institute, Florida).

Generation of stable cell lines

The MCF10DCIS and BT474 cell lines where stably transduced with lentivirus expressing shRNA for PADI2 or non-targeting shRNA control. Mission shRNA lentivirus plasmids for PADI2 (TRCN0000051447 – NM_007365.1-995s1c1) and non-targeting control (SHC002) were purchased from Sigma. Lentivirus was prepared and transduced according to manufacturer's instructions. Stable clones were generated after selection with 2 µg/ml of puromycin for 2-3-weeks. The MCF10AT cell line was previously generated from MCF10A cells that were stably transfected with T24 H-Ras under G418 selection (38). Because of this, we generated a pcDNA3.1-hyg (+) vector expressing FLAG-PADI2 by subcloning FLAG-PADI2 from the previously validated pcDNA3.1-neo (+) overexpression vector (pcDNA3.1-FLAG-PADI2 (16)) using NheI and XhoI restriction sites. MCF10AT cells were transfected with the pcDNA3.1-hyg-FLAG-PADI2 plasmid using X-tremeGene 9 (Roche), and stable clones selected in 100 µg/ml hygromycin.

Transient siRNA

Pooled small interfering RNA (siRNA) oligonucleotides (ON-TARGET plus human SMARTpool) against *PADI2* and *ERBB2* were purchased from Dharmacon RNA Technologies (Thermo Scientific). For siRNA transfection of MCF10DCIS and BT474 cell lines, cells were seeded at 100,000/well in 6-well plates, and transfected with 50–100 nM of the pooled oligonucleotide mixture by using X-tremeGENE siRNA transfection reagent (Roche) following manufacturer's protocols. Cells were grown for 72h before subsequent analysis by western blot or qPCR.

Chromatin-immunoprecipitation (ChIP)

Chromatin immunoprecipitation (ChIP) experiments were performed as previously described (16,39). Briefly, MCF10DCIS and BT474 cells were grown to ~80 to 90% confluence, cross-linked with 1% PFA for 10 min at 37^{o}C, and quenched with glycine (125 mM) for 5 min at 4^{o}C. The cells were lysed (1% SDS, 10 mM EDTA, 50 mM Tris·HCl, pH 7.9, 1x protease inhibitor cocktail) and sonicated under conditions yielding fragments ranging from 300bp to 700bp. The material was clarified by centrifugation, diluted 10-fold in dilution buffer (0.5% Triton X-100, 2 mM EDTA, 150 mM NaCl, 20 mM Tris·HCl, pH 7.9, 1x protease inhibitor cocktail), and pre-cleared with protein A-agarose beads. The pre-cleared, chromatin-containing supernatant was used in immunoprecipitation reactions with antibodies against PADI2 (12110-1-AP, ProteinTech) and H3Cit26 (ab19847, Abcam). Ten percent of the supernatant was saved as reference control. The immunoprecipitated genomic DNA was cleared of protein and residual RNA by digestion with proteinase K and RNase (Roche), respectively. The DNA was then extracted with phenol:chloroform:isoamyl alcohol and precipitated with ethanol. ChIP analysis of the *HER2/ERBB2* promoter and downstream ERE (intron 4) was performed using quantitative real-time PCR (qPCR) to determine the enrichment of immunoprecipitated DNA relative to the input DNA, using primers as previously described (27). Each ChIP experiment was conducted a minimum of three times with independent chromatin isolates to ensure reproducibility.

Western blotting

Western blotting was carried out as previously described (13). Primary antibodies against the following proteins were incubated overnight at 4^{o}C: PADI2 (12110-1-AP, ProteinTech), ERBB2 (A0485, Dako), pERBB2-Y1248 (2247S, Cell Signaling), EGFR (ab2430, Abcam), pEGFR-

Y1173 (4407, Cell Signaling), AKT (4691P, Cell Signaling), pAKT-S473 (4060P, Cell Signaling), MAPK (4695, Cell Signaling), pMAPK-T202/Y204 (4370P, Cell Signaling), AIB1 (2126S, Cell Signaling), and ER-alpha (SC-542, Santa Cruz). To confirm equal protein loading, membranes were stripped and re-probed with anti-β-actin (ab8227, Abcam).

Quantitative real-time PCR (qPCR)

RNA was purified using the Qiagen RNAeasy kit, including on-column DNase treatment to remove genomic DNA. The resulting RNA was reverse transcribed using the ABI High Capacity RNA-to-cDNA kit according to the manufacturer's protocol (Applied Biosystems). TaqMan Gene Expression Assays (ABI) for human *PADI2* (Hs00247108_m1), *ERBB2* (Hs01001580_m1), *EGFR* (Hs01076078_m1), *AIB1* (Hs00180722_m1), *ESR1* (Hs00174860_m1), and *GAPDH* (4352934E), were used for qPCR. Expression levels were analyzed using the $2^{-\Delta\Delta C(t)}$ method (40). Data are shown as means ± SD from three independent experiments, and were separated using Student's t-test.

Flow-cytometry

Monolayers of MCF10DCIS, BT474, CHO-K1, and NIH3T3 cells were seeded into 25 cm^2 flasks (2 x 10^6 cells) and treated with increasing concentrations of BB-Cl-amidine or vehicle (DMSO, 0.6125μM, 1.25 μM, 2.5 μM, and 5.0 μM). Cells were harvested after 48h using Accutase (Innovative Cell Technologies), fixed, permeabilized, and blocked in FACS Buffer (0.1M Dulbecco's phosphate buffered saline, 0.02% sodium azide, 1.0% bovine serum albumin, and 0.1% Triton X-100) containing 10% normal goat serum and stained (except the isotype controls) with rabbit anti-cleaved Caspase-3 antibody (Cell Signaling). Isotype controls were

treated with normal rabbit IgG (Vector Laboratories). All samples were stained with secondary goat anti-rabbit IgG conjugated to Alexa-488 (Invitrogen) and DAPI (Invitrogen) according to the manufacturer's instructions. Cells were analyzed on a FACS-Calibur (BD Biosciences) or a Gallios (Beckman Coulter) flow-cytometer and data analyzed for percent apoptotic cells (cleaved caspase-3-positive) and cell cycle analysis with FlowJo software (TreeStar Inc.). Data are shown as means ± SD from three independent experiments, and were separated using Student's t-test.

Assays for cellular malignancy

Anchorage-independent growth assays were performed on MCF10DCIS-P2KD and MCF10AT-PADI2 cells, along with their respective control cell lines (MCF10DCIS-SC and MCF10AT-emtpy). Briefly, the cells were plated at a density of 5,000 cells/ml in medium containing 0.3% agarose onto media containing 0.6% agarose in 6-well dishes. Cultures were fed once a week and colonies counted after 3-weeks of growth. Each assay was repeated and means represent ± SD from three independent experiments (* $p < 0.05$). Focus formation assays were carried out on cells grown in 6-well plates. Cells were fixed with 4% PFA and stained with crystal violet for subsequent analysis of focus formation.

Statistical analysis

All experiments were independently repeated at least three times unless otherwise indicated. Values were expressed as the mean $\pm$ the SD. Means were separated using Student's t-test.

REFERENCES

1. Coughlin, S. S., and Ekwueme, D. U. (2009) Breast cancer as a global health concern. *Cancer Epidemiol* **33**, 315-318

2. Jemal, A., Siegel, R., Xu, J., and Ward, E. (2010) Cancer statistics, 2010. *CA Cancer J Clin* **60**, 277-300

3. Osborne, C. K., and Schiff, R. (2011) Mechanisms of endocrine resistance in breast cancer. *Annu Rev Med* **62**, 233-247

4. Knowlden, J. M., Hutcheson, I. R., Jones, H. E., Madden, T., Gee, J. M., Harper, M. E., Barrow, D., Wakeling, A. E., and Nicholson, R. I. (2003) Elevated levels of epidermal growth factor receptor/c-erbB2 heterodimers mediate an autocrine growth regulatory pathway in tamoxifen-resistant MCF-7 cells. *Endocrinology* **144**, 1032-1044

5. Shou, J., Massarweh, S., Osborne, C. K., Wakeling, A. E., Ali, S., Weiss, H., and Schiff, R. (2004) Mechanisms of tamoxifen resistance: increased estrogen receptor-HER2/neu cross-talk in ER/HER2-positive breast cancer. *J Natl Cancer Inst* **96**, 926-935

6. Arpino, G., Wiechmann, L., Osborne, C. K., and Schiff, R. (2008) Crosstalk between the estrogen receptor and the HER tyrosine kinase receptor family: molecular mechanism and clinical implications for endocrine therapy resistance. *Endocr Rev* **29**, 217-233

7. Slamon, D. J., Godolphin, W., Jones, L. A., Holt, J. A., Wong, S. G., Keith, D. E., Levin, W. J., Stuart, S. G., Udove, J., Ullrich, A., and et al. (1989) Studies of the HER-2/neu proto-oncogene in human breast and ovarian cancer. *Science* **244**, 707-712

8. Esteva, F. J., Valero, V., Booser, D., Guerra, L. T., Murray, J. L., Pusztai, L., Cristofanilli, M., Arun, B., Esmaeli, B., Fritsche, H. A., Sneige, N., Smith, T. L., and Hortobagyi, G. N. (2002) Phase II study of weekly docetaxel and trastuzumab for patients with HER-2-overexpressing metastatic breast cancer. *J Clin Oncol* **20**, 1800-1808

9. Seidman, A., Hudis, C., Pierri, M. K., Shak, S., Paton, V., Ashby, M., Murphy, M., Stewart, S. J., and Keefe, D. (2002) Cardiac dysfunction in the trastuzumab clinical trials experience. *J Clin Oncol* **20**, 1215-1221

10. Huang, Y., Nayak, S., Jankowitz, R., Davidson, N. E., and Oesterreich, S. (2011) Epigenetics in breast cancer: what's new? *Breast Cancer Res* **13**, 225

11. Jovanovic, J., Ronneberg, J. A., Tost, J., and Kristensen, V. (2010) The epigenetics of breast cancer. *Mol Oncol* **4**, 242-254

12. Vo, A. T., and Millis, R. M. (2012) Epigenetics and breast cancers. *Obstet Gynecol Int* **2012**, 602720

13. Cherrington, B. D., Morency, E., Struble, A. M., Coonrod, S. A., and Wakshlag, J. J. (2010) Potential role for peptidylarginine deiminase 2 (PAD2) in citrullination of canine mammary epithelial cell histones. *PLoS One* **5**, e11768

14. Cherrington, B. D., Zhang, X., McElwee, J. L., Morency, E., Anguish, L. J., and Coonrod, S. A. (2012) Potential role for PAD2 in gene regulation in breast cancer cells. *PLoS One* **7**, e41242

15. McElwee, J. L., Mohanan, S., Griffith, O. L., Breuer, H. C., Anguish, L. J., Cherrington, B. D., Palmer, A. M., Howe, L. R., Subramanian, V., Causey, C. P., Thompson, P. R., Gray, J. W., and Coonrod, S. A. (2012) Identification of PADI2 as a potential breast cancer biomarker and therapeutic target. *BMC Cancer* **12**, 500

16. Zhang, X., Bolt, M., Guertin, M. J., Chen, W., Zhang, S., Cherrington, B. D., Slade, D. J., Dreyton, C. J., Subramanian, V., Bicker, K. L., Thompson, P. R., Mancini, M. A., Lis, J. T., and Coonrod, S. A. (2012) Peptidylarginine deiminase 2-catalyzed histone H3 arginine 26 citrullination facilitates estrogen receptor alpha target gene activation. *Proc Natl Acad Sci U S A* **109**, 13331-13336

17. Chumanevich, A. A., Causey, C. P., Knuckley, B. A., Jones, J. E., Poudyal, D., Chumanevich, A. P., Davis, T., Matesic, L. E., Thompson, P. R., and Hofseth, L. J. (2011) Suppression of colitis in mice by Cl-amidine: a novel peptidylarginine deiminase inhibitor. *Am J Physiol Gastrointest Liver Physiol* **300**, G929-938

18. Lange, S., Gogel, S., Leung, K. Y., Vernay, B., Nicholas, A. P., Causey, C. P., Thompson, P. R., Greene, N. D., and Ferretti, P. (2011) Protein deiminases: new players in the developmentally regulated loss of neural regenerative ability. *Dev Biol* **355**, 205-214

19. Willis, V. C., Gizinski, A. M., Banda, N. K., Causey, C. P., Knuckley, B., Cordova, K. N., Luo, Y., Levitt, B., Glogowska, M., Chandra, P., Kulik, L., Robinson, W. H., Arend, W. P., Thompson, P. R., and Holers, V. M. (2011) N-alpha-benzoyl-N5-(2-chloro-1-iminoethyl)-L-ornithine amide, a protein arginine deiminase inhibitor, reduces the severity of murine collagen-induced arthritis. *J Immunol* **186**, 4396-4404

20. Miller, F. R., Santner, S. J., Tait, L., and Dawson, P. J. (2000) MCF10DCIS.com xenograft model of human comedo ductal carcinoma in situ. *J Natl Cancer Inst* **92**, 1185-1186

21. Shekhar, M. P., Kato, I., Nangia-Makker, P., and Tait, L. (2013) Comedo-DCIS is a precursor lesion for basal-like breast carcinoma: identification of a novel p63/Her2/neu expressing subgroup. *Oncotarget* **4**, 231-241

22. So, J. Y., Lee, H. J., Kramata, P., Minden, A., and Suh, N. (2012) Differential Expression of Key Signaling Proteins in MCF10 Cell Lines, a Human Breast Cancer Progression Model. *Mol Cell Pharmacol* **4**, 31-40

23. Luo, Y., Arita, K., Bhatia, M., Knuckley, B., Lee, Y. H., Stallcup, M. R., Sato, M., and Thompson, P. R. (2006) Inhibitors and inactivators of protein arginine deiminase 4: functional and structural characterization. *Biochemistry* **45**, 11727-11736

24. Slack, J. L., Causey, C. P., and Thompson, P. R. (2011) Protein arginine deiminase 4: a target for an epigenetic cancer therapy. *Cell Mol Life Sci* **68**, 709-720

25. Kalaany, N. Y., and Sabatini, D. M. (2009) Tumours with PI3K activation are resistant to dietary restriction. *Nature* **458**, 725-731

26. Farnie, G., Willan, P. M., Clarke, R. B., and Bundred, N. J. (2013) Combined inhibition of ErbB1/2 and Notch receptors effectively targets breast ductal carcinoma in situ (DCIS) stem/progenitor cell activity regardless of ErbB2 status. *PLoS One* **8**, e56840

27. Hurtado, A., Holmes, K. A., Geistlinger, T. R., Hutcheson, I. R., Nicholson, R. I., Brown, M., Jiang, J., Howat, W. J., Ali, S., and Carroll, J. S. (2008) Regulation of ERBB2 by oestrogen receptor-PAX2 determines response to tamoxifen. *Nature* **456**, 663-666

28. Mishra, S. K., Mandal, M., Mazumdar, A., and Kumar, R. (2001) Dynamic chromatin remodeling on the HER2 promoter in human breast cancer cells. *FEBS Lett* **507**, 88-94

29. Kan, R., Jin, M., Subramanian, V., Causey, C. P., Thompson, P. R., and Coonrod, S. A. (2012) Potential role for PADI-mediated histone citrullination in preimplantation development. *BMC Dev Biol* **12**, 19

30. Serra, V., Scaltriti, M., Prudkin, L., Eichhorn, P. J., Ibrahim, Y. H., Chandarlapaty, S., Markman, B., Rodriguez, O., Guzman, M., Rodriguez, S., Gili, M., Russillo, M., Parra, J. L., Singh, S., Arribas, J., Rosen, N., and Baselga, J. (2011) PI3K inhibition results in enhanced HER signaling and acquired ERK dependency in HER2-overexpressing breast cancer. *Oncogene* **30**, 2547-2557

31. Heppner, G. H., and Wolman, S. R. (1999) MCF-10AT: A Model for Human Breast Cancer Development. *Breast J* **5**, 122-129

32. Dawson, P. J., Wolman, S. R., Tait, L., Heppner, G. H., and Miller, F. R. (1996) MCF10AT: a model for the evolution of cancer from proliferative breast disease. *Am J Pathol* **148**, 313-319

33. Hu, M., Peluffo, G., Chen, H., Gelman, R., Schnitt, S., and Polyak, K. (2009) Role of COX-2 in epithelial-stromal cell interactions and progression of ductal carcinoma in situ of the breast. *Proc Natl Acad Sci U S A* **106**, 3372-3377

34. Hu, M., Yao, J., Carroll, D. K., Weremowicz, S., Chen, H., Carrasco, D., Richardson, A., Violette, S., Nikolskaya, T., Nikolsky, Y., Bauerlein, E. L., Hahn, W. C., Gelman, R. S., Allred, C., Bissell, M. J., Schnitt, S., and Polyak, K. (2008) Regulation of in situ to invasive breast carcinoma transition. *Cancer Cell* **13**, 394-406

35. Shekhar, M. P., Tait, L., Pauley, R. J., Wu, G. S., Santner, S. J., Nangia-Makker, P., Shekhar, V., Nassar, H., Visscher, D. W., Heppner, G. H., and Miller, F. R. (2008) Comedo-ductal carcinoma in situ: A paradoxical role for programmed cell death. *Cancer Biol Ther* **7**, 1774-1782

36. Hartman, Z. C., Wei, J., Osada, T., Glass, O., Lei, G., Yang, X. Y., Peplinski, S., Kim, D. W., Xia, W., Spector, N., Marks, J., Barry, W., Hobeika, A., Devi, G., Amalfitano, A., Morse, M. A., Lyerly, H. K., and Clay, T. M. (2010) An adenoviral vaccine encoding full-length inactivated human Her2 exhibits potent immunogenicty and enhanced therapeutic efficacy without oncogenicity. *Clin Cancer Res* **16**, 1466-1477

37. Hartman, Z. C., Yang, X. Y., Glass, O., Lei, G., Osada, T., Dave, S. S., Morse, M. A., Clay, T. M., and Lyerly, H. K. (2011) HER2 overexpression elicits a proinflammatory IL-6 autocrine signaling loop that is critical for tumorigenesis. *Cancer Res* **71**, 4380-4391

38. Miller, F. R., Soule, H. D., Tait, L., Pauley, R. J., Wolman, S. R., Dawson, P. J., and Heppner, G. H. (1993) Xenograft model of progressive human proliferative breast disease. *J Natl Cancer Inst* **85**, 1725-1732

39. Zhang, X., Gamble, M. J., Stadler, S., Cherrington, B. D., Causey, C. P., Thompson, P. R., Roberson, M. S., Kraus, W. L., and Coonrod, S. A. (2011) Genome-wide analysis reveals PADI4 cooperates with Elk-1 to activate c-Fos expression in breast cancer cells. *PLoS Genet* **7**, e1002112

40. Livak, K. J., and Schmittgen, T. D. (2001) Analysis of relative gene expression data using real-time quantitative PCR and the 2(-Delta Delta C(T)) Method. *Methods* **25**, 402-408

CHAPTER SIX

CONCLUSIONS

SUMMARY OF CHAPTERS

Prior to my work, very little was known about the role of PADI2 in breast cancer progression. That is because the roles of PADIs in female reproductive tissues were poorly understood. Thus, in **Chapter 2**, we investigated the expression patterns of PADIs in female reproductive tissues. We found that both PADI2 and PADI4 are expressed in uterine and mammary epithelial cells (1). Interestingly, we also found that their expression is regulated by estrogen. When we ovariectomized the mice so that they can no longer produce estrogen, there were almost undetectable levels of PADI2 and PADI4 in their uteri and mammary glands. However, when we treated the ovariectomized mice with estrogen, PADI2 and PADI4 expression was upregulated in both the uterus and mammary glands.

Recent studies have found PADI2 as one of the top hit genes that correlates with breast cancer (2-4); however, no study has investigated the role of PADI2 in breast cancer. In **Chapter 3**, I investigated the role of PADI2 in breast cancer progression. I found that depletion of PADI2 results in altered cell morphology where the cells turned from mesenchymal to epithelial-like cells. I found that depletion of PADI2 downregulates the expression levels of Rho family of GTPases (RhoA, Rac1, and Cdc42) that are involved in regulating actin cytoskeleton while upregulates cell adhesion maker, E-cadherin. In addition, I found that EGF induced cell migration robustly enhanced PADI2 expression and activity. However, treatment with BB-Cl-Amidine suppressed tumor cell migration *in vitro*. Using primary mouse mammary organoid, we found that EGF promotes ductal migration and invasion but is severely impaired after BB-Cl-Amidine treatment. Together, these show that PADI2 is involved in tumor cell migration and invasion and that BB-Cl-Amidine can be used as a potential therapeutics.

As mentioned in the introduction, there are two PADI inhibitors (Cl-Amidine and BB-Cl-Amidine) that were generated by our close collaborator, Dr. Paul Thompson (5). In **Chapter 4**, I described the methods in which I used to test the efficacy of the second generation PADI inhibitor, BB-Cl-Amidine (6). I performed soft agar colony formation assays using the MCF10DCIS.com cells that highly express PADI2 and found that the use of only 1 μM of BB-Cl-Amidine was enough to suppress their colony number and colony size. There was a 44% decrease in the number of colonies after BB-Cl-Amidine treatment and the size of the colony is smaller from the range of 70 μm-150 μm to 20 μm-100 μm. This shows that BB-Cl-Amidine may be a potential therapy for breast cancer and is a more potent inhibitor than Cl-Amidine.

MCF10DCIS.com cells that were used in my previous chapters are HER2+ breast cancer. Previous study from our laboratory has shown that PADI2 expression is correlated with HER2 expression. Thus, in **Chapter 5**, we tested whether PADI2 plays a role in HER2 expression and vice versa. We first found that depletion of PADI2 in MCF10DCIS.com and BT474 cells also decreased HER2 expression. Interestingly, we found that PADI2 (as well as H3R26Cit) binds to the HER2 promoter and its downstream ERE. This means that PADI2 may be altering histone structure for favorable transcription of HER2 target genes. This may explain why depletion of PADI2 (either by knockdown or use of BB-Cl-Amidine) results in reduced HER2 expression and activity. Interestingly, we also found that increase in HER2 also upregulates PADI2 expression. This suggests that PADI2 and HER2 might be involved in a positive feedback loop. Lastly, we found that BB-Cl-Amidine can successfully promote apoptosis in PADI2 positive MCF10DCIS.com and BT474 cells without affecting the “normal”, PADI2 negative, NIH-3T3 and CHO-K1 cells. This shows that PADI inhibitor can specifically target PADI2 expressing breast cancer cells.

FUTURE DIRECTION – ROLE OF PADI2 IN TAMOXIFEN RESISTANCE

Recent studies suggest ER and HER2 crosstalk promotes tamoxifen resistance (7,8). Due to our previous findings on the role of PADI2 as an ER-cofactor (9,10) and the role of PADI2 in regulating HER2 expression (**Chapter 5**), I investigated the potential role of PADI2 in tamoxifen resistance. However, due to lack of time, this project is still work in progress. The following section details the best of these data supporting the role of PADI2 in the development of tamoxifen resistance.

Contributions

Manuscript preparation: Horibata, S. and Coonrod, S.A.

Conception and Design: Horibata, S., Coonrod, S.A., and Danko, C.D.

Development of methodology: Horibata, S., Rice, E., Coonrod, S.A., Danko, C.D.

BB-Cl-Amidine and Cl-Amidine: Provided by Thompson, P.R.

Acquisition of data:

Figure 6.1A-E: Horibata, S. (and Rogers, K assisted with staining in Figure 6.1D and 6.1E.)

Figure 6.2: Horibata, S. (and Rogers, K. assisted with staining in Figure 6.2C and 6.2D.)

Figure 6.3: Horibata, S.

Figure 6.4: Horibata, S. and Rice, E. performed the PRO-seq and Danko, C.G. conducted the computational analysis.

Figure 6.5: Figure 6.5A, 6.5B, 6.5D: Horibata, S. and Rice, E. performed the PRO-seq and Danko, C.G. conducted the computational analysis; Figure 6.5C and 6.5E: Horibata, S.; Figure 6.5F: Zhang, H.

Introduction

Approximately, 75% of all breast cancers are estrogen receptor (ER) positive and most breast cancer deaths occur in women with this subtype of breast cancer (7,11-13). The commonly prescribed estrogen blocker for ER+ breast cancers is tamoxifen. However, despite initial success to this treatment, 40-50% of patients will have tamoxifen resistance (14). Thus, a major challenge for the breast cancer field is to develop new therapies that will prevent tumor recurrence and metastasis.

Our recent genome-wide studies have demonstrated that PADI2 is required for ER binding (9), and that H3R26Cit marks overlaps with ER-binding sites in the genome, with 99.97% of ER peaks overlapping with H3R26Cit peaks at all time-points following estrogen (E2) (10). Since PADI2 is required for ER signaling, we tested whether PADI2 is involved in tamoxifen resistance.

PADI2 is highly upregulated in tamoxifen resistance cells

The most commonly used model of ER+ breast cancer cells are MCF-7 cells. Recently however, Gonzalez-Malerva et al. has shown that MCF-7 cells are heterogeneous in nature contain both tamoxifen sensitive ($B7^{TamS}$ and $C11^{TamS}$) and resistant ($H9^{TamR}$ and $G11^{TamR}$) cells (15) (**Figure 6.1A**). Taking advantage of this naturally occurring tamoxifen resistance, we investigated the role of PADI2 in tamoxifen resistance.

To investigate whether PADI2 may play a role in tamoxifen resistance, we tested for PADI2 levels in these cells using qPCR and Western blotting. We found that PADI2 mRNA and

Figure 6.1: PADI2 upregulation in tamoxifen resistant MCF-7 subclones. (A) Tamoxifen sensitive B7 ^{TamS} and C11^{TamS} and tamoxifen resistant H9 ^{TamR} and G11^{TamR} were cultured in the presence of increasing dose of tamoxifen for 4 days. The cells were fixed with 4% PFA and were stained with crystal violet staining. The relative survival rates of the cells were measured using the measured absorbance at OD_{595}. Assay represents mean and ± SD from three independent experiments ($p < 0.05$). **(B)** Total RNA was isolated from B7 ^{TamS}, C11^{TamS}, H9 ^{TamR}, and G11^{TamR} cells. Their *PADI2* mRNA levels were determined by qRT-PCR (SYBR) using B7^{TamS} cells as a reference and β-actin normalization. Assay represents mean and ± SD from three independent experiments (* and ** $p < 0.05$). **(C)** The whole cell lysates of B7 ^{TamS}, C11^{TamS}, H9 ^{TamR}, and G11^{TamR} cells were immunoblotted with PADI2. The blot was also proved with β-actin antibody for control. **(D)** Immunofluorescent assay was performed on B7 ^{TamS} and G11^{TamR} cells and were proved with anti-PADI2 antibody and **(E)** anti-pan-citrulline antibody and DAPI (nuclei).

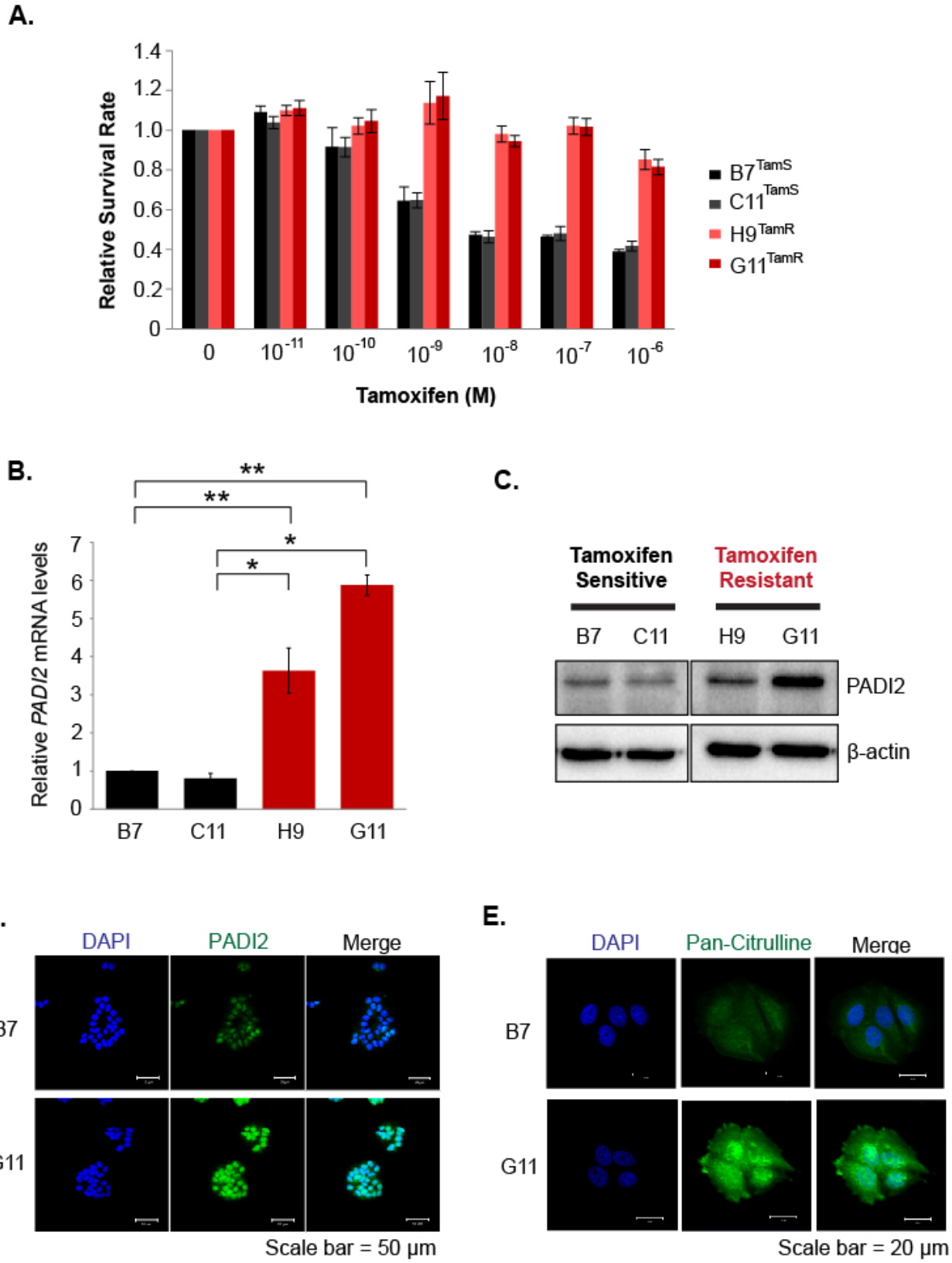
A.
Relative Survival Rate
1.4
1.2
1.0
0.8
0.6
0.4
0.2
0
0
10-11
10-10
10-9
10-8
10-7
10-6
Tamoxifen (M)
B7TamS
C11TamS
H9TamR
G11TamR
B.
Relative PADI2 mRNA levels
**
**
*
*
7
6
5
4
3
2
1
0
B7
C11
H9
G11
C.
Tamoxifen Sensitive
Tamoxifen Resistant
B7
C11
H9
G11
PADI2
β-actin
D.
DAPI
PADI2
Merge
B7
G11
Scale bar = 50 μm
E.
DAPI
Pan-Citrulline
Merge
B7
G11
Scale bar = 20 μm

protein expressions are robustly upregulated in $H9^{TamR}$ and $G11^{TamR}$ cells compared to the $B7^{TamS}$ and $C11^{TamS}$ cells (**Figure 6.1B and 6.1C**). Interestingly, there is high PADI2 expression and activity in the nucleus of the $H9^{TamR}$ and $G11^{TamR}$ cells (**Figure 6.1D and 6.1E**). We also found that PADI2 protein expression was elevated in a complementary tamoxifen resistant model cell lines, MCF7/HER2-18 cells (8,16), when compared to its control cell line, MCF7/NEG (**Figure 6.2A, 6.2B, 6.2C, and 6.2D**). These results strongly suggest that PADI2 is upregulated in tamoxifen resistance cell lines.

Tamoxifen resistant MCF-7 cells are more sensitive to PADI inhibitor than the tamoxifen sensitive MCF-7 cells

Since PADI2 is highly upregulated in tamoxifen resistance cell lines, we tested whether inhibition of PADI2 via the use of PADI inhibitor, BB-Cl-Amidine, would affect the survival rates of $B7^{TamS}$, $C11^{TamS}$, $H9^{TamR}$, and $G11^{TamR}$ cells. Interestingly, we found that tamoxifen resistant $H9^{TamR}$ and $G11^{TamR}$ cells are more sensitive to BB-Cl-Amidine treatment than the $B7^{TamS}$ and $C11^{TamS}$ cells (**Figure 6.3A and 6.3B**). $B7^{TamS}$ and $C11^{TamS}$ are also killed by the BB-Cl-Amidine. We hypothesize that this occurs because inhibition of PADI2 represses ER target gene activations and potentially affect their cell survival (**Figure 6.3A and 6.3B**). Moreover, we found robust increases in citrullination in $G11^{TamR}$ cells compared to $B7^{TamS}$ cells. However, BB-Cl-Amidine treatment greatly reduced citrullination of $G11^{TamR}$ cells; thus, this result potentially suggests why $H9^{TamR}$ and $G11^{TamR}$ cells are sensitive to BB-Cl-Amidine treatment (**Figure 6.3C**). This shows that targeting PADI2 may be a potential answer to treat tamoxifen resistant breast cancer.

Figure 6.2: PADI2 is upregulated in tamoxifen resistant MCF7/HER2-18 line. (A) Total RNA was isolated from MCF7/NEG and MCF7/HER2-18 cells. Their *PADI2* mRNA levels were determined by qRT-PCR (SYBR) using MCF7/NEG cells as a reference and β-actin normalization. Assay represents mean and ± SD from three technical experiments. **(B)** The whole cell lysates of MCF7/NEG and MCF7/HER2-18 cells were immunoblotted with HER2, phospho-HER2, and PADI2. The blot was also proved with β-actin antibody for control. **(C)** Immunofluorescent assay was performed on MCF7/NEG and MCF7/HER2-18 cells and were proved with anti-HER2 antibody and **(D)** anti-PADI2 antibody and DAPI (nuclei).

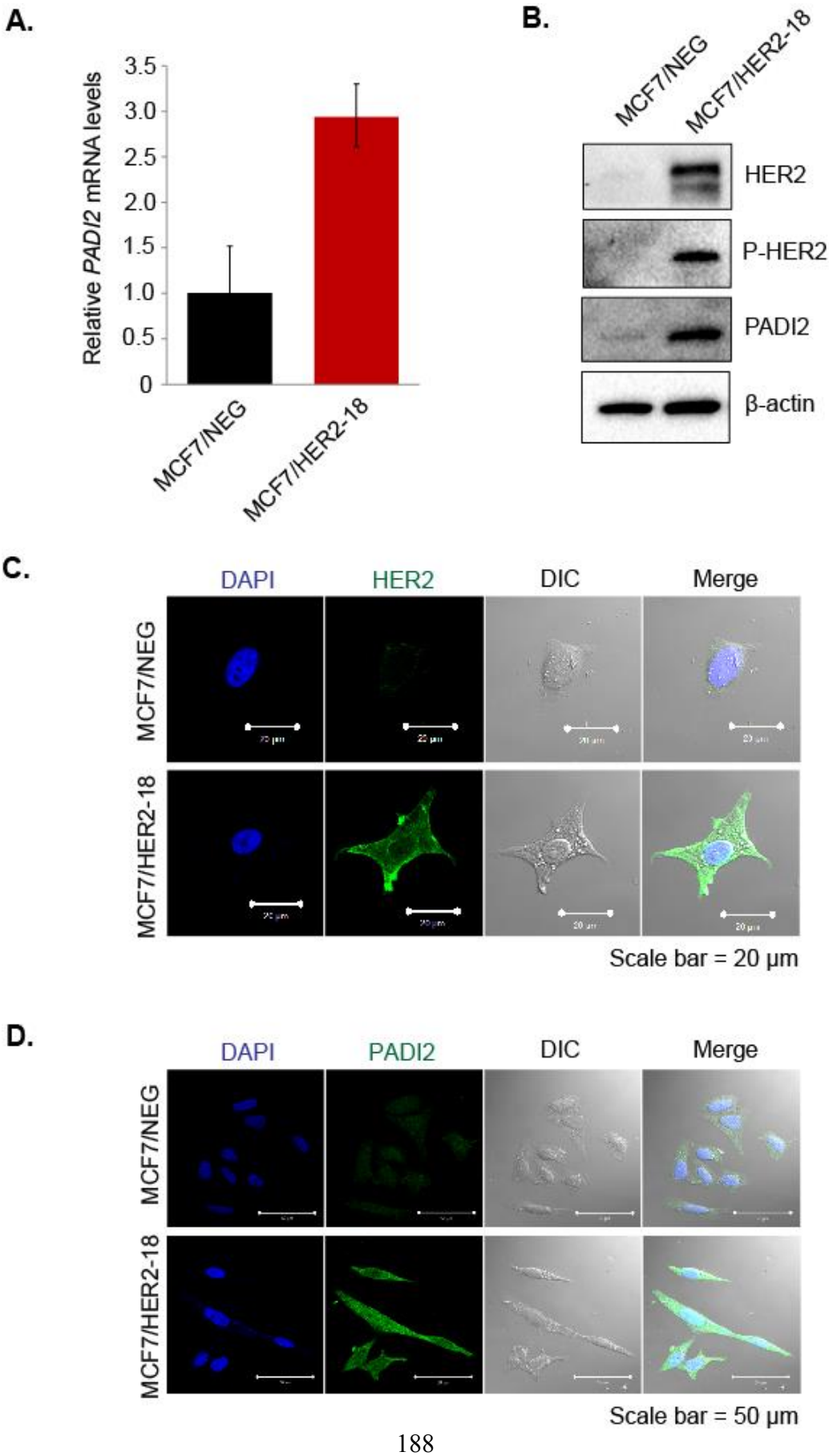
A.
Relative PADI2 mRNA levels
3.5
3.0
2.5
2.0
1.5
1.0
0.5
0
MCF7/NEG
MCF7/HER2-18
B.
MCF7/NEG
MCF7/HER2-18
HER2
P-HER2
PADI2
β-actin
C.
DAPI
HER2
DIC
Merge
MCF7/NEG
MCF7/HER2-18
Scale bar = 20 μm
D.
DAPI
PADI2
DIC
Merge
MCF7/NEG
MCF7/HER2-18
Scale bar = 50 μm

Figure 6.3: Tamoxifen resistant MCF-7 subclones are more sensitive to BB-Cl-Amidine treatment. (A) Tamoxifen sensitive B7 ^{TamS} and C11^{TamS} and tamoxifen resistant H9 ^{TamR} and G11^{TamR} were cultured in the presence of increasing dose of BB-Cl-Amidine for 4 days. The cells were fixed with 4% PFA and were stained with crystal violet staining. The relative survival rates of the cells were measured using the measured absorbance at OD_{595}. Assay represents mean and ± SD from three independent experiments. **(B)** Tamoxifen sensitive B7 ^{TamS} and C11^{TamS} and tamoxifen resistant H9 ^{TamR} and G11^{TamR} were cultured in the presence of 3 μM of BB-Cl-Amidine for 48 hours and were imaged. **(C)** The whole cell lysates of B7 ^{TamS} and G11^{TamR} cells treated without (DMSO) or with BB-Cl-Amidine were immunoblotted with anti-pan-citrulline antibody. The blot was also proved with β-actin antibody for control.

A.

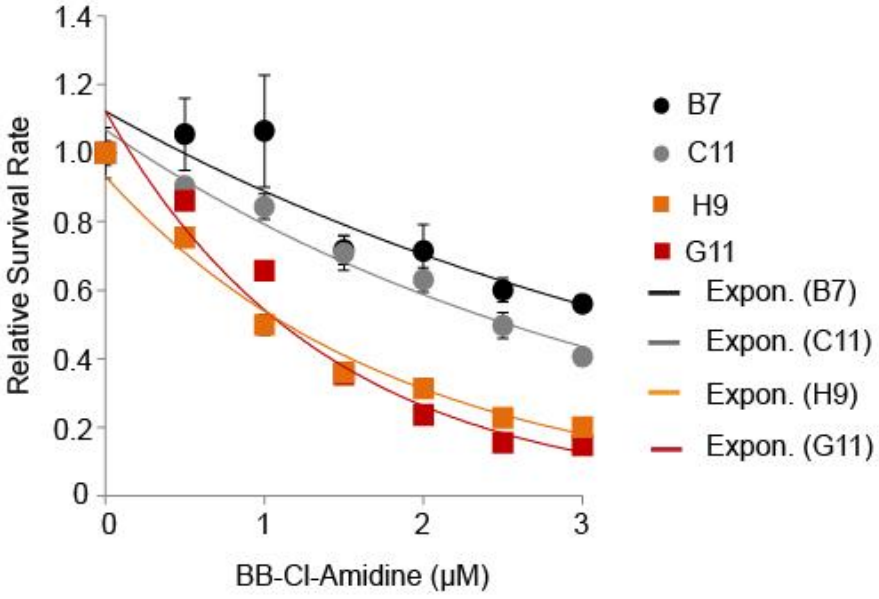
1.4
1.2
1.0
0.8
0.6
0.4
0.2
0
Relative Survival Rate
0
1
2
3
BB-Cl-Amidine (μM)
B7
C11
H9
G11
Expon. (B7)
Expon. (C11)
Expon. (H9)
Expon. (G11)

B.

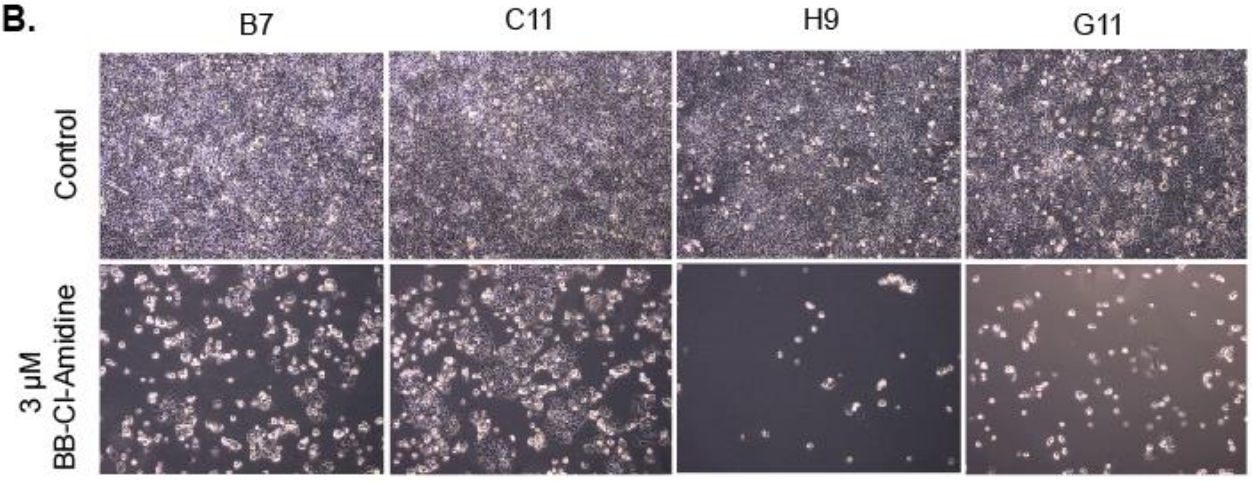
B7
C11
H9
G11
Control
3 μM
BB-Cl-Amidine

C.

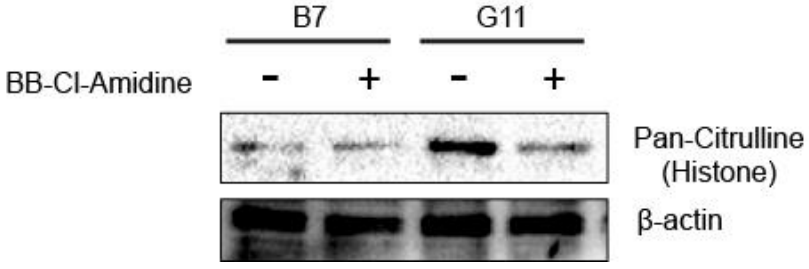
B7
G11
BB-Cl-Amidine
-
+
-
+
Pan-Citrulline
(Histone)
β-actin

Gene expression patterns of TamS and TamR cells revealed by PRO-seq

We next performed Precision nuclear Run-On sequencing (PRO-seq) assay on $B7^{TamS}$, $C11^{TamS}$, $H9^{TamR}$, and $G11^{TamR}$ cells to map the genome-wide distribution and orientation of transcriptionally engaged RNA polymerase II at a base-pair resolution and to identify genes involved in tamoxifen resistance (17). Gene expression analysis demonstrates that both TamS lines cluster together, whereas TamR lines cluster independently **(Figure 6.4A)**, possibly suggesting that multiple independent mechanisms cause resistance in $G11^{TamR}$ and $H9^{TamR}$ lines. Nonetheless, all four lines have highly similar overall gene expression patterns (Spearman's ranked correlation >0.95). In other words, the cause of differential responses to tamoxifen therapy likely resides within these small differences in gene expressions (Spearman's ranked correlation <0.05).

We next performed MA (M (log ratios) A (mean average)) plot analysis of gene expression patterns between TamS and TamR cells. We identified 527 genes with significant changes between TamS and TamR cells (341 up-regulated and 186 down-regulated genes) **(Figure 6.4B)**. Interestingly, we found that two of the most highly expressed genes in the TamS lines were the ER targets, *GREB1* **(Figure 6.5A)** and *PGR* **(Figure 6.5B)**, and expression of these genes was virtually lost in the TamR lines. Recent studies have found that GREB1 and PGR appear to play a critical role in ER complex assembly and activity in breast cancer cells (18-20). The observations that the expression of these ER co-factors is lost in the TamR lines suggest that ER signaling may be defective in the TamR lines. In support of this prediction, we found that both tamoxifen (ER-antagonist; **Figure 6.1A)** and fulvestrant (ER degrader; **Figure 6.5C)** suppressed the growth of the TamS lines while having no effect on TamR cell growth.

Figure 6.4: PRO-seq analysis of TamS and TamR cells provides insight to tamoxifen resistance. (A) Spearman's ranked correlation of TamS ($B7^{TamS}$ and $C11^{TamS}$) and TamR ($H9^{TamR}$ and $G11^{TamR}$) gene expression patterns. **(B)** MA plot showing differential gene expression of TamS ($B7^{TamS}$ and $C11^{TamS}$) and TamR ($H9^{TamR}$ and $G11^{TamR}$) cells.

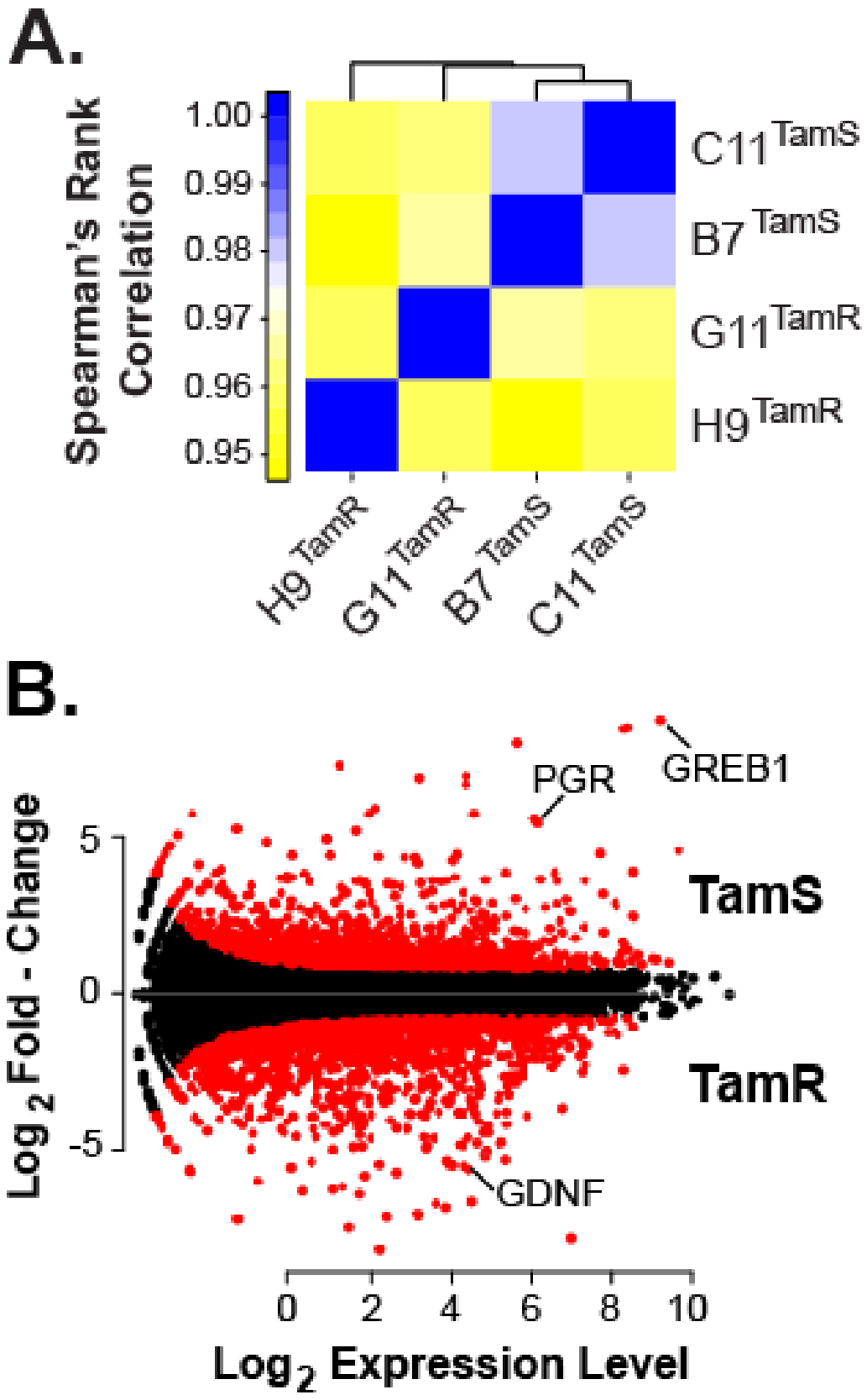
A.
Spearman's Rank Correlation
1.00
0.99
0.98
0.97
0.96
0.95
C11 TamS
B7 TamS
G11 TamR
H9 TamR
H9 TamR
G11 TamR
B7 TamS
C11 TamS
B.
Log2 Fold - Change
5
0
-5
PGR
GREB1
TamS
TamR
GDNF
0
2
4
6
8
10
Log2 Expression Level

Figure 6.5: PRO-seq analysis reveals differential gene expression between TamS and TamR cells. (A) Browser shot of PRO-seq data at *GREB1* and **(B)** *PGR* at loci. Note that ER target gene expressions (*GREB1* and *PGR*) are lost in TamR cells. (Red peaks = Plus DNA strand. Blue peaks = Minus DNA strand). **(C)** Cell survival assay on TamS and TamR cells treated with fulvestant (ER degrader) suggest that TamR cell growth is not dependent upon ER. Error bar is calculated using three biological replicates. **(D)** Browser shot of PRO-seq data at *GDNF* locus. Note that *GDNF* expression is lost in TamS cells. (Red peaks = Plus DNA strand. Blue peaks = Minus DNA strand). **(E)** Treatment of $B7^{TamS}$ cells with recombinant GDNF confers resistance to tamoxifen. **(F)** Western blot of $B7^{TamS}$ cells treated with recombinant GDNF shows increase in PADI2 protein levels in a dose-dependent manner.

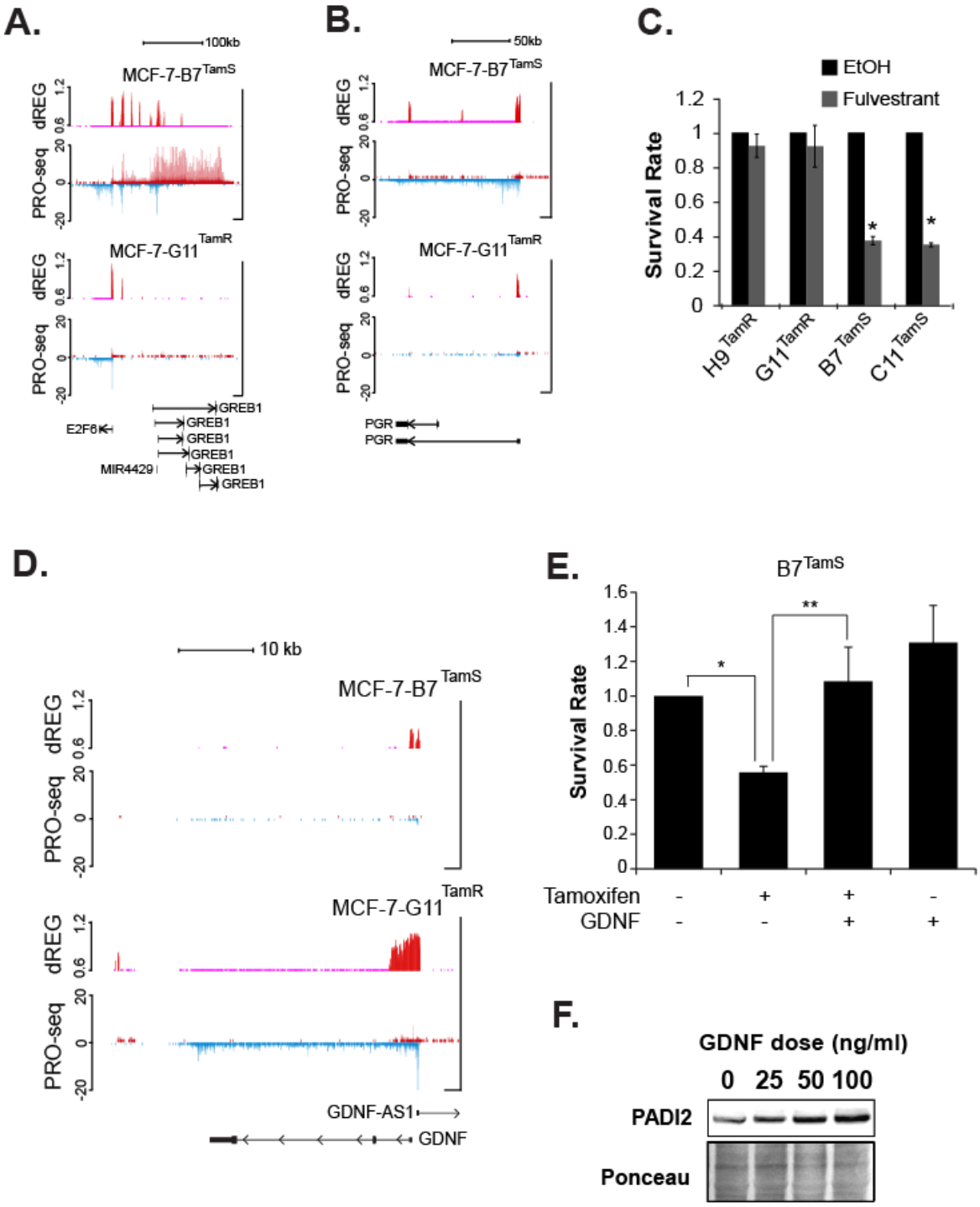
A.
100kb
MCF-7-B7TamS
dREG
PRO-seq
MCF-7-G11TamR
GREB1
E2F6
MIR4429
B.
50kb
PGR
C.
EtOH
Fulvestrant
Survival Rate
H9TamR
G11TamR
B7TamS
C11TamS
D.
10 kb
GDNF-AS1
GDNF
E.
B7TamS
Tamoxifen
GDNF
F.
GDNF dose (ng/ml)
0 25 50 100
PADI2
Ponceau

In TamR cells, we found a robust increase in *GDNF*, glial cell line-derived neurotrophic factor, that was absent in TamS cells **(Figure 6.5D)**. To test whether GDNF may confer tamoxifen resistance to TamS cells, we treated $B7^{TamS}$ cells with recombinant GDNF and then treated the cells with tamoxifen. We found that GDNF prevented tamoxifen-induced cell death in the TamS cells **(Figure 6.5E)**. Interestingly, we also found that these $B7^{TamS}$ cells treated with recombinant GDNF exhibited highly upregulated PADI2 expression **(Figure 6.5F)**. Given that there are also high GDNF and PADI2 expressions in TamR cells, it may be possible that GDNF regulates PADI2 expression.

Altogether, we find that GDNF is differentially expressed in TamS and TamR cells and that GDNF can induce tamoxifen resistance in TamS cells.

Closing Remarks:

Previous studies have identified that PADI2 is highly expressed in breast cancer. However, no previous study to our knowledge, has looked in detail of the role of PADI2 in mammary tumorigenesis. In this thesis, I have investigated the role of PADI2 in breast cancer progression and found that PADI2 is involved in mammary tumor cell migration and invasion. Additionally, we found that PADI2 regulates expression of a well-known breast cancer oncogene, HER2. Furthermore, we found that PADI inhibitor, BB-Cl-Amidine, can effectively target PADI2-positive breast cancer cells to undergo apoptosis. These findings suggest that PADI inhibition may be used as a therapeutic option to treat breast cancer. Hopefully, my thesis work will provide a foundation for the development of therapeutic strategies to treat breast cancer patients.

REFERENCES

1. Horibata, S., Coonrod, S. A., and Cherrington, B. D. (2012) Role for peptidylarginine deiminase enzymes in disease and female reproduction. *J Reprod Dev* **58**, 274-282

2. Mackay, A., Tamber, N., Fenwick, K., Iravani, M., Grigoriadis, A., Dexter, T., Lord, C. J., Reis-Filho, J. S., and Ashworth, A. (2009) A high-resolution integrated analysis of genetic and expression profiles of breast cancer cell lines. *Breast Cancer Res Treat* **118**, 481-498

3. Blick, T., Hugo, H., Widodo, E., Waltham, M., Pinto, C., Mani, S. A., Weinberg, R. A., Neve, R. M., Lenburg, M. E., and Thompson, E. W. (2010) Epithelial mesenchymal transition traits in human breast cancer cell lines parallel the CD44(hi/)CD24 (lo/-) stem cell phenotype in human breast cancer. *J Mammary Gland Biol Neoplasia* **15**, 235-252

4. Bertucci, F., Borie, N., Ginestier, C., Groulet, A., Charafe-Jauffret, E., Adelaide, J., Geneix, J., Bachelart, L., Finetti, P., Koki, A., Hermitte, F., Hassoun, J., Debono, S., Viens, P., Fert, V., Jacquemier, J., and Birnbaum, D. (2004) Identification and validation of an ERBB2 gene expression signature in breast cancers. *Oncogene* **23**, 2564-2575

5. Knight, J. S., Subramanian, V., O'Dell, A. A., Yalavarthi, S., Zhao, W., Smith, C. K., Hodgin, J. B., Thompson, P. R., and Kaplan, M. J. (2015) Peptidylarginine deiminase inhibition disrupts NET formation and protects against kidney, skin and vascular disease in lupus-prone MRL/lpr mice. *Ann Rheum Dis* **74**, 2199-2206

6. Horibata, S., Vo, T. V., Subramanian, V., Thompson, P. R., and Coonrod, S. A. (2015) Utilization of the Soft Agar Colony Formation Assay to Identify Inhibitors of Tumorigenicity in Breast Cancer Cells. *J Vis Exp*, e52727

7. Osborne, C. K., and Schiff, R. (2011) Mechanisms of endocrine resistance in breast cancer. *Annu Rev Med* **62**, 233-247

8. Shou, J., Massarweh, S., Osborne, C. K., Wakeling, A. E., Ali, S., Weiss, H., and Schiff, R. (2004) Mechanisms of tamoxifen resistance: increased estrogen receptor-HER2/neu cross-talk in ER/HER2-positive breast cancer. *J Natl Cancer Inst* **96**, 926-935

9. Zhang, X., Bolt, M., Guertin, M. J., Chen, W., Zhang, S., Cherrington, B. D., Slade, D. J., Dreyton, C. J., Subramanian, V., Bicker, K. L., Thompson, P. R., Mancini, M. A., Lis, J. T., and Coonrod, S. A. (2012) Peptidylarginine deiminase 2-catalyzed histone H3 arginine 26 citrullination facilitates estrogen receptor alpha target gene activation. *Proc Natl Acad Sci U S A* **109**, 13331-13336

10. Guertin, M. J., Zhang, X., Anguish, L., Kim, S., Varticovski, L., Lis, J. T., Hager, G. L., and Coonrod, S. A. (2014) Targeted H3R26 deimination specifically facilitates estrogen receptor binding by modifying nucleosome structure. *PLoS Genet* **10**, e1004613

11. Harvey, J. M., Clark, G. M., Osborne, C. K., and Allred, D. C. (1999) Estrogen receptor status by immunohistochemistry is superior to the ligand-binding assay for predicting response to adjuvant endocrine therapy in breast cancer. *J Clin Oncol* **17**, 1474-1481

12. Ali, S., and Coombes, R. C. (2002) Endocrine-responsive breast cancer and strategies for combating resistance. *Nat Rev Cancer* **2**, 101-112

13. Jemal, A., Siegel, R., Xu, J., and Ward, E. (2010) Cancer statistics, 2010. *CA Cancer J Clin* **60**, 277-300

14. Ma, C. X., Sanchez, C. G., and Ellis, M. J. (2009) Predicting endocrine therapy responsiveness in breast cancer. *Oncology (Williston Park)* **23**, 133-142

15. Gonzalez-Malerva, L., Park, J., Zou, L., Hu, Y., Moradpour, Z., Pearlberg, J., Sawyer, J., Stevens, H., Harlow, E., and LaBaer, J. (2011) High-throughput ectopic expression screen for tamoxifen resistance identifies an atypical kinase that blocks autophagy. *Proc Natl Acad Sci U S A* **108**, 2058-2063

16. Benz, C. C., Scott, G. K., Sarup, J. C., Johnson, R. M., Tripathy, D., Coronado, E., Shepard, H. M., and Osborne, C. K. (1992) Estrogen-dependent, tamoxifen-resistant tumorigenic growth of MCF-7 cells transfected with HER2/neu. *Breast Cancer Res Treat* **24**, 85-95

17. Kwak, H., Fuda, N. J., Core, L. J., and Lis, J. T. (2013) Precise maps of RNA polymerase reveal how promoters direct initiation and pausing. *Science* **339**, 950-953

18. Mohammed, H., D'Santos, C., Serandour, A. A., Ali, H. R., Brown, G. D., Atkins, A., Rueda, O. M., Holmes, K. A., Theodorou, V., Robinson, J. L., Zwart, W., Saadi, A., Ross-Innes, C. S., Chin, S. F., Menon, S., Stingl, J., Palmieri, C., Caldas, C., and Carroll, J. S. (2013) Endogenous purification reveals GREB1 as a key estrogen receptor regulatory factor. *Cell Rep* **3**, 342-349

19. Mohammed, H., Russell, I. A., Stark, R., Rueda, O. M., Hickey, T. E., Tarulli, G. A., Serandour, A. A., Birrell, S. N., Bruna, A., Saadi, A., Menon, S., Hadfield, J., Pugh, M., Raj, G. V., Brown, G. D., D'Santos, C., Robinson, J. L., Silva, G., Launchbury, R., Perou, C. M., Stingl, J., Caldas, C., Tilley, W. D., and Carroll, J. S. (2015) Corrigendum: Progesterone receptor modulates ERalpha action in breast cancer. *Nature* **526**, 144

20. Mohammed, H., Russell, I. A., Stark, R., Rueda, O. M., Hickey, T. E., Tarulli, G. A., Serandour, A. A., Birrell, S. N., Bruna, A., Saadi, A., Menon, S., Hadfield, J., Pugh, M., Raj, G. V., Brown, G. D., D'Santos, C., Robinson, J. L., Silva, G., Launchbury, R., Perou, C. M., Stingl, J., Caldas, C., Tilley, W. D., and Carroll, J. S. (2015) Progesterone receptor modulates ERalpha action in breast cancer. *Nature* **523**, 313-317